# DESIGN RULES FOR CONFORMAL COOLING CHANNELS IN PLASTIC INJECTION MOULDS PRODUCED THROUGH DIRECT METAL LASER SINTERING OF MARAGING STEEL

**IMDAADULAH ADAM**

Dissertation submitted in fulfilment of the requirements for the Degree

**MASTER OF ENGINEERING**

**in**

**MECHANICAL ENGINEERING**

in the

Department of Mechanical and Mechatronics Engineering

Faculty of Engineering, Built Environment and Information Technology

at the

Central University of Technology, Free State

Supervisor: Prof WB du Preez, PhD, Pr Sci Nat

Co-supervisor: Dr J Combrinck, D Eng Mech Eng

BLOEMFONTEIN

May 2019

Declaration of independent work

**DECLARATION WITH REGARD TO**

**INDEPENDENT WORK**

I, IMDAADULAH ADAM, identity number and student number ,
do hereby declare that this research project submitted to the Central University of Technology, Free State for the Degree MASTER OF ENGINEERING: ENGINEERING: MECHANICAL, is my own independent work; and complies with the Code of Academic Integrity, as well as other relevant policies, procedures, rules and regulations of the Central University of Technology, Free State; and has not been submitted before to any institution by myself of any other person in fulfilment (or partial fulfilment) of the requirements for the attainment of any qualification.

_____ 13 May 2019

**SIGNATURE OF STUDENT** **DATE**

*Dedicated to the memory of Anwar Khan: you taught me that failure is never an option.*

# Acknowledgements

Prof Willie du Preez and Dr Jacques Combrinck, I would like to express special gratitude to you for your guidance, moral support and wisdom. It was a great pleasure to work under your supervision.

Johan Els, André Heydenrych and the entire team at the Centre for Rapid Prototyping and Manufacturing, your tireless efforts in producing the components used in this study are gratefully acknowledged.

Marius Zwemstra, I am grateful for all your efforts in assisting me with SIGMASOFT® simulation software.

Altech-UEC, the use of one of your injection mould toolsets in this study is acknowledged with sincere gratitude.

To the Faculty of Natural and Agricultural Sciences at the University of the Free State as well as the Department of Mechanical and Nuclear Sciences at the North-West University, the use of your facilities is greatly appreciated.

To the South African Department of Science and Technology, your financial support through the Collaborative Program in Additive Manufacturing (Contract № CSIR-NLC-CPAM-15-MOA-CUT-01) is gratefully acknowledged.

To my family, a sincere thank you for believing in me and encouraging me to be the best I can be.

To my friends and colleagues, thank you for all your support and encouragement.

Above all else, I am sincerely grateful to the Almighty for providing me with this opportunity, as well as the strength to accomplish this personal milestone.

# Abstract

Additive Manufacturing (AM) is fast becoming a common process in the manufacturing and tooling industry at large. Subsequently, AM has been identified as one of the key technologies in Industry 4.0 through the design freedom and versatility in the possible shortened lead times offered.The application of AM has recently become quite appealing in the Injection Moulding (IM) industry. The development of metal powders for Selective Laser Melting (SLM) has created the potential for SLM to be used for the manufacture of high-volume production IM tooling inserts. The design capabilities of tool designers have been enhanced through the use of AM in the tool making environment by lending its greatest advantage: freedom of design. Since AM offers virtual freedom of design, this has led to the implementation of conformal cooling channels for tooling, which has shown to be instrumental in enhancing productivity and ultimately increasing profitability. The cooling of IM tools is a vital stage in the IM process which has a direct impact on the profitability and productivity of the process. The efficiency of injection mould tooling is positively influenced by an enhanced cooling rate achieved through conformal cooling, which in turn has a positive influence on the quality of the parts produced.

The aim of this study was to further enhance the use of AM in the IM industry through the refinement of design rules for conformal cooling channels. By utilizing Finite Element Analysis (FEA)-based techniques and practical experiments, the end goal has been achieved through the determination of physical limitations of conformal cooling channels built through the Direct Metal Laser Sintering (DMLS) process, an AM technique used to fuse metal powders through application of a high-power-density laser.

Furthermore, one of the challenges faced during this study led to the development of a stress-relieving heat treatment for maraging steel components built using the DMLS process. This was achieved through subsequent applications of a combination of heat treatments followed by 3D-scanning techniques and hardness measurements. This process was iterated until a virtually stress-free component was achieved.

Ultimately, the refined design rules were applied to an IM toolset in an attempt to compare the cooling efficiency and productivity of conformal cooling channels produced using AM and that of conventionally machined cooling channels.The results indicated that conformal cooling has a significant impact on the reduction of cycle times resulting in an improved cooling efficiency.

In a broader perspective, a design process was documented to further augment the design thought process as applied AM in the IM tooling industry. Together with the documentation of the refined design rules for conformal cooling channels, this provides a valuable tool to the IM design industry at large.

# Publications emanating from this study

Adam, I., du Preez, W.B. & Combrinck, J., 2016. Design Considerations for Additive Manufacturing of Conformal Cooling Channels in Injection Moulding Tools. *Interim*, 15(1), pp.35–44. ISSN 1684-498X. 19th Annual Faculty of Engineering and Information Technology Research Seminar, 26 Oct 2016, Central University of Technology, Free State, Bloemfontein, South Africa

Adam, I., Du Preez, W.B. & Combrinck, J., 2017. Stress relieving of maraging steel injection mould inserts built through additive manufacturing. *RAPDASA*, pp.70–72. ISBN 978-0-620-77239-4. 18th Annual Rapid Product Development Association of South Africa conference, 7–10 Nov 2017, Inkosi Albert Luthuli International Conference Centre, Durban, South Africa

Adam, I., Du Preez, W.B. & Combrinck, J., Zwemstra, M., 2018. Conformal Cooling Channel Design For Direct Metal Laser Sintering Of Maraging Steel Mould Inserts. *RAPDASA*, pp.224–234. ISBN 978-0-620-80987-0. 19th Annual Rapid Product Development Association of South Africa conference, 6–9 Nov 2018, Protea Parktonian, Braamfontein, Johannesburg, South Africa

# Contents

# List of Figures

# List of Tables

# Abbreviations

| | |
|---|---|
| 3D | Three Dimensional |
| ABS | Acrylonitrile Butadien Styrene |
| AM | Additive Manufacturing |
| BJ | Binder Jetting |
| CAD | Computer Aided Design |
| DMLS | Direct Metal Laser Sintering |
| EBM | Electron Beam Melting |
| EOS | Electro-Optical Systems GmbH |
| FDM | Fused Deposition Modelling |
| FEA | Finite Element Analysis |
| IM | Injection Moulding |
| LENS | Laser Engineered Net Shaping |
| LOM | Laminated Object Manufacturing |
| MAM | Metal Additive Manufacturing |
| MS1 | Maraging Steel |
| OEM | Original Equipment Manufacturer |
| PP | Polypropylene |
| SLA | Stereolithography |
| SLS | Selective Laser Sintering |
| SLM | Selective Laser Melting |
| UTS | Ultimate Tensile Strength |
| YS | Yield Strength |

# List of Symbols

| | |
|---|---|
| $E$ | Young's Modulus of mould material |
| $G$ | Shear Modulus of mould material |
| $D_H$ | Hydraulic diameter of cooling channel |
| $P_m$: | Injection pressure |
| $x_m$: | Distance between mould surface and cooling channel |
| $\theta$: | Deflection between mould surface and cooling channel |
| $\tau$: | Shear stress experienced under an applied injection pressure |
| $\sigma$: | Stress experienced under an applied injection pressure |

# Chapter 1

## Introduction

*An introduction to the nature of this study, where the aims, objectives and approach will be outlined.*

---

### 1.1 Background

Additive Manufacturing (AM), or 3D Printing as it is more commonly known, encompasses the technologies used to produce three-dimensional (3D) components in a layer fashion directly from a Computer Aided Design (CAD) file. While this technology was first introduced in the 1980s to mainly produce prototype components, with recent developments, AM is fast becoming a common process in various manufacturing industries including the tooling industry at large (Matias and Rao, 2015).

Through its versatility and relatively short manufacturing times, AM is beginning to appeal to original equipment manufacturers (OEMs), to produce jigs and fixtures in the automotive industry at a fraction of the cost and time it would take to manufacture these using conventional methods. Although the initial work has mostly been done using Acrylonitrile Butadiene Styrene (ABS) plastics and the Fused Deposition Modelling (FDM) process (Eidenschink & Günter 2009; Hiemenz 2012, 2015; Stratasys 2013, 2012), the way has been paved for further research and development on using metals and other forms of AM processes in both the automotive and aerospace industries.

AM has been highlighted as a key technology in Industry 4.0, specifically in the manufacturing sector (Wohlers Report 2018) and from this an important question arises: what does AM have to offer the tooling industry? Until recently, however, AM has mainly been used in the injection moulding (IM) industry for prototyping as well as research and product development (Combrinck, Boosyen & van der Walt 2012). By making use of AM to produce high-volume production tooling, such as IM tools, tool designers are no longer limited by conventional machining methods and can design and produce IM tools with intricate geometries and conformal cooling channels.

The introduction of conformal cooling channels is a great advantage offered by AM in the IM industry (van As, Combrinck, Booysen & de Beer 2015), because the cooling of the moulds used in IM is

crucial in determining the productivity and efficiency of the IM process. Unlike conventional cooling channels, which are restricted due to the limitations of conventional machining techniques, AM-produced conformal cooling channels follow the contours of the mould cavity and core, providing even cooling across the entire mould (Li, 2001). Because cooling accounts for up to two-thirds of the IM cycle time, AM conformal cooling channels can improve the efficiency of cooling, reducing cooling time and improving productivity.

With the fast growing interest in AM in the tooling industry, it has become apparent that limited knowledge exists in terms of design rules for components to be manufactured by means of AM technology. As laid out in the recommendations of the South African AM Technology Strategy (de Beer, du Preez, Greyling, Prinsloo, Sciamarilla, Trollip, Vermeulen & Wohlers 2016), summarized in Figure 1 below, the need for design and design optimization exists and not only does it have a significant impact on the tooling sector but also across a broader spectrum of AM sectors.

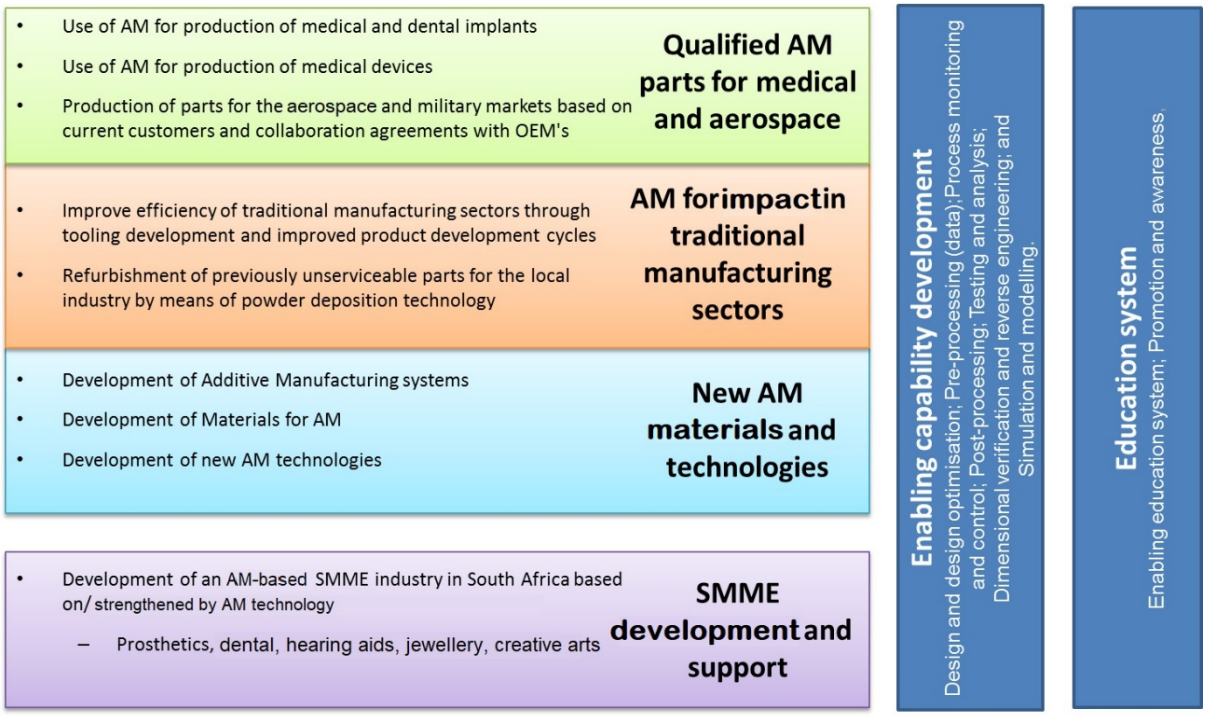


*Figure 1: Summary of the recommendations of the South African AM Technology Strategy*

## 1.2 Problem Statement

"Designing a good-looking car is absolutely easy as pie. Designing a car that a company can afford, the manufacturing guys can assemble, the engineers can engineer is difficult"

– Gale Halderman, Original Ford Mustang Designer.

By applying Gale Halderman's idea to the tooling industry it is evident that designing a high-volume production IM tool that offers affordability, pleasing product aesthetics, functionality and most importantly, manufacturability, is quite challenging. However, with the advancement of AM technologies, this is fast becoming achievable; hence the need for refined AM design guidelines and specific rules with regard to IM tools with conformal cooling channels arises and will be explored in this study. Consequently, design guidelines specific to the design of conformal cooling channels will be investigated in this study. Refined design guidelines and rules to be utilized by tool designers and AM designers will be developed, thereby transforming the boundaries of tool manufacture in an ever-evolving Industry 4.0.

## 1.3 Aim

The aim of this research is to identify and refine existing AM design rules as applied to conformal cooling for use in a high-volume production IM tooling environment. Refined AM design rules, taking into consideration existing AM design constraints, in a user-friendly format for the tool making industry will be documented, thereby contributing to a more efficient and profitable IM industry.

## 1.4 Objectives

The objectives of this research are as follows:

- Research and identify existing AM design constraints as applied to IM tooling with conformal cooling channels built in maraging steel.
- Develop and refine specific design rules to improve the cooling efficiency of conformal cooling channels in IM tooling inserts produced in maraging steel.
- Demonstrate the effectiveness of the conformal cooling through application to an industry mould.
- Document a design process for conformal cooling channels in a format that would be user-friendly for practitioners in the tooling industry.

## 1.5 Approach

The flow diagram shown in Figure 2 presents a general layout of the approach to this study. From this it is evident that after a thorough literature study, design constraints will be investigated and design rules will be highlighted for further refinement. Through the application of Computer Aided Design (CAD) techniques and Finite Element Analysis (FEA)-based simulations a set of IM inserts will be designed and produced using the Direct Metal Laser Sintering (DMLS) AM process. The IM inserts will be tested and the data which was collected will be analyzed and documented.

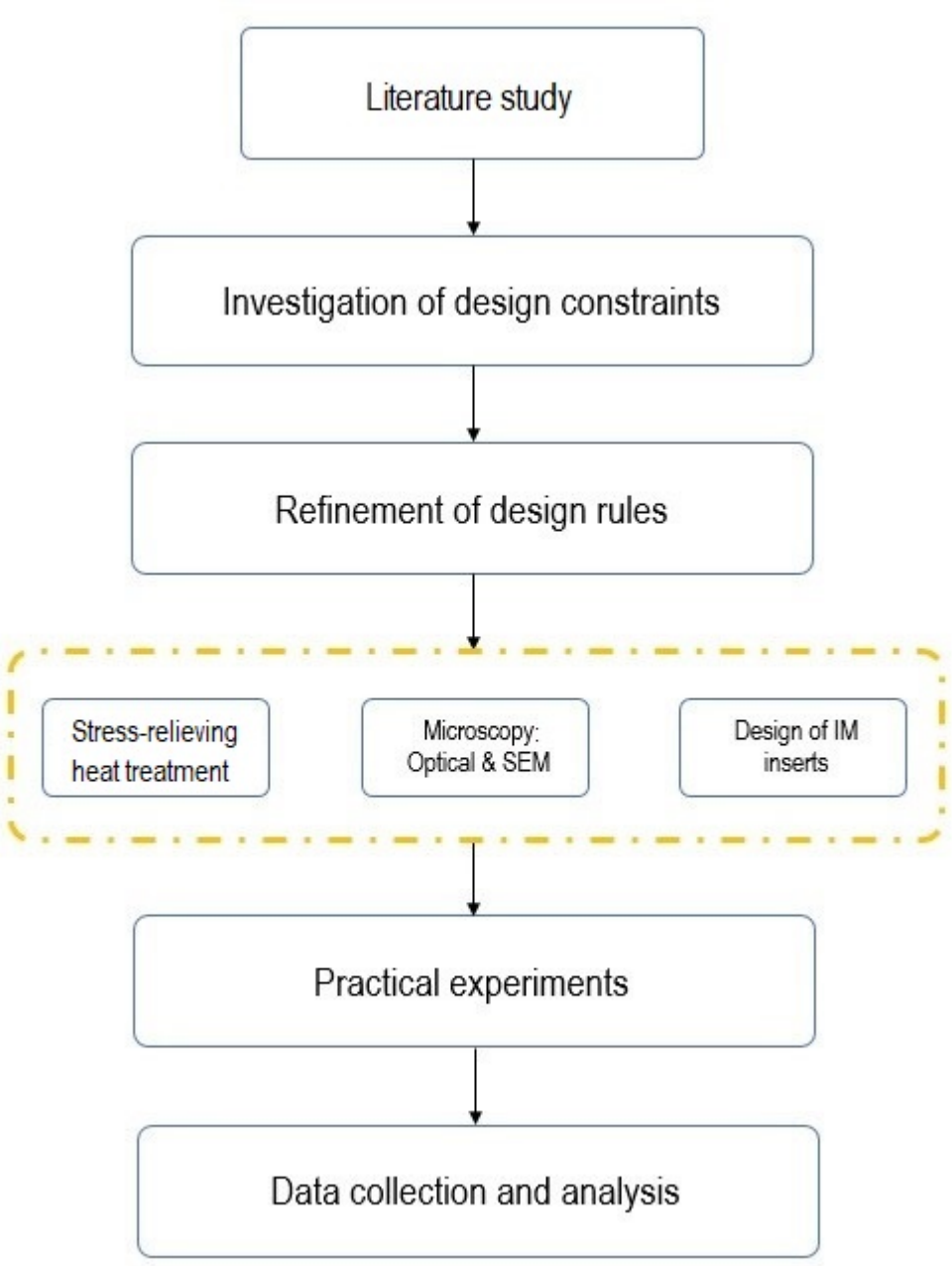


*Figure 2: Flow diagram representing an overview of the general approach to this study*

## 1.6 Delimitations

This study will focus on the use of cooling channels having a circular cross-section as applied to the injection moulding process. While cooling channel lengths and flow rates form a part of the total scope of parameters influencing the IM mould cooling efficiency, these will not be investigated as separate parameters in this study.

*Summary*

*Since IM is one of the most commonly used methods of plastic processing, over the years it has become adequately efficient. However, further improvement and optimization in the context of the digitalization drive of Industry 4.0 is justified, and through the use of available technologies such as AM, this is now feasible. It has been shown that AM offers virtual freedom of design of complicated components, which offers a significant benefit to the IM tooling industry for realizing more efficient conformal cooling channels. By pushing the design boundaries of conformal cooling channels, this study aims to enhance the design rules for conformal cooling channels, thereby contributing to a more efficient and profitable IM industry and tooling industry at large.*

# Chapter 2

## Literature Review

*An evaluative report of the information found in literature, which describes, summarizes and clarifies the literature relevant to this study. Thereby a theoretical and practice-related base for the research conducted in this study is provided.*

---

Plastic Injection Moulding (IM), the ubiquitous moulding process which is used for manufacturing various components from toys to critical medical devices, can be considered the most commonly used plastic manufacturing process in which there is a constant demand for a high-quality product which is economical to produce.

### 2.1 Injection Moulding

The IM process, whereby molten plastic is injected into a mould under pressure, is considered one of the most widely used applications in the polymer processing industry. The mould toolset usually consists of two halves which are clamped into position and kept at a constant temperature. Hot molten plastic is then forced under pressure into the mould and allowed to cool down. After the plastic has solidified, the clamps are released, the moulded component is ejected, and the cycle is subsequently repeated. In this way, geometrically identical objects ranging in size from toy building blocks to vehicle components are mass produced (Whale, Fowkes, Hocking & Hill 1995). A representation of the IM process is shown in Figure 3.

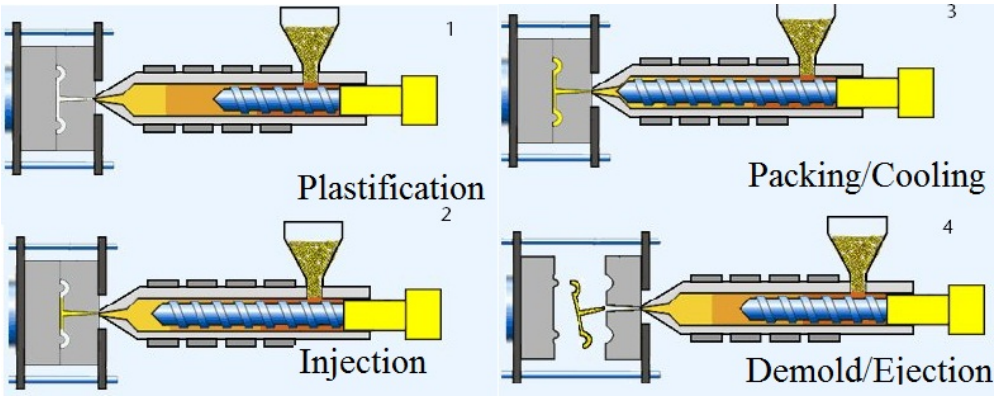


*Figure 3: Representation of the injection moulding process*

### Stage 1:

During the initial stage, the two halves of the toolset are pressed together by a clamping unit forming an enclosed volume inside the tool which replicates the shapes of the product to be moulded.

### Stage 2:

During the second stage of the process, molten polymer is injected into the IM tool. During the injection stage, approximately 95% of the volume inside the mould is filled. Although the exact time of the injection is challenging to control, it can be estimated by injection pressure, injection power and volume of the injected shot. The injection process is followed by a packing process, whereby the remainder of the volume is filled at a slower rate in order to compensate for the shrinkage effect of the cooling material inside the mould.

### Stage 3:

Cooling of the molten material starts immediately after having reached the surface of the tool. The IM tooling is typically equipped with cooling channels which serve to cool the toolset to a specified temperature, depending on the ejection temperature of a particular polymer. Typically, the cooling stage contributes approximately 60% of the total cycle time (van As *et al.*, 2015).

### Stage 4:

During the final stage of the IM process, the component is ejected from the toolset. As the material has cooled down and solidified, the tool is opened exposing a finished product. The product is ejected from the tool by ejector pins, followed by the product falling out of the tool.

## 2.2 Tooling Design

Tooling design essentially comprises the design, analysis and construction of tooling equipment, and methods and procedures to increase manufacturing productivity (Rao, 2007). This is a complex design process which is mainly governed by the function for which the tool is being designed as well as high levels of accuracy. Tooling is generally grouped under the following categories (Rao, 2007):

- Jigs and fixtures: used to hold a part in place while work is carried out on the part.
- Press and forming tools: used to form high volumes of a product using hydraulic, mechanical or pneumatic pressure.
- Moulding tools: used to rapidly and consistently produce high volumes of the same product.

The success of mass production depends directly on the ease of assembly and production, and subsequently there is a need for the design and manufacture of purpose-built tooling which facilitates

ease of assembly. This tooling is used to enhance production operations such as product assembly, forming, machining, moulding, and inspection (Elanchezhian, Sunder Selwyn & Vijaya Ramnath, 2005).

### 2.2.1. Jigs and fixtures

Jigs and fixtures are designed and manufactured with the intent to hold, support and locate a specific work piece and ensure that the part is machined within a specified tolerance. The use of jigs and fixtures allows for efficient mass production (Elanchezhian, Sunder Selwyn and Vijaya Ramnath, 2005).

### 2.2.2. Press and forming tooling

Press and forming tooling may be considered an integral part of the modern mass production machine shop. Large numbers of components can be produced in a short time with relative ease. These components range from furniture and vehicle bodies to cooking and eating utensils (Elanchezhian, Sunder Selwyn & Vijaya Ramnath, 2005).

## 2.3 Additive Manufacturing Processes

Additive Manufacturing (AM), or "three-dimensional (3D) Printing" as it is commonly known, has been highlighted as one of the key technologies in Industry 4.0 (Wohlers 2018). AM is a process whereby material is added layer by layer to produce a desired part directly from a Computer Aided Design (CAD) file. While this is a generic definition of AM, many AM system manufacturers have created unique process names in order to differentiate themselves from their competitors. However, many of these systems share similar processes; hence the ASTM International Committee F42 on Additive Manufacturing Technologies strove to approve a list of AM process definitions. Furthermore, in a collaborative effort between the ASTM and ISO standards organisation, the ASTM terminology was replaced with the ISO/ASTM 52900 standard. In the ISO/ASTM 52900 standard, the additive manufacturing processes are categorized into seven main categories (Wohlers et al. 2018, Elwany 2014):

- Material extrusion: Material is dispensed through a nozzle to produce each layer.
- Material jetting: Droplets of material are deposited selectively to produce each layer.
- Binder jetting: Liquid binding agent selectively joins powder particles in a powder bed.
- Sheet lamination: Sheets of material representing layer cross-sections are bonded one over the other.
- Vat photopolymerization: Liquid photopolymer is typically cured by a laser.

- Powder bed fusion: A thermal energy source, typically a laser or electron beam, selectively fuses powder material in a powder bed.
- Directed energy deposition: Similar to powder bed fusion, metal powder is injected into a melt pool to form a layer pattern (Heigel, Michaleris & Reutzel, 2015).

### 2.3.1 Material Extrusion

#### Fused Deposition Modelling (FDM)

FDM is an AM process in which a thin filament of plastic feeds into a machine where a print head extrudes it and deposits the polymer filament in a 2D layer based on the data from a 2D slice of a 3D CAD model. These 2D layers are stacked onto each other and fused together to create a specific 3D part or shape.

Materials used in this process are typically plastics such as Polycarbonate (PC), Acrylonitrile Butadiene Styrene (ABS), Polyphenylsulfone (PPSF), Polycarbonate- Acrylonitrile Butadiene Styrene (PC-ABS) blends, and Polycarbonate-ISO (PC-ISO) which correspond to a specific International Standards Organization (ISO) standard for the food and medical industry (Wong & Hernandez, 2012).

### 2.3.2 Material Jetting

#### Polyjet

This is an AM process that uses inkjet technologies to manufacture physical models. The inkjet head moves along the *x* and *y* axes depositing a photopolymer which is cured by ultraviolet lamps after each layer is finished. The layer thickness achieved in this process is approximately 16 $\mu$m, so the produced parts have a high resolution (Wong *et al.* 2012).

### 2.3.3 Binder Jetting

Binder Jetting is a process whereby a binding agent is injected onto loose material powders and is heated up which causes the binder to dry. A new layer of powder is then spread over the previously “printed” layer and this process continues in this fashion until a complete part has been manufactured.

#### Prometal

Prometal is an AM process used to build injection tooling and forming dies. This is a powder-based process in which stainless steel is used. The powder is located in a powder bed that is controlled by build pistons that lower the bed after each layer is completed. A feed piston supplies the material for each layer. The printing process occurs when a liquid binder is spurted out in jets onto a steel powder

bed. Upon completion, residual powder is removed and the product is finished using either a sintering process or an infiltration process. During the sintering process, the product is heated to approximately 180 °C for 24 hours. This allows the liquid binder to harden. During the infiltration process, the product is heated to approximately 1100 °C and infused with bronze powder typically at a ratio of 60% stainless steel and 40% bronze (Wong *et al.* 2012).

### 2.3.4 Sheet Lamination

#### Laminated Object Manufacturing

Laminated Object Manufacturing (LOM) is a process that combines additive and subtractive techniques to build a part layer by layer. In this process, the material, typically metal foils and metal, plastic, ceramic, organic, and composite sheets, is supplied in sheet form and are bonded together by pressure and heat application and a thermal adhesive coating (Mueller & Kochan, 1999). A carbon dioxide laser cuts the material to the shape of each layer as designed using CAD software (Feygin & Sung, 1999; (Wong *et al.* 2012)).

### 2.3.5 Vat photopolymerization

#### Stereolithography

Stereolithography is a liquid-based AM process whereby a laser selectively hardens a photo-sensitive resin (contained in a vat) to form a solid polymer layer on a piston-controlled build platform. The build platform is lowered, allowing another layer to be formed on top of the previous layer, eventually creating a solid 3D part (Elwany, 2014).

### 2.3.6 Powder Bed Fusion

#### Laser Sintering

Laser sintering is a process whereby layers of powder particles are selectively fused or melted on a building platform by a laser beam. This process is typically used for both metals and polymers.

#### Selective Laser Sintering (SLS)

SLS is an AM process in which a powder, typically a polymer, is sintered or fused by a carbon dioxide laser beam. The build chamber is heated to almost the melting point of the material. The laser fuses the powder to a specific geometry for each layer as specified by the CAD software design (Wong *et al.* 2012).

#### Selective Laser Melting (SLM)

Direct Metal Laser Sintering (DMLS), a trademark of the AM machine supplier Electro-Optical Systems (EOS) GmbH, is a leading derivative of the application of SLM. It is a layer manufacturing

process for various types of metals whereby thin layers of powder particles are selectively sintered (melted) on a building platform and these two-dimensional (2D) layers are simultaneously fused onto the previous layers by a scanning laser beam, as shown in Figure 4.

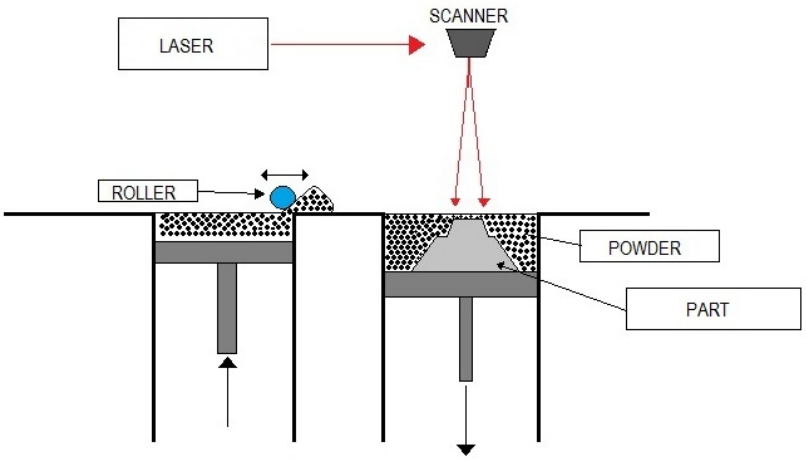


*Figure 4: Graphic representation of the direct metal laser sintering process*

Through subsequent lowering of the building platform and addition of a new powder layer, the layered structure of the 3D component is produced (Ferreira, 2004).

Another commercial variation of SLM is LaserCusing, the trademark of Concept Laser. Similar to DMLS, LaserCusing also makes use of a laser and in this process the metal particles are also fused in a layered fashion (Buijs, 2005).

#### Electron Beam Melting

This process makes use of a high-voltage electron beam in order to melt material powder. The process takes place in a high-vacuum chamber which avoids oxidation issues and makes it very suitable for building metal parts. EBM also can process a great variety of alloyed metals. One of the future uses of this process is manufacturing in outer space, since it operates in a high-vacuum chamber (Wong *et al.* 2012).

### 2.3.7 Directed Energy Deposition

#### Laser Engineered Net Shaping

In this AM process, a part is built by melting metal powder that is injected into a specific location. The powder is melted by a high-powered laser beam and solidifies when cooled down forming a layer of the desired product. The process occurs in a closed chamber with a protective argon atmosphere and permits the use of a great variety of metals and combinations of them like stainless steel, nickel-based alloys, titanium-6 aluminium-4 vanadium, tool steel, copper alloys, etc. This

process can also be used to repair parts that would be impossible or expensive to do using other processes (Wong *et al.* 2012).

With the development of AM processes, it has become possible to create metal parts by using AM technologies such as the DMLS, Prometal or LENS processes. Metal alloys used for AM processes include aluminium, cobalt-chrome, nickel alloys, maraging steel, stainless steels and titanium alloys (EOS, 2013). With the availability of EOS maraging steel (MS1) powder and an EOSINT M280 system at the Central University of Technology, Free State (CUT), this study will make use of the DMLS process using MS1.

## 2.4 Use of Metal Powders in Additive Manufacturing

The application of AM to produce high-volume production tooling is fast becoming a reality. Typically, high-volume tooling is produced using a metal alloy which can withstand the constant pressure and stresses that occur during the IM process. With AM fast becoming a leading form of manufacturing in various industries, the use of different materials has evolved along with the various AM techniques. Formerly used for the "printing" of plastics and polymers, the discovery and invention of laser-based AM techniques have led to the use of metal powders in the AM world (Santos, Shiomi, Osakada & Laoui 2006). This has paved the way for intricate parts to be manufactured directly from metal in the aerospace, automotive and medical fields (Clayton, 2014).

### 2.4.1 Additive manufacturing using maraging steel powder (MS1)

EOS maraging steel (MS1) is a pre-alloyed ultra-high-strength steel, characterized by having very good mechanical properties, and being easily heat-treatable using a simple thermal age-hardening process to obtain excellent hardness and strength. Since this material has good mechanical properties, it is ideal for many tooling applications, as well as for high-performance industrial applications. Its composition corresponds to U.S. classification 18% Ni Maraging 300, European 1.2709 and DIN/EN (1.2312) specification (40CrMnMoS8-6) (EOS, 2014b). Thus, MS1 displays similar properties which makes it ideal for tooling applications such as IM tools (van As et al. 2015). Table 1 shows a summary of MS1 material properties.

*Table 1: Material Properties (EOS 2014b, Schmolz-Bickenbach 2015)*

| *Chemical, Physical and Mechanical Properties* | *Maraging Steel (MS1)* | *1.2312 Tool Steel* |
|---|---|---|
| Chemical Composition (wt-%) | Al (0.05 - 0.15)<br>C (≤ 0.03)<br>Co (8.5 - 9.5)<br>Cr (≤ 0.5)<br>Fe (bal)<br>Mn (≤ 0.1)<br>Mo (4.5 - 5.2)<br>Ni (17 – 19)<br>P (≤ 0.01)<br>S (≤ 0.01)<br>Si (≤ 0.1)<br>Ti (0.6 - 0.8) | C (0.35 – 0.45)<br>Cr (1.8 - 2)<br>Fe (bal)<br>Mn (1.4 -1.6)<br>Mo (0.15 – 0.25)<br>Si (0.3 – 0.5)<br>P (0.03 – 0.005)<br>S (0.05 – 0.1) |
| Minimum recommended layer thickness ( $\mu m$ ) | 40 - 60 | Not applicable |
| Minimum wall thickness (mm) | 0.3 - 0.4 | Not applicable |
| Relative density with standard parameters | Approximately 100% theoretical density | Not applicable |
| Density with standard parameters ( $g/cm^3$ ) | 8.0 - 8.1 | Not applicable |
| Ultimate tensile strength before heat treatment (MPa) | 1100 $\pm$ 100 | 960 |
| Ultimate tensile strength after heat treatment (MPa) | 1950 $\pm$ 100 | Not specified |
| Yield strength before heat treatment (MPa) | 1100 $\pm$ 100 | 850 |
| Yield strength after heat treatment (MPa) | 1900 $\pm$ 100 | Not specified |
| Young's modulus (GPa) | 180 $\pm$ 20 | 205 |
| Hardness before heat treatment (HRC) | 33 – 37 | 32 |
| Hardness after heat treatment (HRC) | 50 – 54 | 51 |
| Thermal conductivity before heat treatment ( $W/m°C$ ) | 15 $\pm$ 0.8 | 34 |
| Thermal conductivity after heat treatment ( $W/m°C$ ) | 20 $\pm$ 1 | Not specified |
| Specific heat capacity ( $J/kg°C$ ) | 450 $\pm$ 20 | 470 |

As seen in Table 1, MS1 shows a combination of good material properties such as high strength, high toughness, good weldability and dimensional stability during aging heat treatment. This superior strength, hardness and toughness is achieved by aging the martensitic phase, making MS1 ideal for high-strength applications as required by the aircraft industry as well as the tooling industry. What sets maraging steels apart from conventional high-strength steels is the hardening mechanism used during the hardening process, where the relatively soft body-centered cubic martensite, which is formed upon cooling, is hardened by the precipitation of intermetallic compounds. It is from this martensitic aging process that the term "maraging steel" is derived.

However, where the cooling of IM tooling is considered, there are physical limitations, such as the strength of the insert material, which sets a limit for the distance $x_m$ between the cooling channel and the mould surface and as such, these limits will be investigated in this study.

### 2.4.2 Heat treatment of MS1

Due to the high tolerances required when fitting an IM tool insert into a pre-machined bolster, a major concern is the geometric deviation of the DMLS insert from the CAD geometry due to residual stresses induced during the DMLS process (Dobransky, Baorn, Simkulet, Kocisko, Ruzbarsky & Vojnova., 2015). Residual stress can be described as a stress present in an object without the influence of any external forces and is introduced into components during thermal processes such as heat treatments, forming or welding (Chou, 2014).

In essence, the DMLS process can be compared to a fast welding process during which the laser beam is scanned over the powder layers and selectively melts and fuses the powder particles together. The very high cooling rate of the melted powder, caused by the rapid movement of the high-temperature laser beam, combined with cyclical reheating of subsequent layers, causes the build-up of tensile stresses in the surface and opposing compressive stresses in the interior of the component. This causes the component to geometrically deviate from the CAD geometry, as illustrated in Figure 5 (Knowles, Becker & Tait 2012).

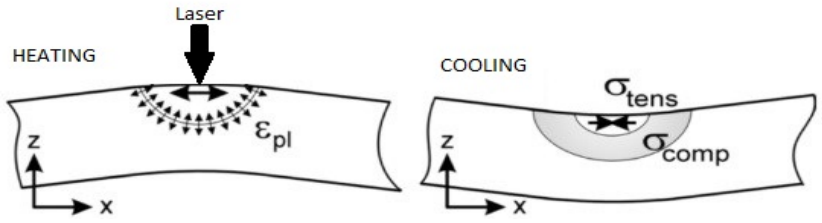


*Figure 5: Rapid heating and cooling of components during the DMLS process which results in deformation of the built components*

While these induced residual stresses may have an impact on the performance and longevity of a component, the geometric deformation of an SLM-produced tool insert could limit or even nullify the benefits to be gained from the SLM technology. The supplier of the MS1 powder used to build these inserts, EOS, does not provide a stress-relieving heat treatment for SLM parts. However, the heat treatment given on the EOS material data sheet, which states that the components be heated to a temperature of 495 °C and allowed to soak for a period of six hours (EOS, 2014a), is an age-hardening treatment. In the case of MS1, which is an age-hardening alloy, it is possible to reach a

hardness of ≥50 HRC after age-hardening making it difficult to achieve the correct fitment tolerances and finishing through machining and other post-processing techniques.

The heat treatment of metals is commonly applied to alter the microstructure of the metal, and is done in order to obtain certain mechanical properties, depending on the application of a specific component. Heat treatment of metals can be achieved through one or a combination of the following processes:

- Annealing: The metal is heated to a high temperature and allowed to cool slowly to room temperature; this results in the metal possessing high ductility but low hardness.
- Hardening: The metal is heated to a certain temperature depending on the carbon content present in the metal and rapidly cooled or quenched in water or oil. This results in a hardened metal.
- Tempering: The metal is heated to a suitable temperature after it has been quenched during hardening. This allows the microstructure of the metal to normalize, resulting in both high strength and hardness.
- Age-hardening: The metal is heated to the aging temperature and kept there for an extended period of time to allow precipitation of alloying elements within the microstructure. These precipitates inhibit the movement of dislocations or cracks in the crystal lattice of the metal, resulting in a stronger metal. This heat treatment technique is used to increase the yield strength of malleable metals, including most structural alloys such as Al, Mg, Ni, Ti, and some steels.

It was found that a build-up of residual stress in DMLS components results in deformation in the component (Knowles et al. 2012); hence there is a need for a stress-relieving heat treatment process.

## 2.5 Design for Additive Manufacturing

Design guidelines for AM and Metal Additive Manufacturing (MAM) in general are still mainly governed by the capabilities of the different AM machines (Samperi, 2014).This leaves designers with the perception that AM allows for total freedom of design, as long as the AM machine can “make” the product. However, the existing design guidelines provide room for the development of more detailed sets of design rules specifically for MAM in the tooling industry in terms of not only the capabilities of the AM machines, but also more importantly, the quality of the desired final product (critical surface finish, etc.) (Samperi, 2014). By making use of these guidelines and rules, not only is the product itself enhanced but also the end-user features of the product (Schmid & Eidenschink,

2014). The trend towards using AM in the tooling industry has gained momentum through its introduction to the IM industry and has made it possible for R&D engineers and designers to make changes to an IM tool within a short space of time and at a fraction of the cost of conventional machining.

The use of AM design guidelines in the tooling industry is a necessity as it allows designers to optimize the required tooling characteristics according to the specific AM process used, as well as the end user needs. A good example of this is shown in Figure 5 (Schmid & Eidenschinck, 2014).

Figure 6 shows a flow diagram used to determine the process required to manufacture FDM tooling. By making use of certain parameters based on AM of ABS plastics, as well as the main function of the tooling, they were able to determine whether it was possible to manufacture the tooling using only FDM or whether additional processes should be used. By developing similar flow diagrams for MAM, the design process of MAM tooling could be simplified.

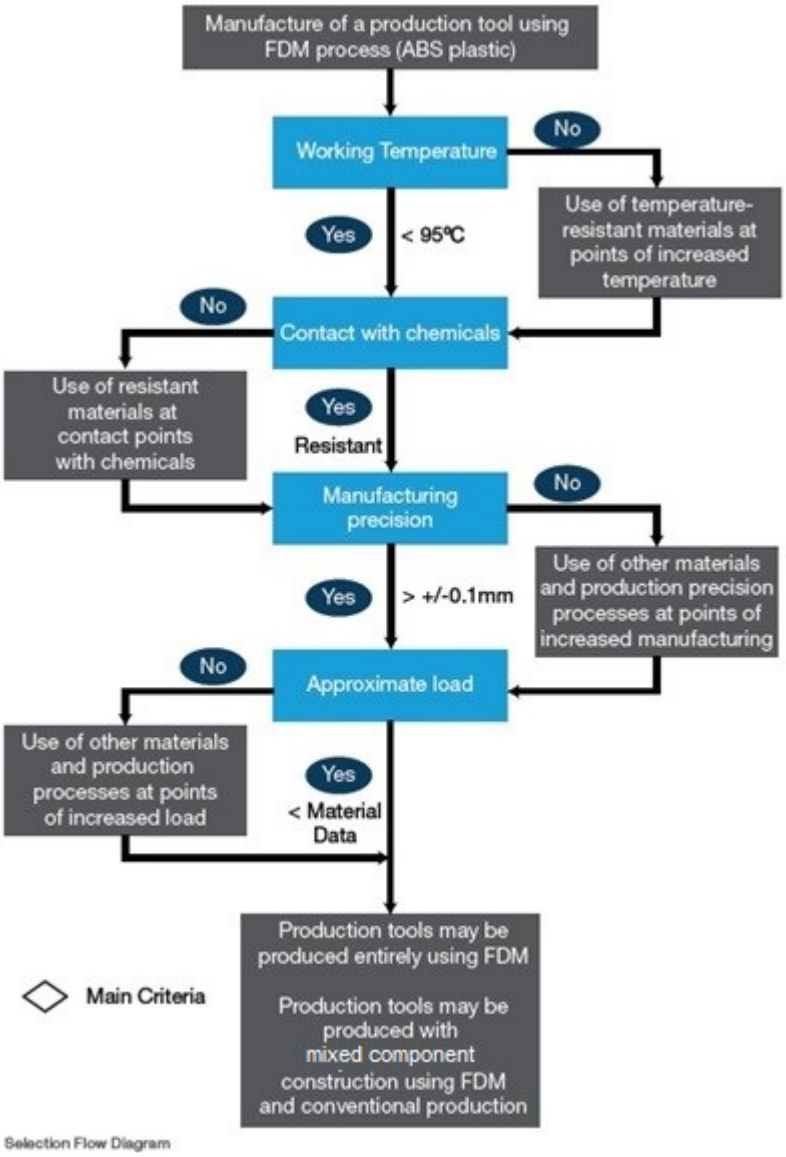


*Figure 6: Design flow diagram for FDM jigs (Schmid* et al., *2014)*

The design process for AM is widely considered as a “one button” process due to the high levels of automation used in AM. Designers tend to forget the preparatory work carried out by engineers and technicians who have the necessary experience and knowledge (Zhang, Bernard, Gupta & Harik., 2014). This leaves significant room for error especially in the tooling industry, as components and tools need to be manufactured to a high level of accuracy. Based on this, the need for design guidelines and rules which could assist designers in making the correct decisions when it comes to the constraints of tool design and manufacture becomes evident.

## 2.6 Design Considerations for Tooling

Traditionally, the design of a product focused primarily on the manufacturability of the product using conventional methods resulting in the aesthetics and functionality of the product being sacrificed at times. However, with the introduction of AM technology, as well as the technological advancements of manufacturing processes, designers are able to apply all these facets to the design process with ease (Sandberg, 2007). Since very few rules or limitations exist with regard to the manufacture of a product, designers are given a set of guidelines to consider when designing for AM (EOS, 2007).

These include:

- Conventional machining methods should be used as far as possible.
- DMLS and other AM technologies should be reserved for products where:
  - Electro Discharge Machining (EDM) is required
  - 5-axis milling is required.
  - Multiple clamping while machining is necessary.
  - Hybrid tooling is a viable option

The abovementioned processes are not only costly but also time-consuming. Figure 7 illustrates how the use of AM to produce tooling products saves time and ultimately cuts manufacturing costs.

By utilizing AM, there is no longer a need to develop and manufacture special EDM electrodes. Also, the time-consuming Computer Numerical Control (CNC) processes are minimized, allowing the tool to be put into production at an earlier stage.

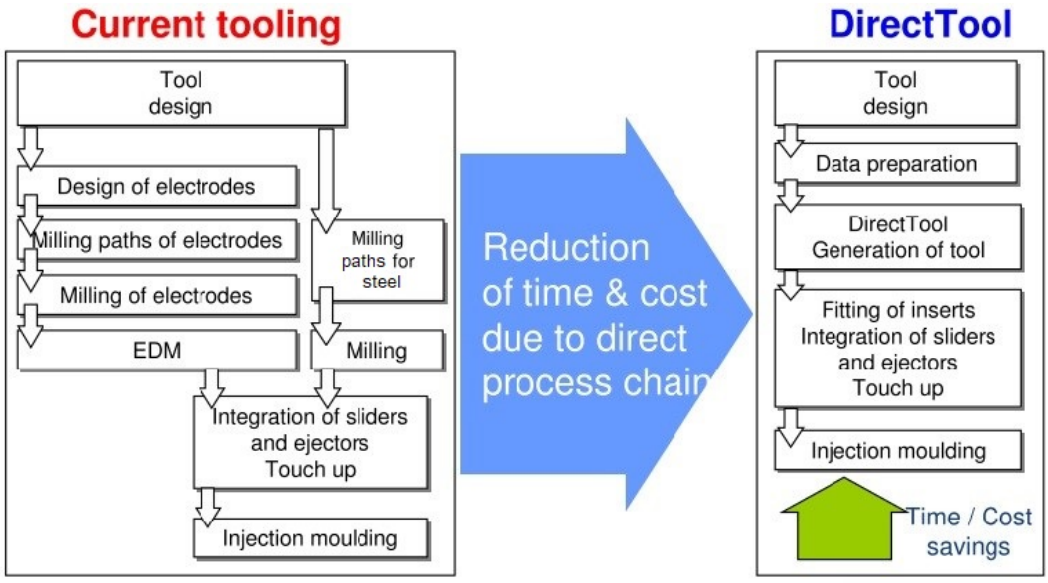


*Figure 7: Reduction of time and cost of tooling by using AM (EOS 2007)*

EDM, as seen in Figure 7, plays an important role in the conventional manufacture and production of IM tooling, where the need for sharp corners and thin ribs or slots is required. EDM is also used in tooling applications where cutting tool limitations are prominent and small diameter cutters experience frequent breakages.

EDM is a process whereby material is removed via a series of rapidly recurring electrical current discharges between two electrodes which are separated by a dielectric liquid such as paraffin. The electrodes are generally distinguished as the tool-electrode and the work-piece electrode, where the tool-electrode is generally designed separately and machined using CNC machines. The tool-electrode and the work-piece electrode have different polarities which result in an electrical current flow between the two surfaces. (Wu, Zhou, Xu, Yang, Zing & Xu, 2016)

In hybrid tooling, a tool insert manufactured through AM is fitted into a steel bolster which is manufactured using conventional machining methods. The AM insert reduces the machining time required for intricate EDM electrodes and leaves tool makers with simple machining operations for the bolsters

### 2.6.1 Design of conformal cooling channels

Conformal cooling channels refer to channels inside a toolset which conform to the contours of the mould cavity and provide the shortest possible distance between the wall of the mould cavity surface and the cooling channel. These attributes of conformal cooling channels allow the coolant to flow in such a manner that a uniform temperature profile is maintained, resulting in a more efficient heat transfer between the molten polymer and the cooling fluid (Gibson, Rosen & Stucker, 2015). Unlike conventionally drilled channels, it is possible to design AM conformal cooling channels with virtual design freedom in order to access the most challenging shapes and areas in the IM tool. This often results in very complex yet optimized channel shapes which have been shown to have superior cooling efficiency when compared to conventional cooling channels (Gibson, Rosen and Stucker, 2015).

### 2.6.2 Mould strength

With the introduction of AM into the manufacturing environment, the use of SLM of metals allows for the manufacture of IM tooling inserts having more effective conformal cooling channels. Not only are designers able to place cooling channels in “hard-to-reach” parts of the IM tool, but the channels can also be placed closer to the mould surface which further enhances the cooling efficiency (Rao & Schumacher, 2004). While this is theoretically perfect, there are certain physical limitations, such

as the strength of the mould material, which set a limit for the distance $x_m$ between the cooling channel and the mould surface.

When developing the following formulae (Rao *et al.*, 2004), the worst-case scenario was considered, whereby a rectangular channel was loaded with the injection pressure $P_m$ as shown in Figure 8. Since commonly used channels are circular in cross-section, they experience relatively smaller stress and deflection.

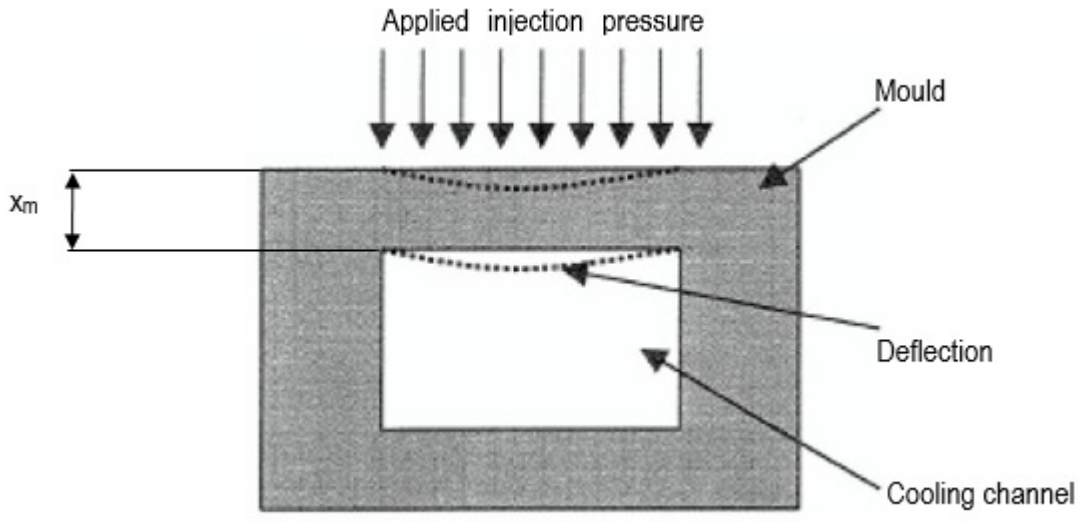


*Figure 8: Deflection of a rectangular channel under applied injection pressure.*

The stress experienced under the applied injection pressure $P_m$ can be expressed by the following:

$$\sigma = \frac{P_m D_H^2}{2x_m} \quad \ldots (1)$$

The shear stress experienced under the applied injection pressure $P_m$ can be expressed by the following:

$$\tau = \frac{3P_m D_H}{4x_m} \quad \ldots (2)$$

The mould deflection experienced under the applied injection pressure $P_m$ can be expressed by the following:

$$\theta = \frac{P_m D_H^2}{x_m}\left[\frac{D_H^2}{32E_m x_m} + \frac{0.15}{G_m}\right] \quad \ldots (3)$$

Where:

$E_m$: Young's Modulus of mould material

$G_m$: Shear Modulus of mould material

$D_H$: Hydraulic diameter of cooling channel

$P_m$: Injection pressure

$x_m$: Distance between mould cavity surface and cooling channel

General guidelines for conformal cooling channels are given as (Mielonen, 2016; Schneider & Carson, 2016):

$D_H$ = 4 mm

$x_{m=}$ 2.5 mm

It is evident that while the mould material properties are important, the above expressions are all dependent on the injection pressure. By making use of the upper limit of the values provided in Table 2, it is possible to compute the values for: $\sigma, \tau \; and \; \theta$. More importantly, it is possible to determine the minimum possible distance $x_m$ between the mould surface and cooling channels, which can be verified by making use of mould simulation software such as SIGMASOFT®.

*Table 2: Injection pressures for typically used plastics in the IM industry (Rao & O'Brien 1998)*

| Material | Necessary Injection Pressure (MPa) | | |
|---|---|---|---|
| | Low viscosity<br><br>Heavy sections | Medium viscosity<br><br>Standard sections | High viscosity<br><br>Thin sections; small gates |
| **ABS** | 80/110 | 100/130 | 130/150 |
| **POM** | 85/100 | 100/120 | 120/150 |
| **PE** | 70/100 | 100/120 | 120/150 |

| | | | |
|---|---|---|---|
| **PA** | 90/100 | 110/140 | >140 |
| **PC** | 100/120 | 120/150 | >150 |
| **PMMA** | 100/120 | 120/150 | <150 |
| **PS** | 80/100 | 100/120 | 120/150 |
| **RigidPVC** | 100/120 | 120/150 | >150 |
| **Thermosets** | 100/140 | 140/175 | 175/230 |
| **Elastomers** | 80/100 | 100/120 | 120/150 |

### 2.6.3 Water meter cover case study

Figure 9 shows some of the challenges faced by the tool design team at FADO. There was very limited space for the cooling channels, air vents and ejector pins in the IM mould. The solution to these challenges was to manufacture the IM tooling using AM, which allowed the design team to utilize conformal cooling channels, as seen in Figure 10. The advantages of utilizing conformal cooling is highlighted in Figure 11, where it is shown that with conformal cooling the heat transfer during the heating phase is more even over a shorter period of time. This not only solved the problems faced by the design team but also lowered the cycle time by 32%, as shown in Figure 12, allowing an estimated saving of EUR 12 000.


*Figure 9: Challenges faced by FADO design team. (http://www.eos.info/tooling)*

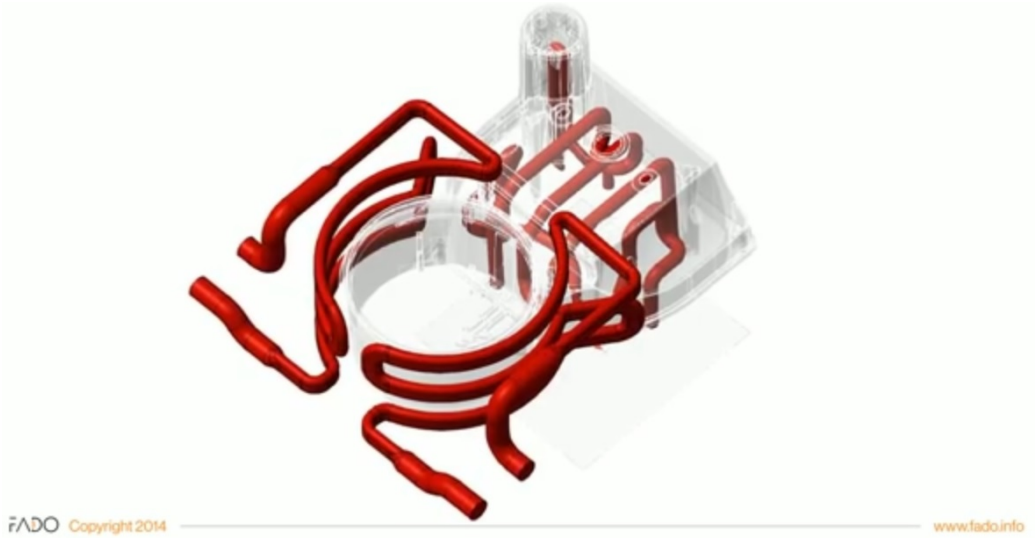


*Figure 10: Water meter cover conformal cooling channels. (http://www.eos.info/tooling)*

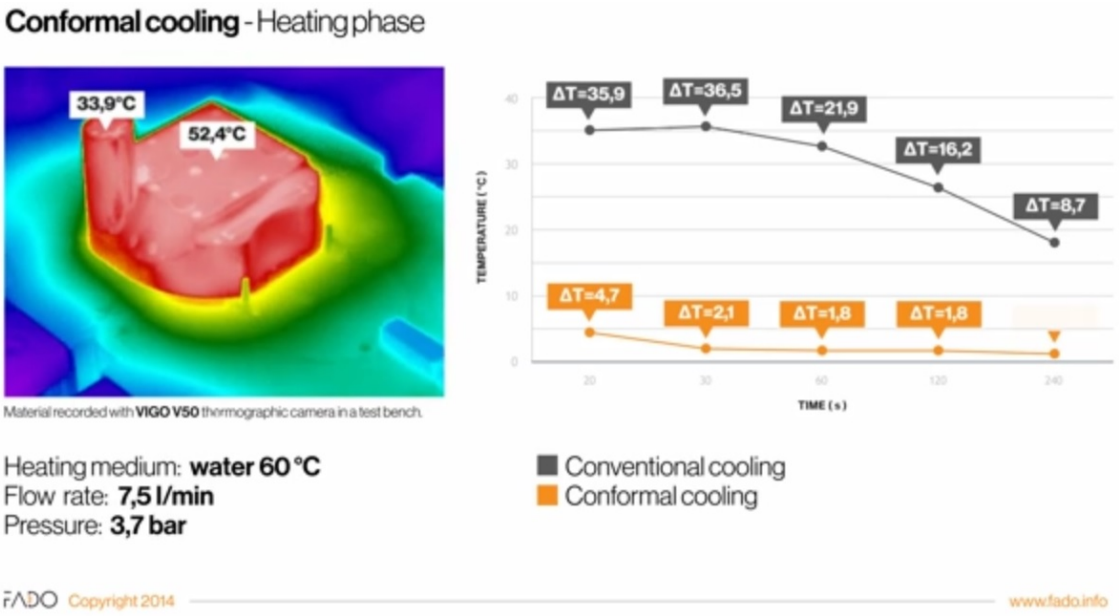


*Figure 11: Heat transfer during the heating phase. (http://www.eos.info/tooling)*

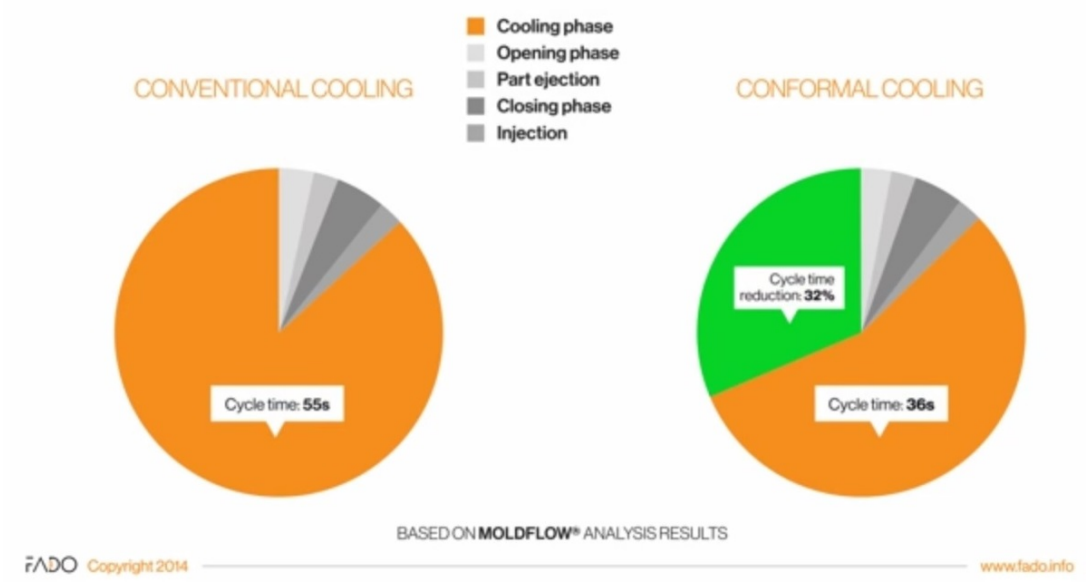


*Figure 12: Reduction in cycle time using conformal cooling. (http://www.eos.info/tooling)*

With reference to the design check list in Table 2 if applied to the design used in this case study, it is seen in Figure 13 that most of the design features, such as holes for ejector pins and cooling channels, have been included in the CAD design and were directly manufactured using DMLS, as shown in Figures 14 and 15.

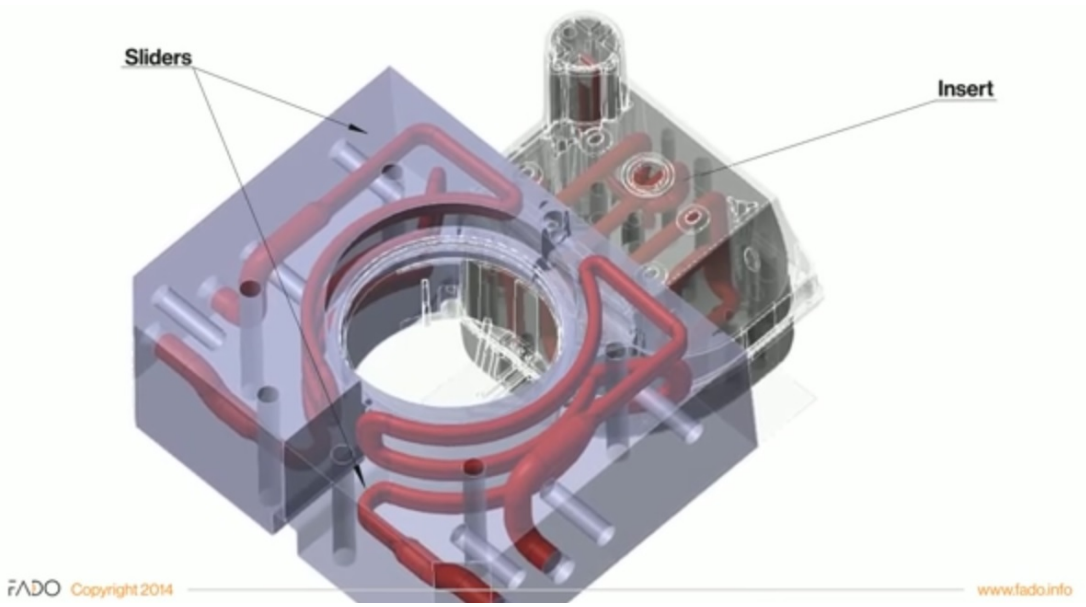


*Figure 13: CAD design of the mould showing design features. (http://www.eos.info/tooling)*

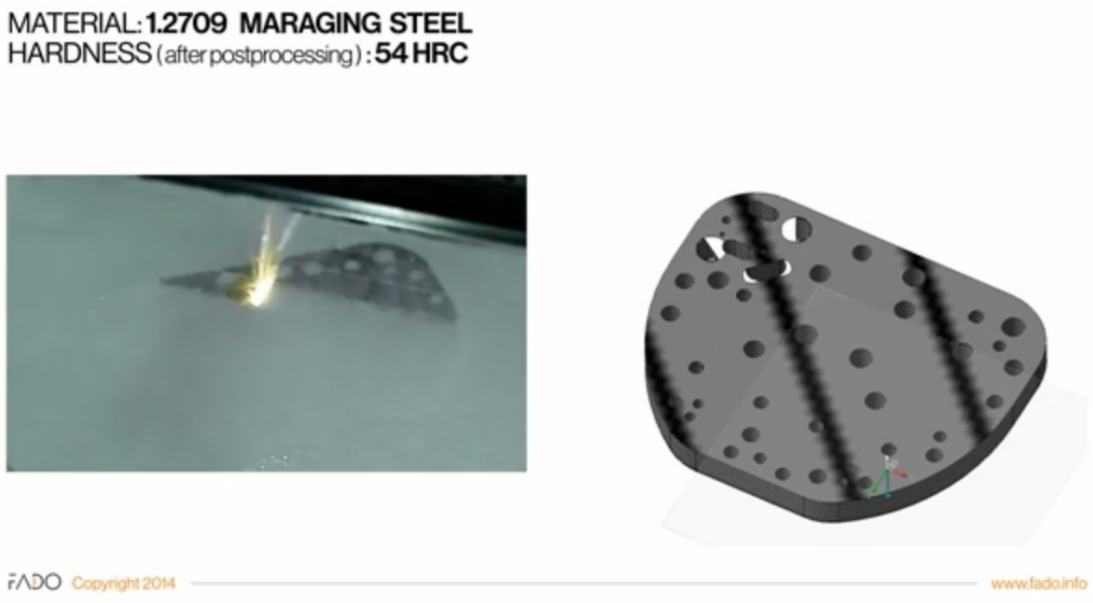


*Figure 14: DMLS manufacture of the mould insert showing the cooling channels and holes for the ejector pins. (http://www.eos.info/tooling)*

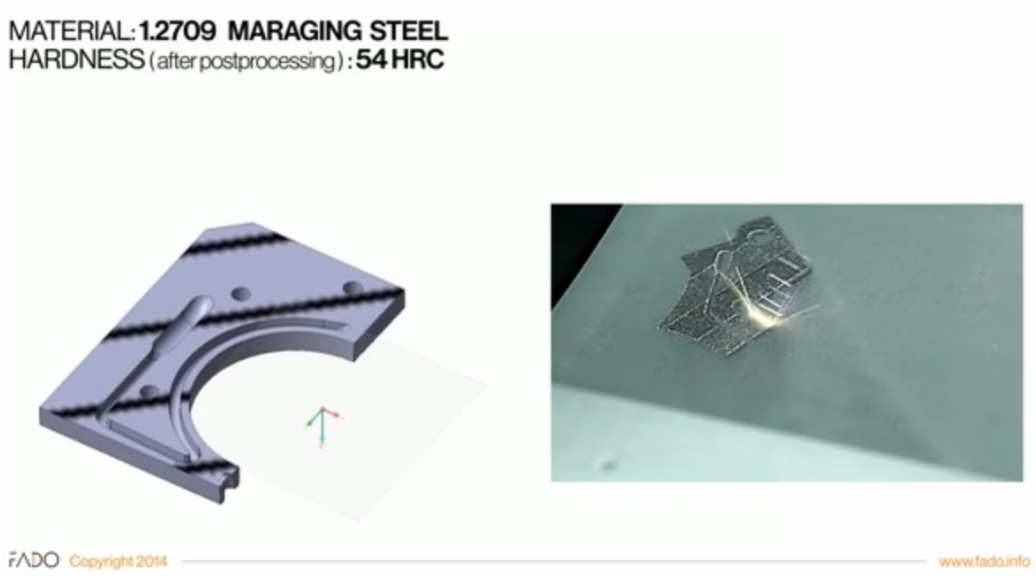


*Figure 15: DMLS manufacture of the mould slider showing the cooling channels and holes for ejector pins. (http://www.eos.info/tooling)*

When considering this case study, it is clear that there was a remarkable reduction in cycle time with the use of AM, which led to a more profitable IM tool; this in itself is a huge advantage for any IM company. Many technical advantages exist such as reduced use of time-consuming and costly CNC and EDM operations. The direct manufacture using AM allows companies to have a tool with geometrically complex aspects manufactured in a fraction of the time it would take to manufacture

using conventional methods. In addition, the ability to add conformal cooling could lead to significantly reduced production cycle times.

### 2.6.4 General additive manufacturing design rules

Table 3 shows a design check list for IM tool inserts manufactured using the DMLS process. This check list provides the designer with some basic design guidelines during the design process of IM tooling through AM. By making use of a case study, the application of the design check list in Table 3 can be demonstrated. FADO, established in 1984, is a tooling and IM company based in Bydgoszcz, Poland, that has made case studies available through the EOS website and is an official service provider for EOS' DMLS technology. One of their case studies is used here to demonstrate the application of the design guidelines in Table 3. As previously stated, the design for AM as a whole is mainly limited by the AM machine's capabilities (Samperi, 2014).

*Table 3: Summary of Design Rules*

| Design Rules for AM Tooling | |
|---|---|
| EPMA (European Powder Metallurgy Association) | |
| Design Rule | Parameters |
| Minimum wall thickness | 0.2 mm not self-supporting |
| Minimum hole diameter, perpendicular to z-axis | 0.4 mm<10mm without supports |
| Minimum strut diameter | 0.15 mm |
| Maximum H/L ratio | <8:1 without supports |
| Overhangs | $>45^0$ without supports |
| Surface finish | 25–40 μm as built |
| EOS | |
| Design Rule | Parameters |
| Minimum wall thickness | No data |
| Minimum hole diameter, perpendicular to z-axis | No data |
| Minimum strut diameter | 0.15 mm |

| | |
|---|---|
| Maximum H/L ratio | <6:1 without supports |
| Maximum D/L ration for pins | <1:2 without supports |
| Overhangs | >25$^0$ without supports |
| Stratasys | |
| Design Rule | Parameters |
| Minimum wall thickness | 1 mm |
| Minimum hole diameter, perpendicular to z-axis | No data |
| Minimum strut diameter | No data |
| Maximum W/L ratio | No data |
| Maximum D/L ration for pins | No data |
| Overhangs | >35$^0$ without supports |

These design rules give an idea of what is typically achievable by making use of the DMLS process. While not very clear, they provide a solid base to start developing a comprehensive set of rules to be used in the tooling industry as well as the AM industry at large. With the main focus being productivity and accuracy, designers can potentially apply AM design techniques to the design and manufacturing of tooling. This not only offers increased productivity in the IM industry but also allows for tools with complex geometries to be manufactured.

A concise set of guidelines have been set up by the European Powder Metallurgy Association (EPMA) specifically for designers and engineers (EPMA, 2015). These design guidelines are relevant for an SLM process such as DMLS only and are as follows:

- Holes and internal channels: it is recommended that a standard minimum hole size of 0.4 mm be used and a maximum hole size of 10 mm for a build direction which is perpendicular to the “z-axis” of the machine.
- For hole sizes with a diameter greater than 10 mm, support structures are needed, as shown in Figure 16 (a). These structures can be difficult to remove from non-linear channels. It is therefore suggested that the channel profile be modified in such a manner as illustrated in Figure 16 (b).

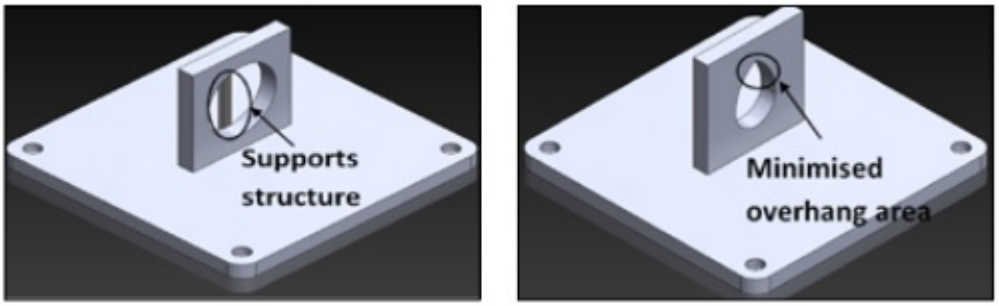


*(a)* *(b)*

*Figure 16: (a) Support structure used in a hole of diameter >10mm. (b) Modified profile to minimize use of support structures. (EPMA 2015)*

- Minimum wall thickness: generally prescribed as 0.2 mm, the minimum wall thickness of a part is dependent on the AM machine capabilities as well as the material used. Figure 17 shows the effect of buckling on a part which was manufactured with a very thin wall thickness. Although the part is fully dense, the part cannot support itself due to the thin wall structure. While this may not be applicable to tooling applications, it must be noted as an important guideline when designing products for AM.

*Figure 17: Thin-walled manifold showing signs of buckling due to thin walls. (EPMA 2015)*

- Maximum height-to-length ratio: it is recommended that the maximum height-to-length ratio does not exceed 8:1. However, if the part has a reasonable supporting structure, the height-to-length ratio may be increased.
- Minimum strut diameter and lattice structures: the minimum recommended strut diameter of 0.15 mm is easily achieved using AM technologies.

Lattice structures are used where weight reduction is an important feature without sacrificing on the strength of a product. This is very useful in the aerospace and automotive industries. Figure 18 shows how this is achieved.

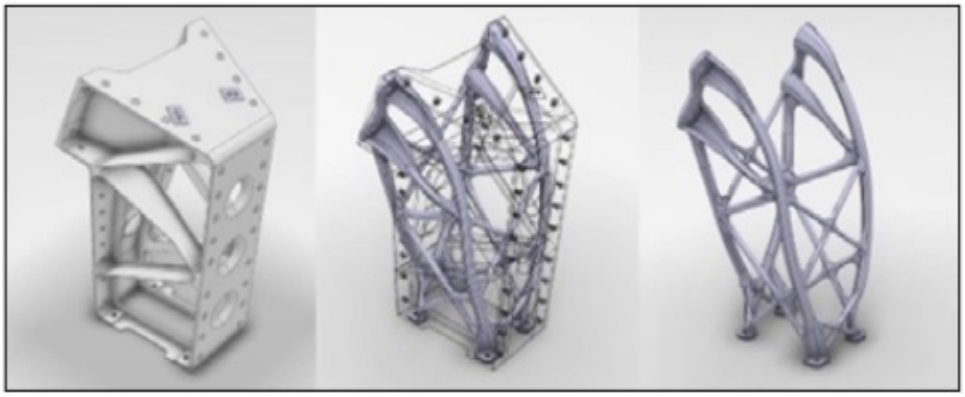

*Figure 18: The use of a lattice structure to reduce the weight of a product. (EPMA 2015)*

The idea of creating "literally anything" without any design limitations by making use of 3D printing is very appealing. It certainly begs an important question: "Are the parts truly functional and practical?" While the answer may be "yes" for fully aesthetic parts, when it comes to fully functional parts, then design rules becomes a necessity especially for specialized fields such as tooling, automotive and aerospace industries as well as the medical field. Table 3 (below) gives a summary of design rules as applied by some of the pioneering 3D printing companies (EPMA 2015, EOS 2014a, Schmid & Eidenschink 2014)

*Summary*

*Literature has shown that the cooling of IM tooling is crucial to the efficiency of the IM process, influencing the cycle time of the IM process as well as the quality of the parts produced. Tool designers have previously been limited to the capabilities of conventional manufacturing methods. While this is effective, the full potential of IM tool cooling systems is yet to be unlocked through the use of AM processes. While certain limitations exist in the design for AM, designers are no longer bound by stringent limitations placed upon them by manufacturing processes. The use of AM in the IM industry has proven to be effective by enhancing the moulds in terms of cooling as well as the use of intricate shapes which are difficult to achieve using conventional machining methods. Despite this, the detailed design guidelines followed are still a closely guarded "trade secret", or proprietary knowledge, and certain standardized more detailed guidelines should be established. By refining design rules for AM specifically for application in the tooling sector, designers will be able to produce sustainable products which will maximize their economic and social impact while reducing any harmful environmental impact caused by waste material, such as cuttings and swarf.*

# Chapter 3

## Research Approach and Methodology

*A presentation of the specific procedures used to generate data that was analyzed and critically evaluated to define the required design rules.*

---

### 3.1 Research Approach

Due to the industry-specific nature of this study, a letter was sent out to the industry inviting companies involved in the plastic IM industry to play a part in this study. This allowed for direct input from industry players in order to gauge the industry needs in terms of pushing the boundaries of tool design. By utilizing feedback from the industry, this study was easily accessible and understood by both tool designers and manufacturers. Site visits were conducted at two companies where IM tools were selected as case studies.

The limitations set out for this study required the use of cooling channels having a circular cross-section. Table 4, shows the selection process used for determining this cross-sectional limitation. The various cross-sections were rated according to the criteria highlighted in Table 4 and scored from 1 to 10 with 1 being the lowest rating and 10 being the highest. These ratings were based on data extracted from a SIGMASOFT® virtual moulding simulation.

*Table 4: Criteria for selecting channel shape to be used in this study.*

| Channel Shape | Heat Transfer | Structural Rigidity | Manufacturability | Average |
|---|---|---|---|---|
| 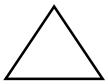 | 7 | 8 | 2 | 17 |
| 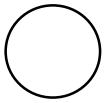 | 6 | 6 | 8 | 20 |
|  | 8 | 5 | 3 | 16 |
| 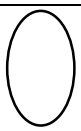 | 2 | 8 | 8 | 18 |

It was found that while a triangular cross-section provided sufficient cooling and structural rigidity, the need for support structures would be necessary during manufacturing, which is unfavourable when removing material during post-processing. It was also noted that stress concentrations manifested at the corners of channels having a triangular cross-section, which would ultimately lead to failure of the IM insert.

Inserts having an oval cross-section appeared to have sufficient heat transfer capabilities and average structural rigidity. However, these channels would require support structures if placed with the large radius perpendicular to the mould cavity surface. If channels having an oval cross-section were placed with the small radius perpendicular to the mould cavity surface, support structures would no longer be required. However, the cooling efficiency would be sacrificed.

While channels having a circular cross-section showed average heat transfer capabilities and structural rigidity, and the manufacturability was shown to be favourable. However, Table 3 shows that circular sections larger than 10 mm in diameter would require support structures during manufacturing.

Based on this comparison between the various cross-sections, it was decided to make use of channels having a circular cross-section.

## 3.2 Methodology

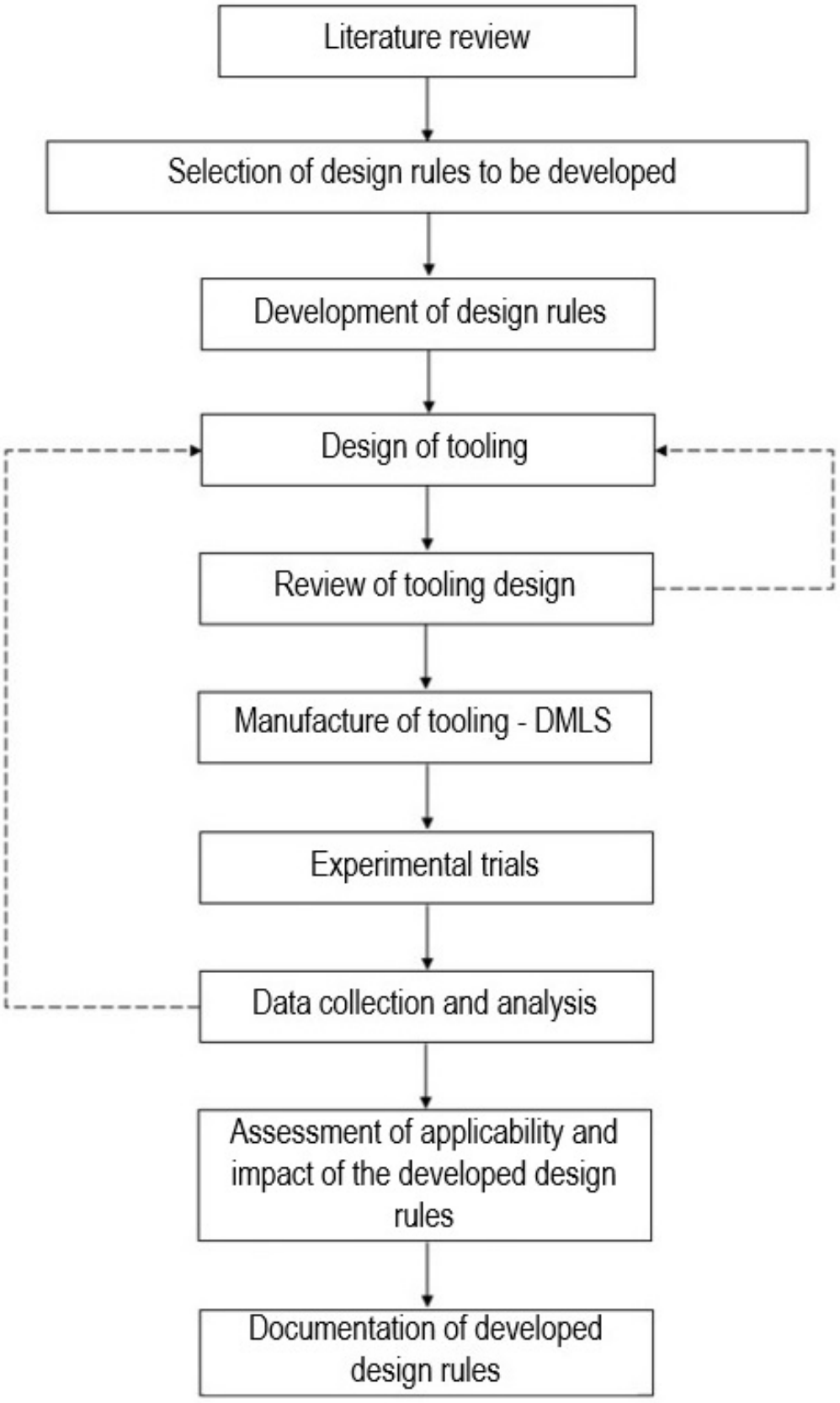


*Figure 19: A diagrammatic representation of the methodology used to refine design rules as applied to conformal cooling channels in IM tooling.*

### 3.2.1 Review and selection of appropriate design rules to be developed

Literature has shown that the greatest benefit offered by AM to the tooling industry is the production of conformal cooling channels through increased design freedom. It was, therefore, decided to enhance the cooling potential of IM tooling, through refining the design constraints for AM conformal cooling channels.

While this study focuses on the further development of design rules for AM conformal cooling channels, a valuable opportunity arose to develop and document a stress-relieving heat treatment process for MS1 components produced using AM. This was of importance since the tolerances required to fit tooling inserts are quite high.

### 3.2.2 Development of design rules

Through a combination of calculations, FEA-based simulation, experimental trials and 3D-scanning techniques, conformal cooling channel design rules were developed and refined, based on existing cooling channel design constraints.

The stress-relieving heat treatment was developed through an iterative process of heat treatments, hardness measurements and 3D-scanning techniques.

### 3.2.3 Design of IM tooling

By applying the developed design rules, IM tooling was designed using SolidWorks CAD software.

### 3.2.4 Tool design analysis & review

The tool design was reviewed and analyzed through the use of the Finite Element Analysis (FEA)-based virtual moulding software SIGMASOFT®.

### 3.2.5 Manufacture of tool using DMLS

Using maraging steel powder (MS1) as a feedstock material for the DMLS process, the tooling inserts were manufactured on an EOSINT M280 DMLS machine. Post-processing for final surface finishing was done using conventional machining techniques such as milling and surface grinding.

### 3.2.6 Experimental trials of tooling

The finished toolset was tested at Hanren Precision Engineering, using a HAIXING HX268 IM machine, with a rated clamping capacity of 270 tons. 150 moulding cycles were successfully completed.

### 3.2.7 Data collection and analyses

Data was collected from the end products and analyzed for any discrepancies from the refined design rules. Focus was placed on determining any deformation along the mould cavity surface, as this served as an indication of the extent of success achieved with the refined design rules.

### 3.2.8 Assessment of the applicability and impact of the developed design rules

The applicability and impact of the refined design rules were assessed and documented according to any observed deformation of the mould cavity. This was both visually inspected and scanned using 3D-scanning techniques to determine if any deformation had occurred. This was further assessed through an experimental comparison of the cycle time achieved between a conventionally produced toolset and an AM produced toolset.

## 3.3 Refinement of Design Constraints

### 3.3.1 Material property determination

In order to verify the material strength specifications of the powder supplier Electro-Optical Systems (EOS) GmbH, mechanical tests were performed on six test specimens, which were built on an EOSINT M280 DMLS machine that was serviced and calibrated according to EOS specifications. Of the six samples, three were in an as-built state and three were stress-relieved and age-hardened. In order to gain further insight into the mechanical test results, optical microscopy was conducted on cross-sections of the specimens. The specimens were mounted, polished and etched with a 10% Nital solution, whereafter the optical microscopy was performed using an Axioskop optical microscope using various magnifications. Further microscopy was performed using a JEOL scanning electron microscope (SEM). Energy-dispersive X-ray spectroscopy (EDS) was conducted on an age-hardened specimen to allow for further understanding of the microstructure. The data collected was then compared with the data sheet provided by EOS. This process is shown in Figure 20.

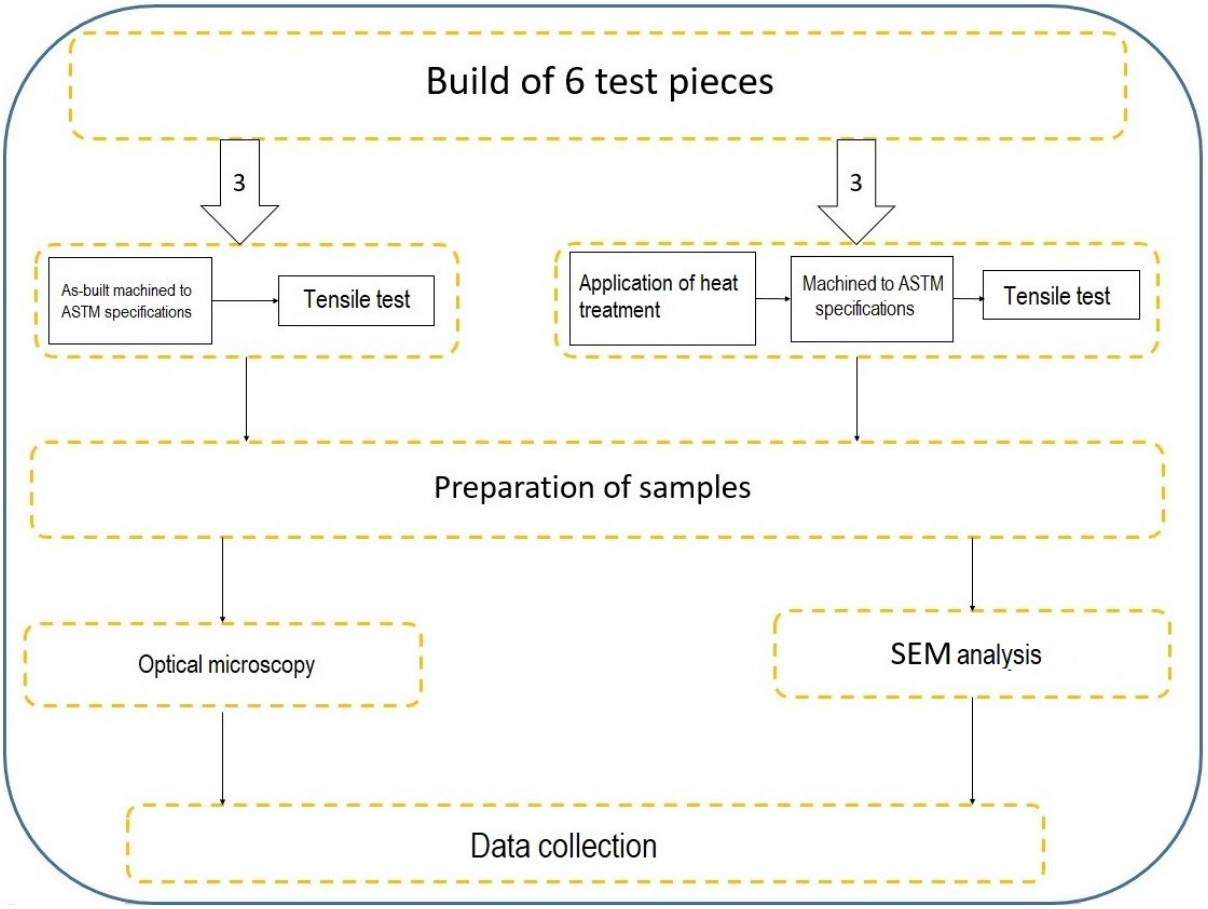


*Figure 20: Process for the material property determination of the test specimens.*

### 3.3.2 Development of a stress-relieving heat treatment

Due to the high tolerances required when fitting an IM tool insert into a cavity of a pre-machined bolster, a major concern was the geometric deviation of the DMLS insert from the CAD geometry due to residual stresses induced during the DMLS process. Since heat treatment of metals is usually applied to alter the microstructure of the metal, a stress-relieving heat treatment was developed to allow for the induced residual stresses to be relieved. Furthermore, the stress-relieving heat treatment would lead to lower hardness and easier machinability of MS1 inserts, thereby enhancing the post-processing of IM inserts. Figure 21 shows the steps followed in the development of the stress-relieving heat treatment.

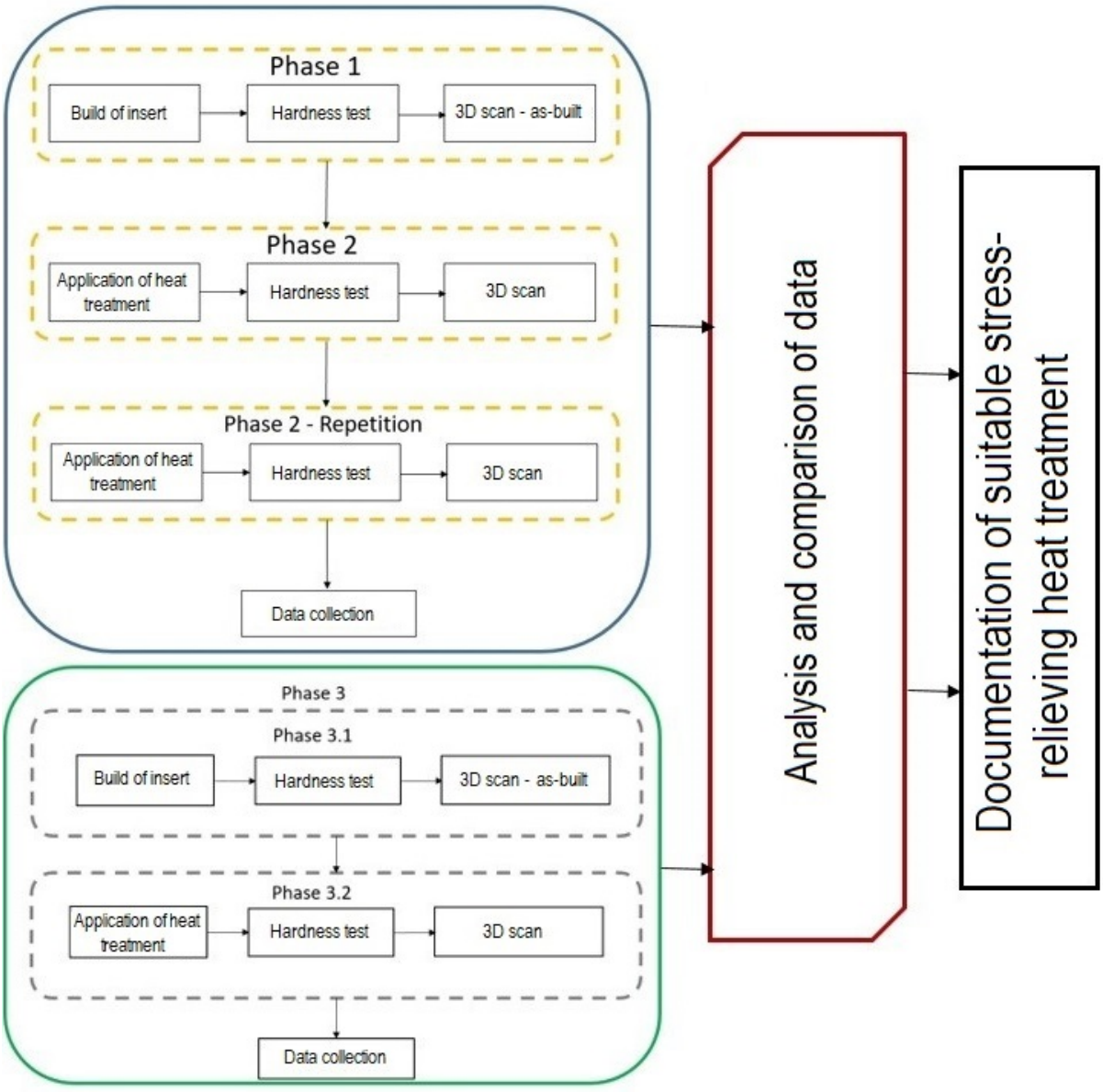


*Figure 21: Stress-relieving heat treatment process development for SLM parts built from MS1 powder.*

In Phase 1 of the investigation, the as-built fixed half of the IM tool insert was cut from the build platform, its hardness was determined and it was scanned using a Kreon Ace arm and a Solano Blue 3D scanner having a tolerance of ± 50 µm. The scanned data was compared to the CAD model of the insert and a deviation of the as-built insert from the CAD geometry was observed. For this comparison, eight points were selected on the tool insert geometry, as shown in Figure 22. For comparison purposes these same data points were used for each insert and the average of the eight data points was calculated to quantify the deviation of the IM tool insert from the CAD model.

The yellow colour shown on the scan data in Figure 22 indicates a deviation from the CAD geometry in the positive Z-axis and the blue indicates a deviation in the negative Z-axis, whereas the green

colour indicates a match with the CAD geometry. The actual deviation from the CAD design at each of these points is also shown. Dz is the deviation along the Z axis, which is the axis perpendicular to the plane of the build platform (the X-Y plane).

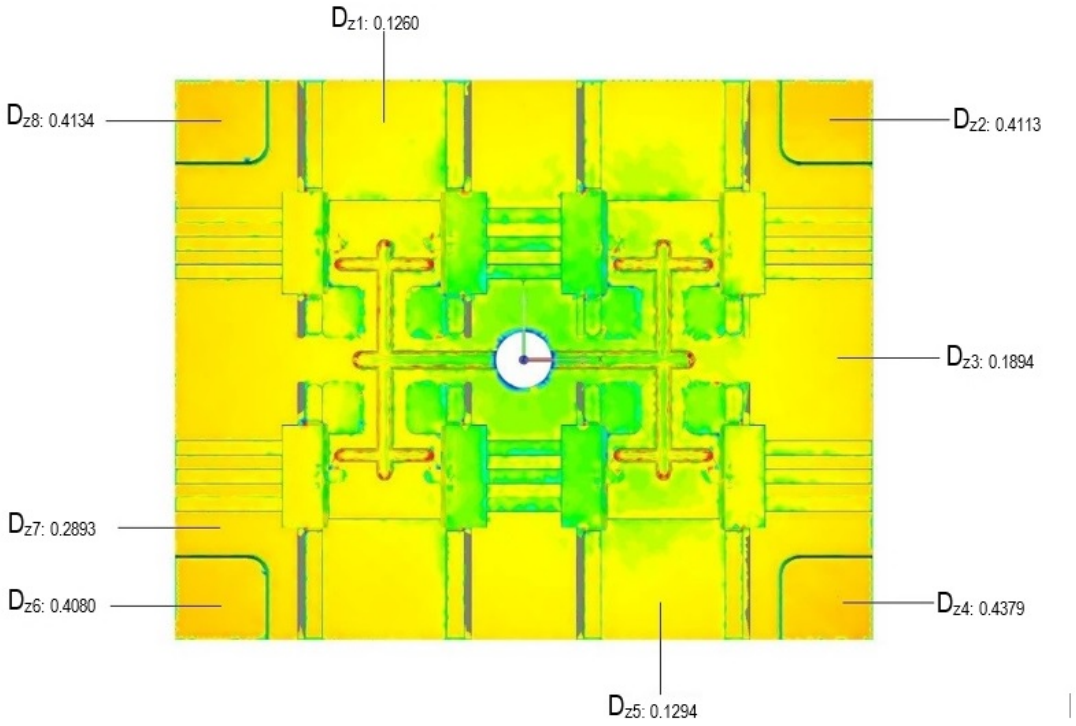


*Figure 22: Location of the 3D-scanned geometry comparison points used on all the inserts.*

Phase 2 describes the initial heat treatment applied to try to eliminate the geometric deviation found in Phase 1. During this phase, the insert that had already been removed from the build platform was heated to a temperature of 890 °C, soaked for a period of one hour and two minutes and allowed to air cool to room temperature. Thereafter, the hardness was measured and the insert was scanned in order to determine the effects of the heat treatment. In order to determine the effect of an increased time at temperature on the IM tool insert, Phase 2 was subsequently repeated with an additional soaking time of one hour.

The results obtained in Phase 2 confirmed the need for a longer soaking at 890 °C, but also showed that a stress-relieving heat treatment after a part had already been cut from the build platform did not effectively prevent deformation of the part. This led to the approach followed in Phase 3.

During Phase 3, the moving half of the IM tool insert was scanned while still attached to the build platform and its hardness was measured. Thereafter, the insert, while attached to the build platform, was subjected to a heat treatment at 890 °C for a soaking period of three hours. Subsequently, the insert was again scanned while still attached to the build platform and its hardness was measured.

Finally, after the insert was cut from the build plate, it was again 3D-scanned and its hardness was measured.

## 3.4 Conformal Cooling Channel Design

### 3.4.1 Design for mould strength

The cooling of IM tooling is crucial to the performance of the toolset, influencing the rate of the IM process as well as the quality of the parts produced. Tool designers have always been limited to the capabilities of conventional manufacturing methods and, while this is effective, the full potential of IM cooling systems is yet to be unlocked.

With the introduction of AM to the IM manufacturing environment, tool designers now have freedom of design which allows for the use of conformal cooling channels which follow the contours of the part, thereby increasing the cooling potential. Not only are designers able to place cooling channels in "hard-to-reach" parts of the IM tool, but cooling channels can also be placed closer to the mould surface which further enhances the cooling efficiency (Rao and Schumacher, 2004). While this is theoretically perfect, certain physical limitations exist, such as the strength of the mould material, which sets a limit for the distance $x_m$ between the cooling channel and the mould surface.

A series of theoretical calculations were performed in order to determine a minimum value for $x_m$ at which the mould material would deform under an applied injection pressure. Based on these values, an acceptable value for $x_m$ was documented. A simple part of 50 mm length, 30 mm width and thickness of 2 mm, was designed to verify this minimum value of $x_m$ through a practical experiment as well as through the use of SIGMASOFT® mould simulation software using the parameters set out in Table 5, further material properties are provided in Appendix 2, Table 23.

*Table 5: SIGMASOFT® simulation parameters used during the SIGMASOFT® simulations during the strength analysis of AM inserts*

| | |
|---|---|
| Mould material | Maraging steel |
| Part material | ABS |
| Injection pressure (MPa) | 140 |
| Mould temperature (°C) | 50 |
| Coolant temperature (°C) | 20 |
| Injection Moulding cycles | 20 |

Figure 23 below shows a view of the CAD design of the simple part.

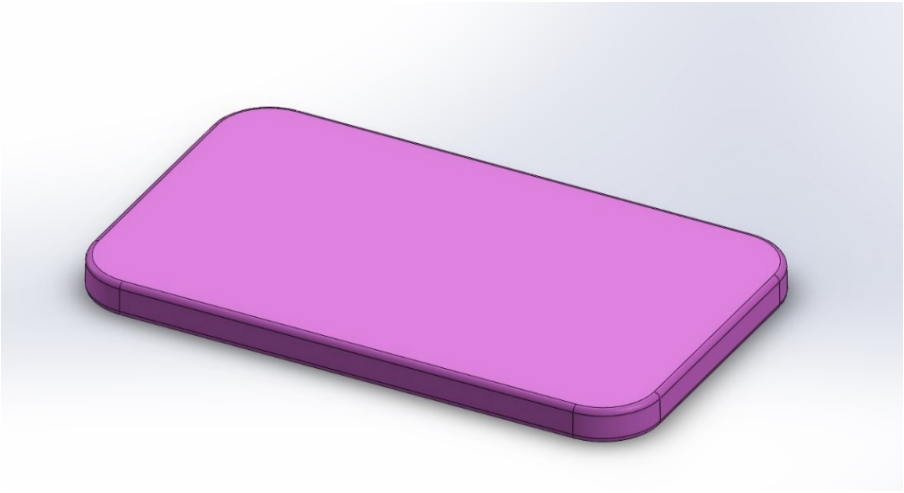

*Figure 23: CAD design of the part used in the mould strength IM trials.*

IM trial inserts were manufactured using DMLS technology. These inserts contained circular cooling channels having hydraulic diameters $D_H$ of 4 mm and 8 mm, respectively. Figure 24 shows a representation of the IM trial inserts. A detailed CAD drawing of the mould strength test insert mould is shown in Figure 53 as provided in Appendix 2.

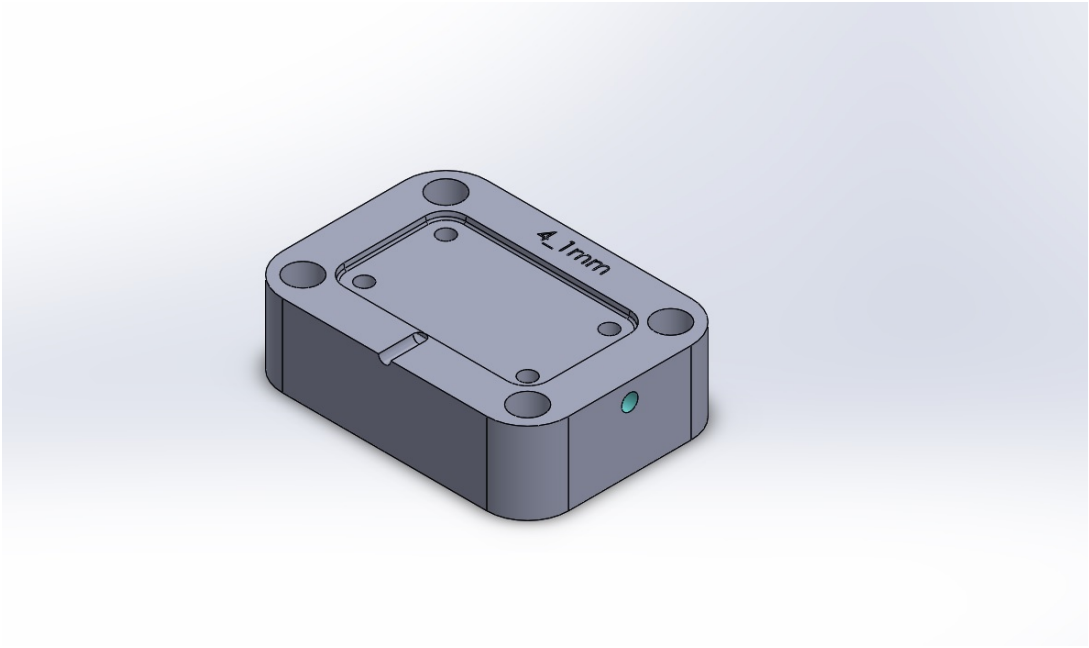


*Figure 24: CAD design of the IM trial insert with 4 mm channel.*

The IM inserts were then assembled into a pre-machined bolster, as presented in Figure 25, and experimental trials were conducted.

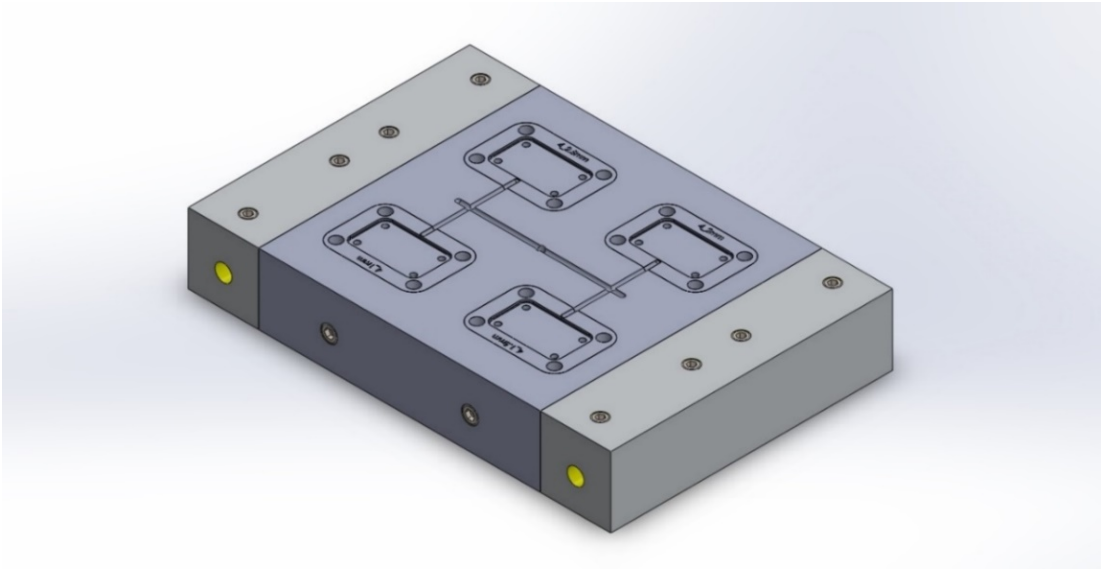

*Figure 25: Assembled IM tooling bolster with inserts for a 4 mm diameter hydraulic cooling channel.*

The IM inserts produced using the DMLS process are shown in Figures 26 to 29.

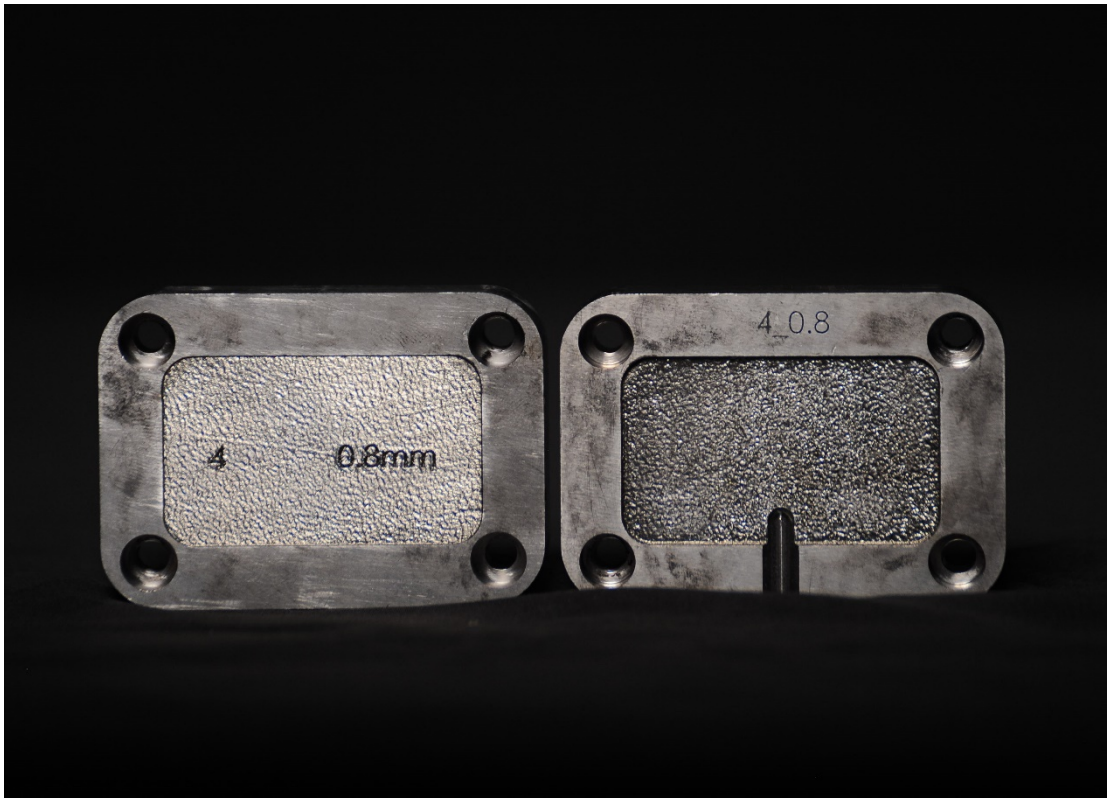


*Figure 26: Inserts having a $D_H$ of 4 mm and $x_m$ of 0.8 mm.*


*Figure 27: Inserts having a $D_H$ of 4 mm and $x_m$ of 1.5 mm.*

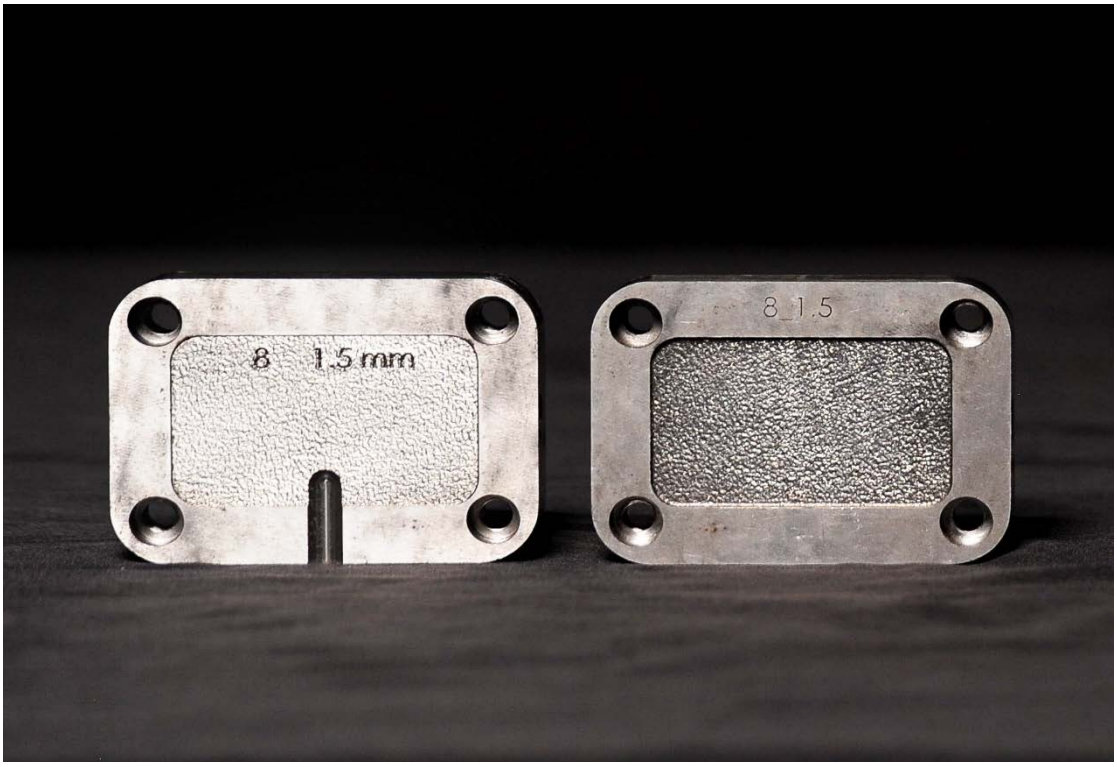


*Figure 28: Inserts having a $D_H$ of 8 mm and $x_m$ of 1.5 mm.*

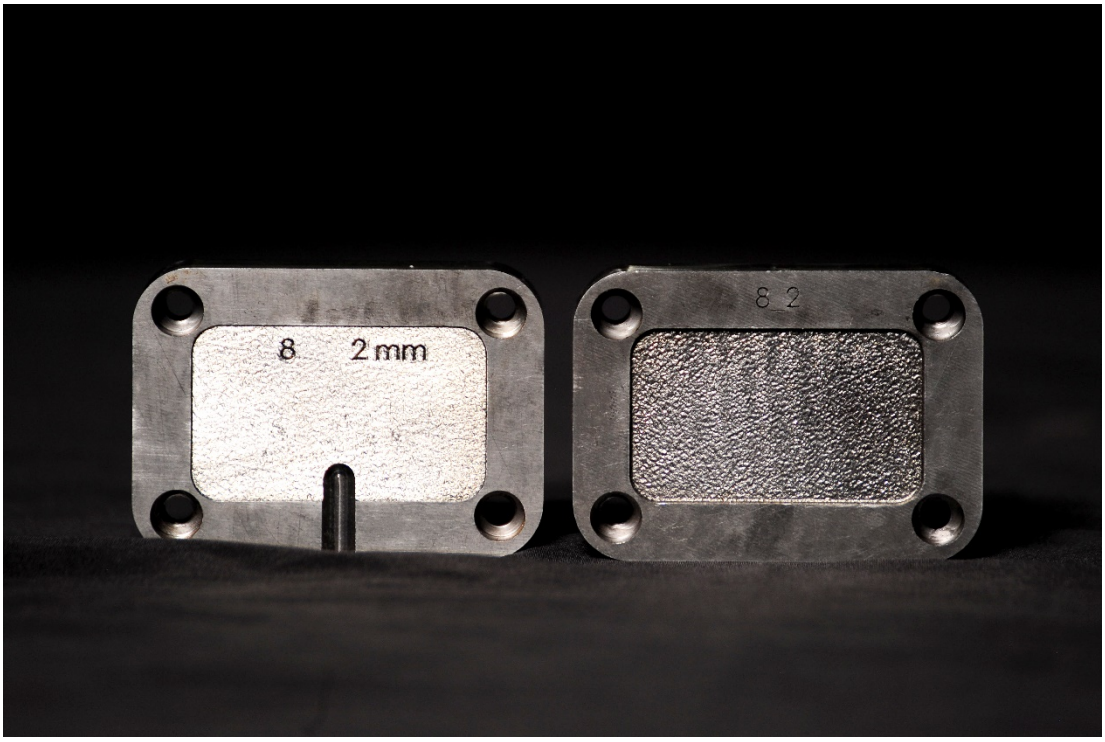


*Figure 29: Inserts having a $D_H$ of 8 mm and $x_m$ of 2 mm.*

Figure 30 shows the inserts before post-processing on the right-hand side and after final machining on the left-hand side of the figure.

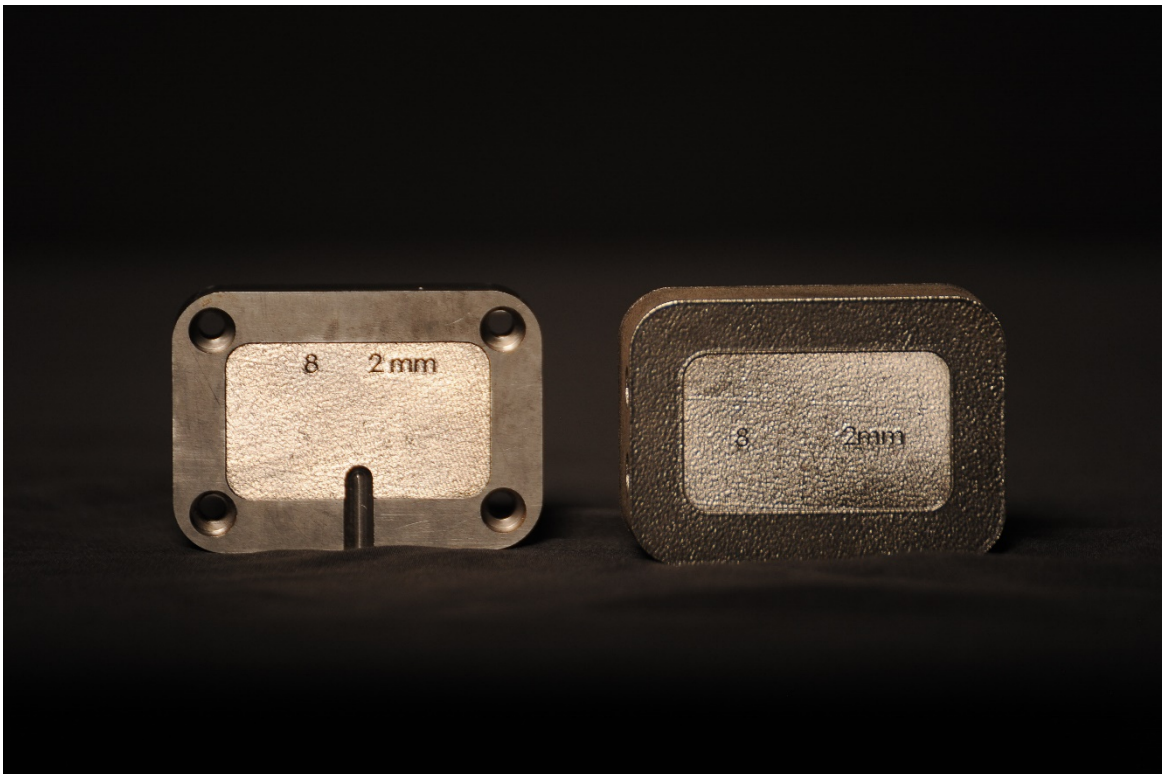


*Figure 30: The experimental insert after post-processing (left) and prior to post-processing (right).*

Experimental trials were conducted using a HAIXING HX268 IM machine, with a rated clamping capacity of 270 tons. The machine was operated at the maximum rated injection pressure of 140 MPa with a clamping pressure of 130 tons. Figure 31 shows the AM insert tooling assembly mounted onto the IM machine. Molten Polypropylene was injected into the inserts for a total of 100 cycles per insert. Upon removal from the toolset, the AM inserts were scanned using a Kreon Ace arm and a Solano Blue 3D scanner with a tolerance of ± 50 µm, in order to determine if any deformation had occurred.

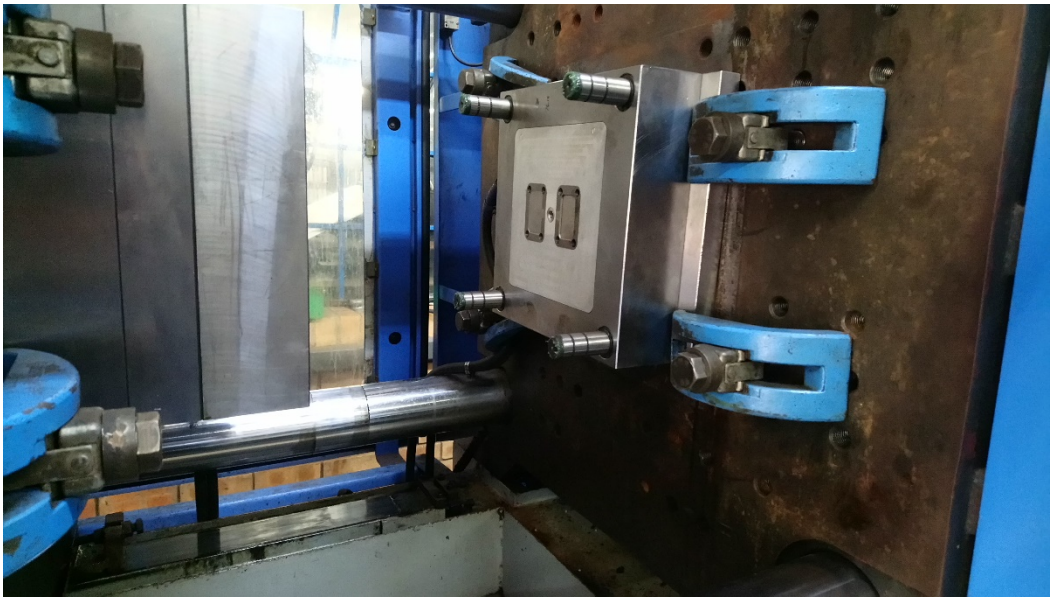

*Figure 31: AM insert tooling assembly mounted onto IM machine.*

### 3.4.2 Application of refined design rules

An even distribution of cooling in IM tooling plays an important part in the production of plastic components. With this in mind, a case study was conducted to compare conventional cooling channels and AM-produced conformal cooling channels. The comparison at this stage in the design process was via virtual moulding FEA-based simulations using SIGMASOFT® software using the simulation parameters set out in Table 6, further material properties are provided in Appendix 2, Tables 23 and 24.

*Table 6: SIGMASOFT® simulation parameters during the comparison between conventional and conformal cooling channels for an industrial case study*

| | |
|---|---|
| Mould material | Maraging steel |
| Part material | Polypropylene |
| Injection pressure (MPa) | 140 |
| Mould temperature (°C) | 50 |
| Coolant temperature (°C) | 20 |
| Injection Moulding cycles | 20 |

The intent with this case study was to obtain a better understanding of the heat flow in the mould cavity before production was carried out. This could provide tool designers with an indication of the financial impact the AM-produced mould would have compared to the current conventionally manufactured mould.

As seen in Figure 32 below, the original cooling channels provided limited cooling to the IM tool, and due to the excessive cyclic heating and cooling of the mould, fine features, circled in Figure 34, became brittle and broke. This resulted in the mould being continuously repaired or remanufactured, and consequently production came to a standstill.

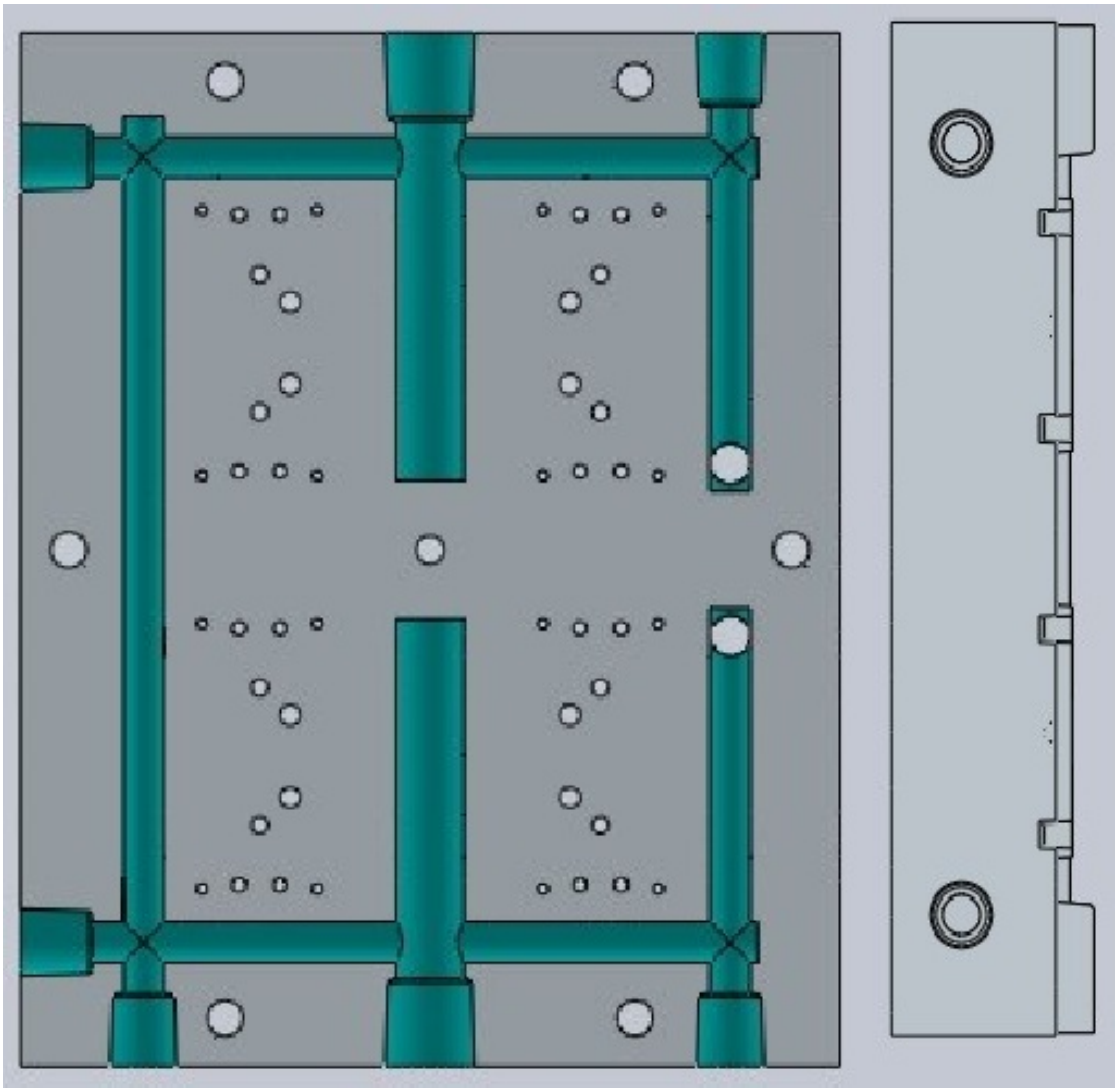

*Figure 32: Representation of the conventionally machined cooling channels.*

It was decided to make use of 6 mm (a) conformal cooling channels, as shown in Figure 33. Due to space constraints around the ejector pins, cooling channels with a diameter of 4 mm (b) and 3.5 mm (c), respectively, were designed. With the added design freedom of AM, it was possible to position the conformal cooling channels closer to the mould cavity.

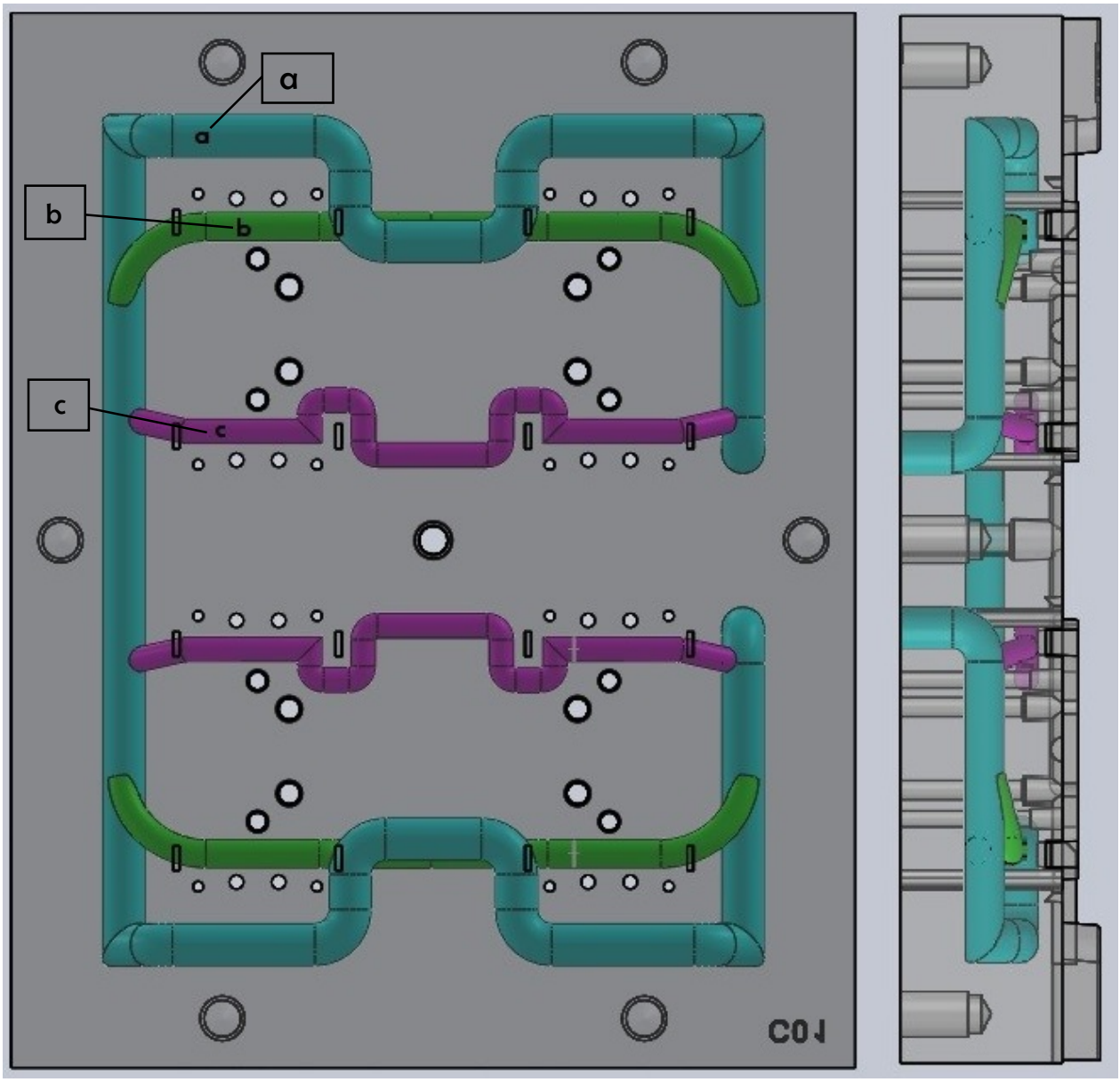


*Figure 33: Top view representing the conformal cooling channels.*

Figure 33 shows that conformal cooling channels could be beneficial to IM tools in the sense that the channels can be placed in such a manner that they provide cooling to areas of the mould which are restricted due to features such as ejector pin holes. Detailed CAD drawings of the Altech-UEC mould are shown in Appendix 2 as Figures 51 and 52, while Figure 54 highlights the dimensions of the moulded part.

Figure 34 shows the DMLS-produced insert in an as-built state. The circled area indicates one of the main areas which were prone to embrittlement as a result of poor cooling.

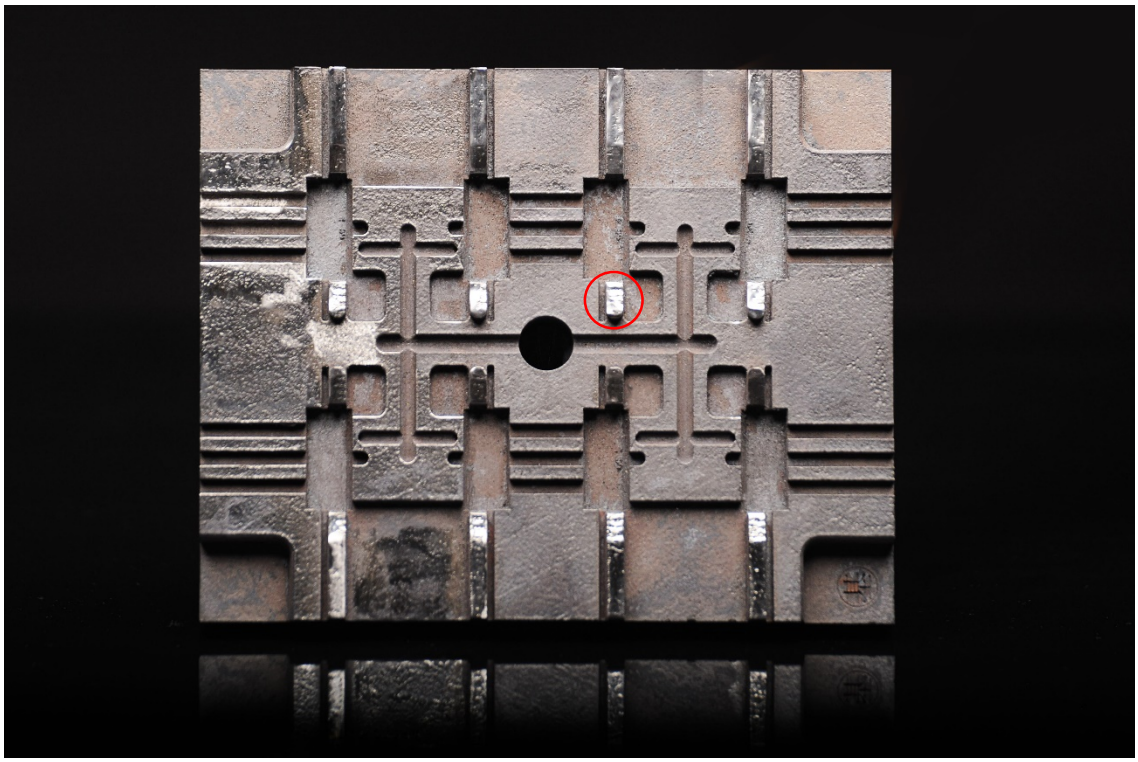

*Figure 34: The DMLS-produced insert in an as-built state, highlighting one of the areas prone to embrittlement.*

Practical comparison trials were conducted on the Altech-UEC IM toolset using a HAIXING HX268 IM machine, with a rated clamping capacity of 270 tons. The machine was operated at an injection pressure of 30 MPa with a clamping pressure of 130 tons. Molten Polypropylene was injected into the inserts for a total of 150 IM cycles.

*Summary*

*The experiments performed in this study have served to pave the way towards achieving the aim and objectives of the study. By combining CAD design, SIGMASOFT® FEA-based simulation techniques, microscopy techniques and practical experiments, the following investigations were carried out:*

- *Material comparison between supplier data and experimental data;*
- *Development of a stress-relieving heat treatment for maraging steel components produced using the DMLS process;*
- *Determination of a minimum safe distance between the cooling channel and the mould cavity surface;*
- *Practical comparison between an IM tool having conformal cooling channels and an IM tool having conventionally machined channels.*

# Chapter 4

## Results & Discussion

*Presentation, analysis and discussion of the information gathered through the experimental approach and methodology adopted for this study.*

---

### 4.1 Industry Response

The research approach used in this study prompted an interaction with the IM industry, which led to a positive reaction towards AM from players in the IM industry. Altech-UEC, a company which produces electronic devices, allowed the use of a complex IM tool that contained fine features with cooling restrictions. This allowed the use of AM to optimize the cooling of this specific IM tool as well as to determine the impact AM-produced IM tools could have on productivity.

#### 4.1.1 Review of design constraints and selection of appropriate design rules to be developed

Existing design constraints were reviewed and it was found that they were very broad and vague with regard to what can be achieved in terms of functional tooling. While this is acceptable as a basic design guideline, these rules have to be further developed in order assist tool designers to generate complex tooling. Literature showed that the greatest benefit offered by AM to the tooling industry was the production of truly conformal cooling channels through design for AM freedom. Therefore, it was decided to enhance the cooling potential of IM tooling, which led to the following design rule being reviewed and developed further:

- Minimum wall thickness between the mould face and cooling channel.

In developing a design guideline for the minimum wall thickness between the mould face and cooling channel, material strength was an important factor; hence an investigation was conducted to verify the material data supplied by EOS through practical experimentation. Further insight into the material composition was gained through microscopy techniques.

While this study focused on the further development of design rules for conformal cooling channels, the stringent fitment tolerances required in the tooling industry gave rise to a valuable opportunity to

develop and document a stress-relieving heat treatment for maraging steel components produced using AM.

Furthermore, this refined design guideline was applied to an IM tool having conformal cooling channels which was produced using the DMLS process. The data extracted during practical trials was then compared to an identical IM tool having conventionally drilled cooling channels.

## 4.2 Refinement of Design Constraints

### 4.2.1 Material property comparison

Table 7 provides a comparison between the mechanical properties determined for the test specimens built through DMLS from MS1 powder and the data as specified by the supplier, EOS.

*Table 7: Comparison of the experimentally determined mechanical properties with the EOS data for as-built and age-hardened specimens*

| *As-built* | *EOS* | *Test Samples* |
|---|---|---|
| Yield Strength (MPa) | 1100 ± 100 | 1022 ± 35.35 |
| Ultimate Tensile Strength (MPa) | 1100 ± 100 | 1161 ± 20.41 |
| Young's modulus (GPa) | 180 ± 20 | 168 ± 2.026 |
| % elongation at break | 8% ± 3% | 7.33% ± 3.65% |
| *Age-hardened* | *EOS* | *Test Samples* |
| Yield Strength (MPa) | 1900 ± 100 | 1967 ± 10.02 |
| Ultimate Tensile Strength (MPa) | 1950 ±100 | 2031 ± 50.90 |
| Young's modulus (GPa) | 180 ± 20 | 189 ± 2.956 |
| % elongation at break | 2% ± 1% | 3.93% ± 2.797% |

The yield strength (YS) of the DMLS specimens in the as-built state was approximately 78 MPa lower than the EOS specification, while in the age-hardened state the YS was approximately 67 MPa higher than the EOS specification. The ultimate tensile strength (UTS) was 61 MPa higher than the EOS specification in the as-built state and 81 MPa higher in the age-hardened state. In the as-built state, the Young's modulus (E) was approximately 12 GPa lower than the specification, while in the age-hardened state it was approximately 9 GPa higher. However, given the measurement uncertainty shown in Table 5, the experimental values lie within the EOS specified range.

The microstructures shown in Figures 35 (a) and (b) highlight the microstructure of the test specimens in the as-built and age-hardened state, respectively. In the as-built state (Figure 35 (a)), a microstructure is presented which shows the typical DMLS layered tracks. In this microstructure it is evident that the metal powder fused thoroughly and an almost parabolic edge characterized the

solidification pattern of each track of the molten powder. From this it can be deduced that each layer solidified on the underlying layer, with the laser tracks overlapping each other, thereby reducing any porosity (Yadroitsev, Krakhmalev & Yadroitsava, 2014) .

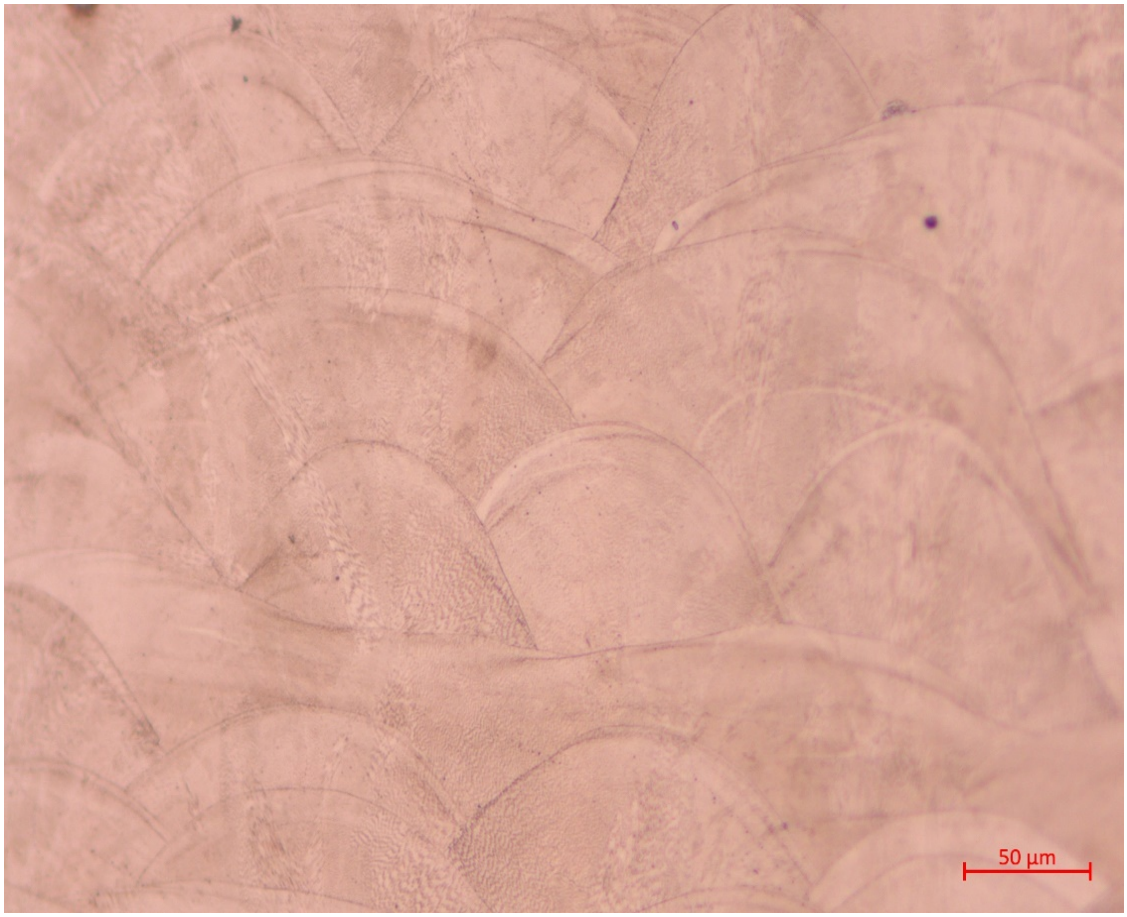


*a) Microstructure of maraging steel in the as-built state*

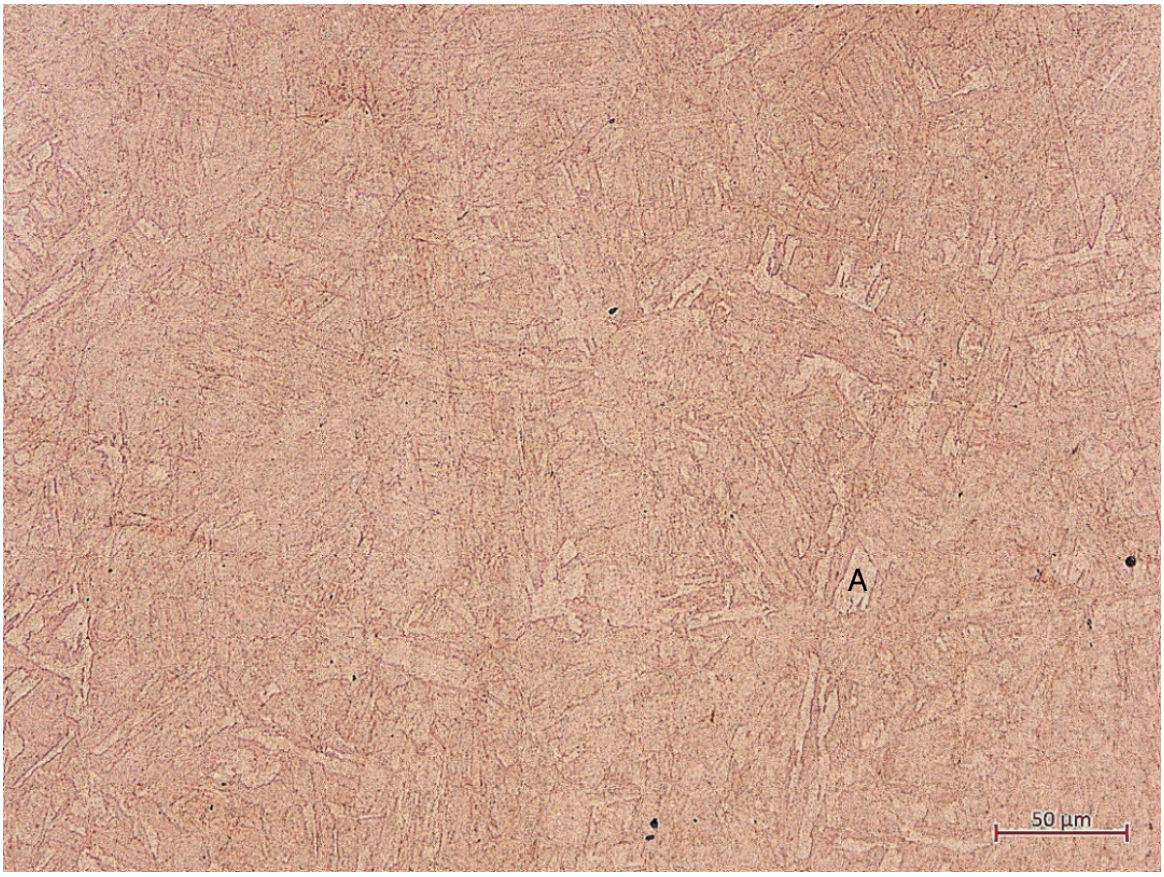


*b) (b) Microstructure of maraging steel after age-hardening*

*Figure 35: DMLS maraging steel (MS1) microstructure as seen through an optical microscope.*

Figure 35 (b), shows the microstructure in the age-hardened state in which the track boundaries shown in Figure 35 (a) are no longer visible and a more homogenous microstructure appears to have formed. This is as result of the stress-relieving annealing heat treatment which was performed prior to the age-hardening. In this treatment, the specimens were soaked at a temperature of 890°C for three hours.

Point A in Figure 35 (b) is a typical precipitate formed during the age-hardening process. Table 8 shows the material composition of this precipitate in the age-hardened state, which was analyzed using the EDS technique.

*Table 8: Material composition of a precipitate of the age-hardened DMLS MS1 sample.*

| *Elements* | *% wt* |
|---|---|
| Fe | 63.54 |
| Ni | 16.76 |
| Co | 9.38 |
| C | 5.71 |
| Mo | 3.8 |
| Ti | 0.83 |

From Table 8, it is evident that the detected percentages of Ni, Co, Mo and Ti confirm that this precipitate has a composition of 16Ni9Co4MoTi, which is typical of an age-hardened maraging steel (Thijs *et al.*, 1990). The 63.54 wt % Fe is from the surrounding steel matrix.

As expected from the age-hardening process, there is an increase in both the YS and UTS when comparing the as-built data with the age-hardened data. This is as a result of the hardening mechanism acting in the age-hardening process, whereby the material is hardened by the precipitation of intermetallic compounds during prolonged exposure to a temperature of 495 °C (Ahn, Park & Kim, 2010). An increase in Young's modulus to 189 GPa after applying the heat treatment was observed. This increase in Young's modulus is as a result of the formation of Ni3(Mo, Ti) precipitates, which restricts the homogenous distribution of nickel in the martensitic matrix (Kempen, Yasa, Thijs, Kruth, van Humbeeck., 2011). The decrease in ductility indicated by the increase in Young's modulus is further confirmed by the reduction of the percentage elongation from 7.33 % in the as-built state to 3.93 % in the age-hardened state.

Figure 36 shows typical SEM secondary electron images (SEIs) of the fracture surfaces of as-built and age-hardened DMLS MS1 tensile specimens. The as-built specimen, shown in Figure 36 (a), fractured after substantial plastic deformation in which the formation of dimples, typical of ductile fracture, is observed. Figure 36 (b) shows an SEM image of the fracture surface of the test sample which was age-hardened. On the latter fracture surface, microcavities are observed which are indicative of the presence of precipitates expected in the age-hardened metal.

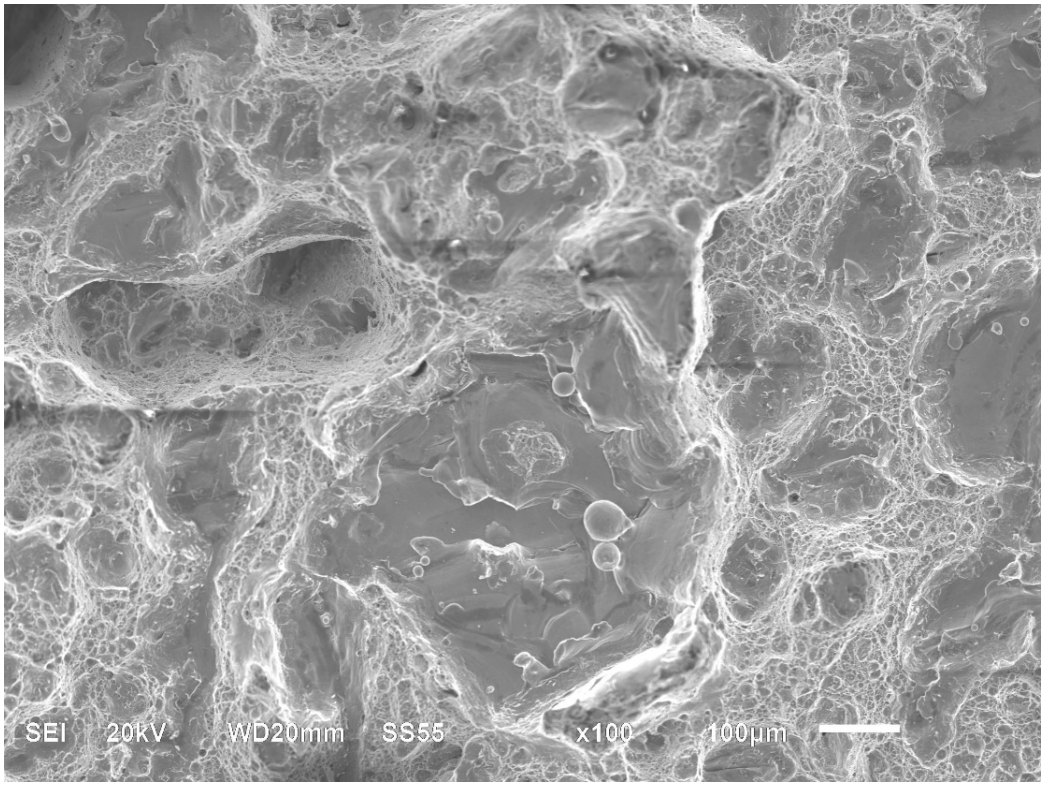


*(a) Ductile fracture in the as-built specimen.*

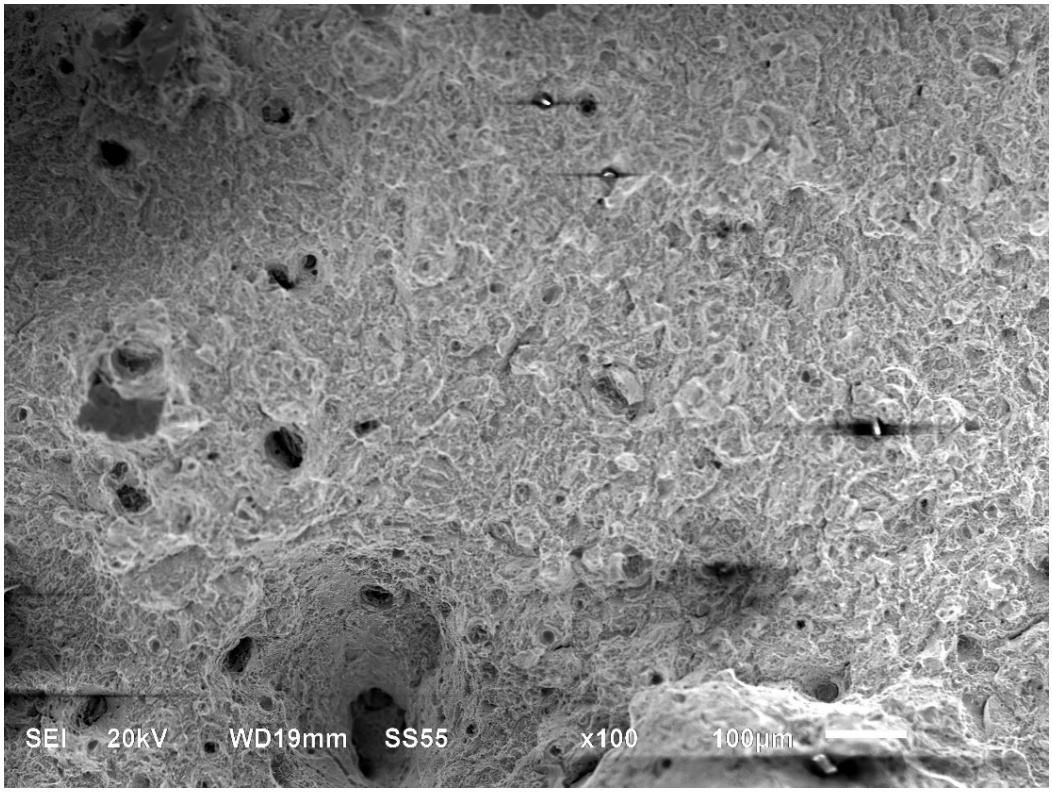


*(b) Inter- and trans-granular fracture in the age-hardened specimen.*

*Figure 36: SEI images of fracture surfaces of the DMLS MS1 as-built and age-hardened tensile specimens.*

Literature has shown that maraging steel is the preferred choice when the laser melting of high-strength components is required (Tiwari 2015). When comparing the results achieved through SEM and optical microscopy, it was found that the material composition is consistent with that of the material supplier as well as that found in literature (Kempen *et al.*, 2011).

### 4.2.2 Stress-relieving heat treatment

The phases used in the development of the stress-relieving heat treatment was discussed in detail in section 3.2.2, where Figure 19 shows the steps followed during the development process. Figure 37 shows the scan data obtained during Phase 1 from the insert as-built and cut from the platform, while Figures 38 and 39 show the scan data from Phase 2. The as-built insert displayed an average deviation over the eight measurement points from the CAD geometry of 0.154 ± 0.05 mm, which is due to the residual stress generated in the insert during the DMLS process. Its hardness was measured as 35 ± 0.5 HRC. The scan results obtained after the successive heat treatments applied during Phase 2 (see Figures 38 and 39) showed that the average deviation with respect to the CAD geometry increased to 0.225 ± 0.08 mm after the first heat treatment and further increased to 0.303 ± 0.05 mm after the second heat treatment. From the hardness measurements it was found that the metal softened after the first heat treatment to 31 ± 0.5 HRC and after the second heat treatment to 26 ± 0.5 HRC.

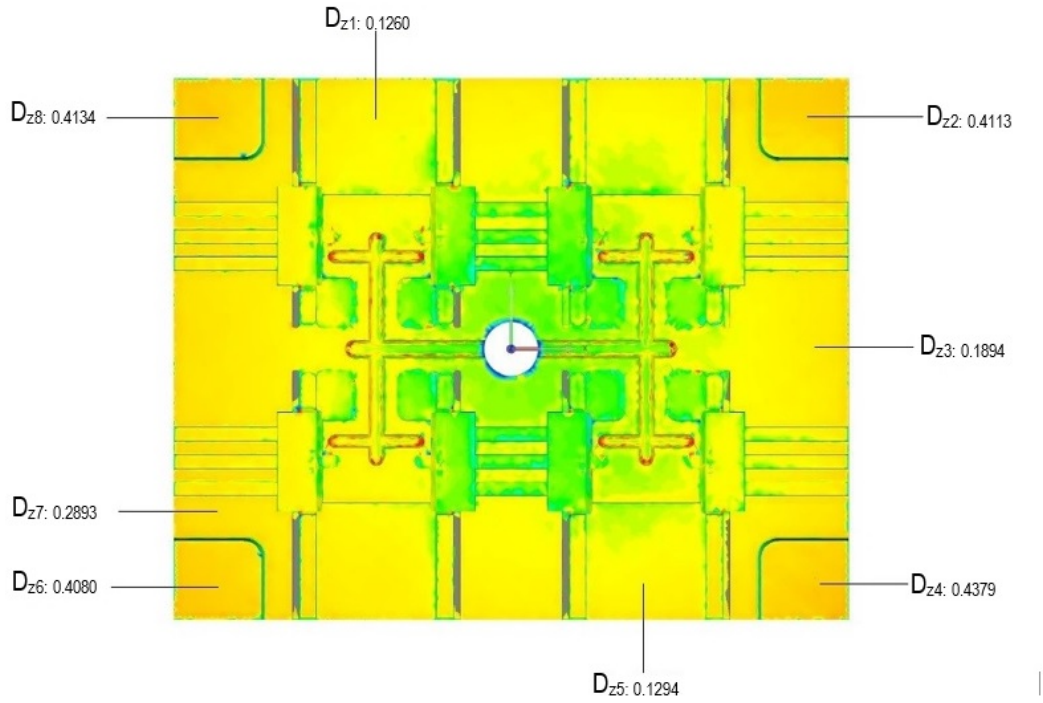


*Figure 37: Scan data from Phase 1, showing an initial average deviation of 0.154 mm after removal from the build platform.*

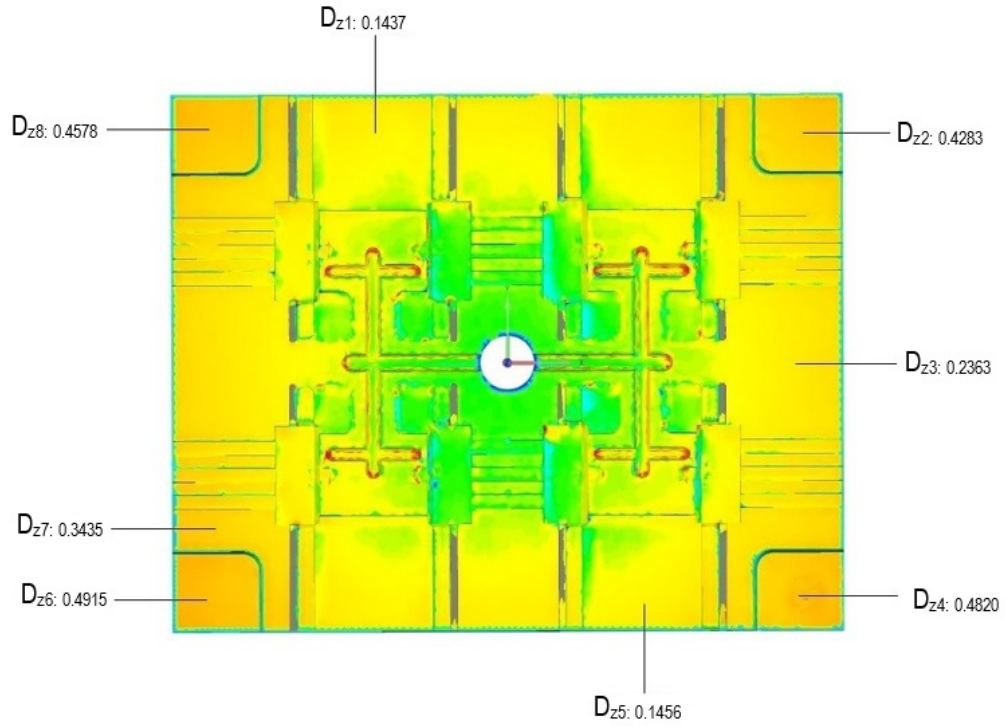


*Figure 38: Scan data from Phase 2 after the first heat treatment, showing an average deviation of 0.225 mm.*

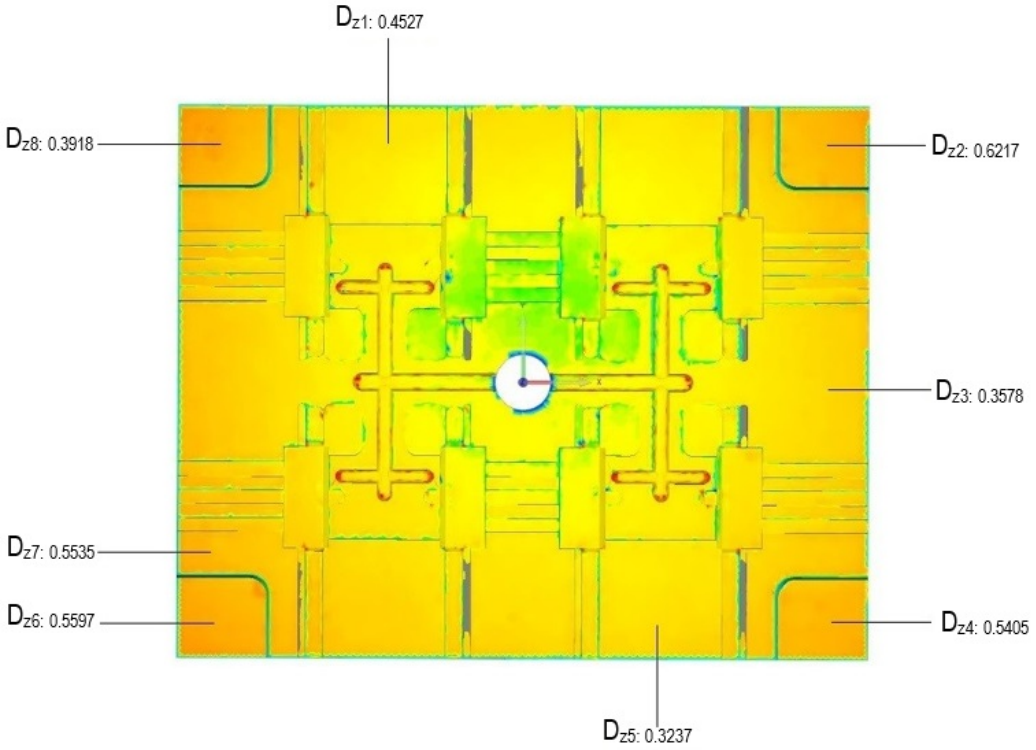


*Figure 39: Scan data from Phase 2 after the second heat treatment, showing an average deviation of 0.303 mm.*

Tables 9 and 10 give a summary of the scan results obtained from the experimental tests conducted during Phases 1 and 2.

*Table 9: Scan and hardness test results for Phase 1 after removal from the platform*

| Phase 1: Removed from platform | | |
|---|---|---|
| Heat treatment : None (As-built) | | |
| Deviation $D_z$ (mm) | | Hardness (HRC) |
| $D_{z1}$ | 0.1260 | 35 ± 0.5 |
| $D_{z2}$ | 0.4113 | |
| $D_{z3}$ | 0.1894 | |
| $D_{z4}$ | 0.4379 | |
| $D_{z5}$ | 0.1294 | |
| $D_{z6}$ | 0.4080 | |
| $D_{z7}$ | 0.2893 | |
| $D_{z8}$ | 0.4134 | |
| Average $D_z$ | 0.154 ±0.05 | |

*Table 10: Scan and hardness test results for Phase 2 after removal from the platform*

| Phase 2: Removed from platform | | |
|---|---|---|
| Heat treatment: 62 min at 890 °C | | |
| Deviation $D_z$ (mm) | | Hardness (HRC) |
| $D_{z1}$ | 0.1437 | 31 ± 0.5 |
| $D_{z2}$ | 0.4283 | |
| $D_{z3}$ | 0.2363 | |
| $D_{z4}$ | 0.4820 | |
| $D_{z5}$ | 0.1456 | |
| $D_{z6}$ | 0.4915 | |
| $D_{z7}$ | 0.3435 | |
| $D_{z8}$ | 0.4578 | |
| Average $D_z$ | 0.225 ±0.08 | |
| Heat treatment: 60 min at 890 °C | | |
| Deviation $D_z$ (mm) | | Hardness (HRC) |
| $D_{z1}$ | 0.4527 | 26 ± 0.5 |
| $D_{z2}$ | 0.6217 | |
| $D_{z3}$ | 0.3578 | |
| $D_{z4}$ | 0.5405 | |
| $D_{z5}$ | 0.3237 | |
| $D_{z6}$ | 0.5597 | |
| $D_{z7}$ | 0.5535 | |
| $D_{z8}$ | 0.3918 | |
| Average $D_z$ | 0.303 ± 0.05 | |

From the Phase 1 and 2 results shown in Tables 9 and 10, it is clear that stress-relieving heat treatments on the insert that was already removed from the build platform did not result in recovery

of its shape to comply better with the CAD geometry. In fact, the deviation increased with the heat treatments applied during Phase 2, as shown in Figures 38 and 39. This indicates that the residual stress induced in the insert during DMLS was of such magnitude that it caused some extent of plastic deformation of the insert which was retained once it was cut from the build platform. This plastic deformation could not be reversed during subsequent heat treatments. However, it was encouraging to find that the heat treatments applied in Phase 2 led to softening of the metal and did not result in age-hardening.

Figures 40 and 41 show the scanned geometry found in Phase 3. Clearly, the stress-relieving heat treatment applied to this insert while still attached to the build platform was effective and provided an un-deformed insert after removing it from the platform.

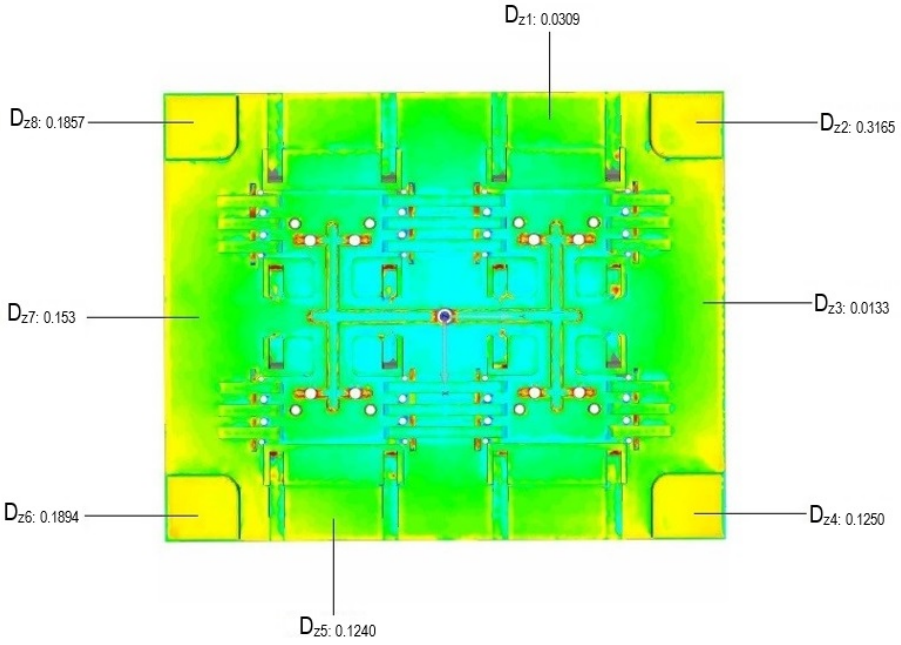


*Figure 40: Scan data of Phase 3, showing an initial average deviation of 0.07mm while attached to the build platform.*

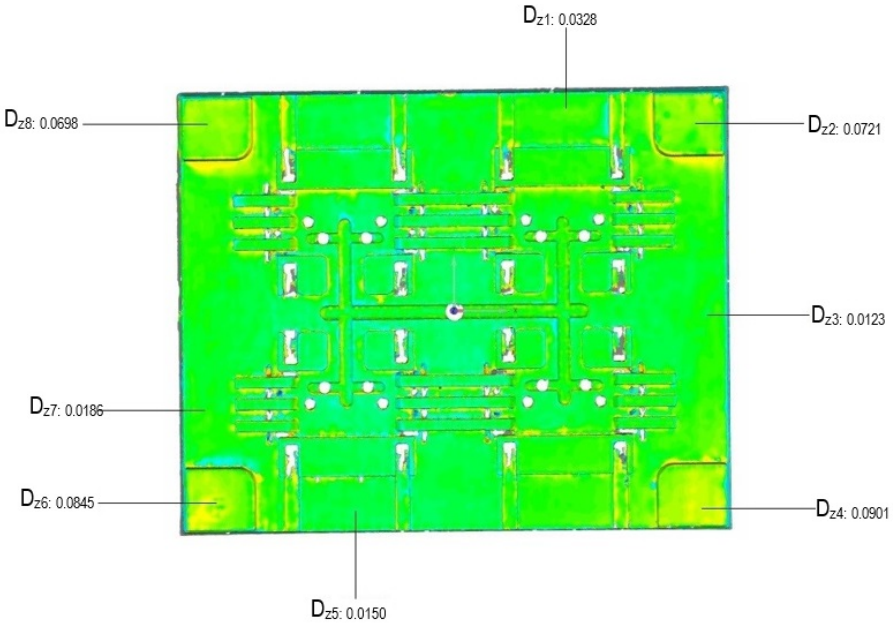


*Figure 41: Scan data of Phase 3 after stress-relieving heat treatment, showing an average deviation of 0.05mm after removal from the build platform.*

Table 11 gives a summary of the test results obtained from the various scans and hardness tests conducted in Phase 3.

*Table 11: Scan and hardness test results for Phase 3 while attached to the platform*

| Phase 3: Attached to platform | | |
|---|---|---|
| Heat treatment: None (As-built) | | |
| Deviation $D_z$ (mm) | | Hardness (HRC) 32 ± 0.5 |
| $D_{z1}$ | 0.0309 | |
| $D_{z2}$ | 0.3165 | |
| $D_{z3}$ | 0.0133 | |
| $D_{z4}$ | 0.1250 | |
| $D_{z5}$ | 0.1240 | |
| $D_{z6}$ | 0.1894 | |
| $D_{z7}$ | 0.1530 | |
| $D_{z8}$ | 0.1857 | |
| Average $D_z$ | 0.07 ±0.01 | |
| Heat treatment: 180 min at 890 °C | | |
| Deviation $D_z$ (mm) | | Hardness (HRC) 22 ± 0.5 |
| $D_{z1}$ | 0.0328 | |
| $D_{z2}$ | 0.0721 | |
| $D_{z3}$ | 0.0123 | |
| $D_{z4}$ | 0.0901 | |
| $D_{z5}$ | 0.0150 | |
| $D_{z6}$ | 0.0845 | |
| $D_{z7}$ | 0.0186 | |
| $D_{z8}$ | 0.0698 | |
| Average $D_z$ | 0.05 ±0.01 | |

*Table 12: Average deviation and hardness for Phase 3 after removal from the platform*

| Phase 3: Removed from platform | | |
|---|---|---|
| Deviation $D_z$ (mm) | | Hardness (HRC) |
| $D_{z1}$ | 0.0328 | 22 ± 0.5 |
| $D_{z2}$ | 0.0721 | |
| $D_{z3}$ | 0.0123 | |
| $D_{z4}$ | 0.0901 | |
| $D_{z5}$ | 0.0150 | |
| $D_{z6}$ | 0.0845 | |
| $D_{z7}$ | 0.0186 | |
| $D_{z8}$ | 0.0698 | |
| Average $D_z$ | 0.05 ± 0.01 | |

From Table 12 it is clear that the heat treatment applied in Phase 3 caused the average deviation from the CAD model to decrease from 0.07 ± 0.01 mm to 0.05 ± 0.01 mm and the hardness to decrease from 32 ± 0.5 HRC to 22 ± 0.5 HRC. This indicates that if the insert is stress-relieved while still attached to the build platform, plastic deformation is limited to a minimum, thus allowing for the geometry of the insert to revert to the CAD geometry during the heat treatment. It is also evident that the increased soaking period of three hours at 890 °C had the desired effect of allowing the microstructure to normalize, ultimately resulting in a residual stress-free insert.

### 4.2.3 Design for mould strength

In order to calculate the minimum value of $x_m$ at which the mould material will fail, the following was considered:

Mould material: Maraging steel (MS1)

$\sigma_{UTS}$: 1950 MPa (after age-hardening)

$\sigma_{YIELD}$: 1900 MPa (after age-hardening)

$P_m$: 140 MPa

*E*: 180 GPa

*G*: 70 GPa

For $D_H$ = 4mm:

From equation (1): $$\sigma = \frac{P_m D_H^2}{2x_m^2}$$

$$2x_m^2\sigma = P_m D_H^2$$

$$x_m = \sqrt{\frac{P_m D_H^2}{2\sigma_{UTS}}}$$

$$x_m = \sqrt{\frac{140 \times 10^6 \cdot (4 \times 10^{-3})^2}{2 \cdot 1950 \times 10^6}}$$

$$= 0.76 \times 10^{-3} \text{ m}$$

$$\approx 0.8\ mm$$

For $D_H$ = 6mm:

From equation (1): $$\sigma = \frac{P_m D_H^2}{2x_m^2}$$

$$2x_m^2\sigma = P_m D_H^2$$

$$x_m = \sqrt{\frac{P_m D_H^2}{2\sigma_{UTS}}}$$

$$x_m = \sqrt{\frac{140 \times 10^6 \cdot (6 \times 10^{-3})^2}{2 \cdot 1950 \times 10^6}}$$

$$= 1.14 \times 10^{-3} \text{ m}$$

$$\approx 1.2\ mm$$

For $D_H$ = 8mm:

From equation (1): $$\sigma = \frac{P_m D_H^2}{2x_m^2}$$

$$2x_m^2\sigma = P_m D_H^2$$

$$x_m = \sqrt{\frac{P_m D_H^2}{2\sigma_{UTS}}}$$

$$x_m = \sqrt{\frac{260 \times 10^6 \cdot (8 \times 10^{-3})^2}{2 \cdot 1950 \times 10^6}}$$

$$= 1.5\ mm$$

For $D_H$ = 10mm:

From equation (1): $$\sigma = \frac{P_m D_H^2}{2x_m^2}$$

$$2x_m^2\sigma = P_m D_H^2$$

$$x_m = \sqrt{\frac{P_m D_H^2}{2\sigma_{UTS}}}$$

$$x_m = \sqrt{\frac{140 \times 10^6 \cdot (10 \times 10^{-3})^2}{2 \cdot 1950 \times 10^6}}$$

$$= 1.89 \times 10^{-3}\ \text{m}$$

$$\approx 2\ mm$$

Table 13 gives the calculated minimum values of $x_m$ for $P_m$ = 140 MPa and set values of $D_H$.

*Table 13: Calculated minimum values of $x_m$ for $P_m$ = 140 MPa*

| $\mathbf{D_H}$ (mm) | 4 | 6 | 8 | 10 |
|---|---|---|---|---|
| $\mathbf{x_m}$(mm) | 0.8 | 1.2 | 1.5 | 2 |

It was decided to conduct experimental trials on AM inserts having conformal cooling channels of $D_H$ of 4 mm and 8 mm, respectively. The results for the experimental trials are given in Table 14 where it is seen that trials were conducted on various minimum values of $x_m$.

*Table 14: Experimental minimum values of $x_m$*

| $\mathbf{D_H}$ (mm) | 4 | 8 |
|---|---|---|
| $\boldsymbol{x_{m1}}$(mm) | 0.8 | 1.5 |
| $\boldsymbol{x_{m2}}$(mm) | 1.5 | 2 |

It was found that no visible deformation could be detected on any of the AM inserts, leading to the conclusion that for a $D_H$ of 4 mm, a safe minimum distance of $x_m$= 0.8 mm is acceptable. For a cooling channel having a $D_H$ of 8 mm, it was found that a safe minimum distance of $x_m$= 1.5 mm was acceptable.

Figure 41 shows the SIGMASOFT® simulation results for an insert having a $D_H$ of 4 mm. From this it was predicted that for an $x_m$ of 0.8mm, the maximum deflection would be 1.396 µm under an injection pressure of 140 MPa. For a channel having a $D_H$ of 4 mm and an $x_m$ of 1.5 mm, a deflection of 2.04 µm was predicted.

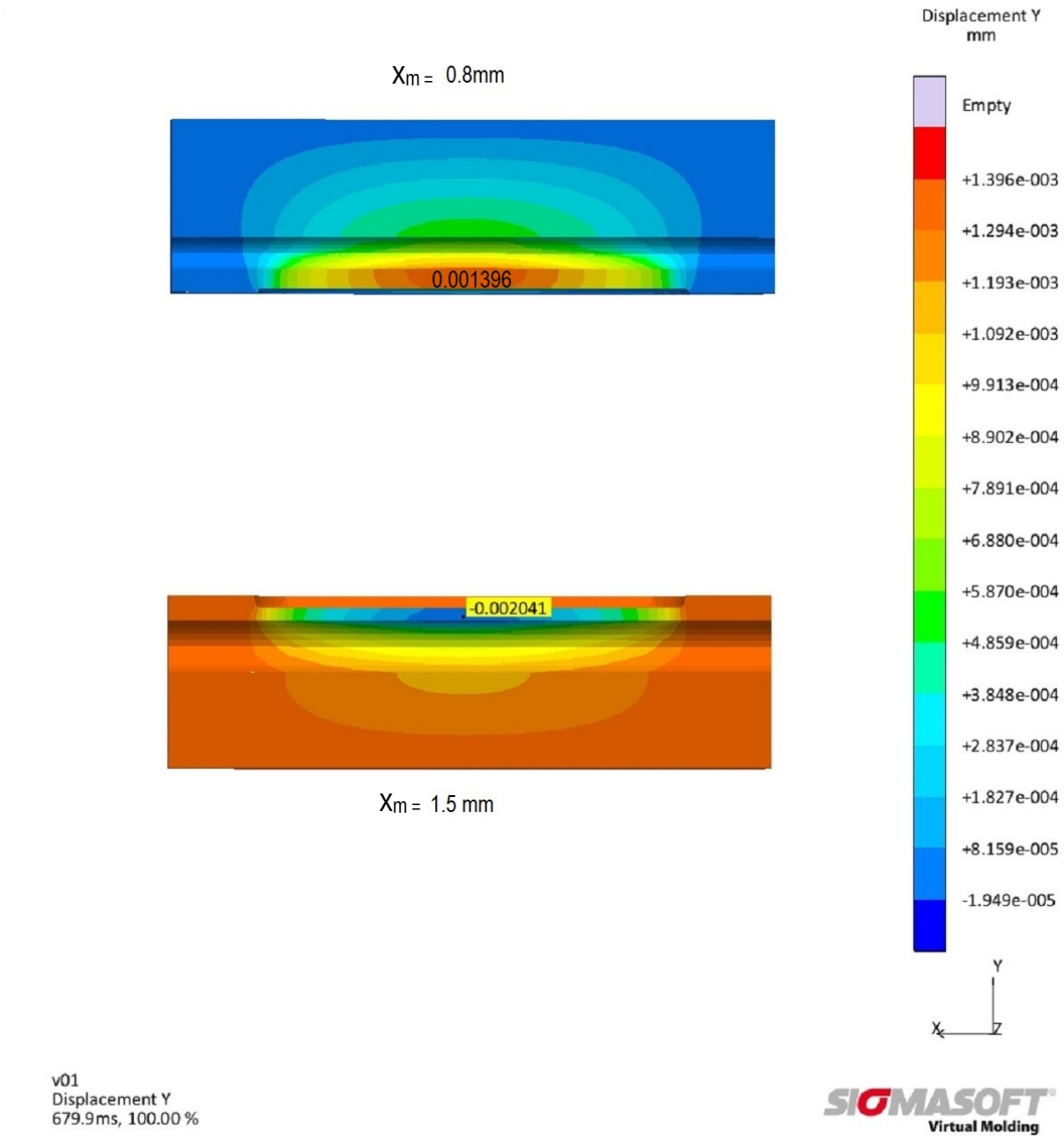


*Figure 42: SIGMASOFT ® deformation prediction results for an insert having a $D_H$ of 4 mm.*

Figure 42 shows the SIGMASOFT® simulation results for an insert having a $D_H$ of 8 mm. From this it was predicted that for an $x_m$ of 1.5 mm, the maximum deflection would be 15.45 µm under an injection pressure of 140 MPa. For a channel having a $D_H$ of 8 mm and an $x_m$ of 2 mm, a deflection of 0.601 µm was predicted.

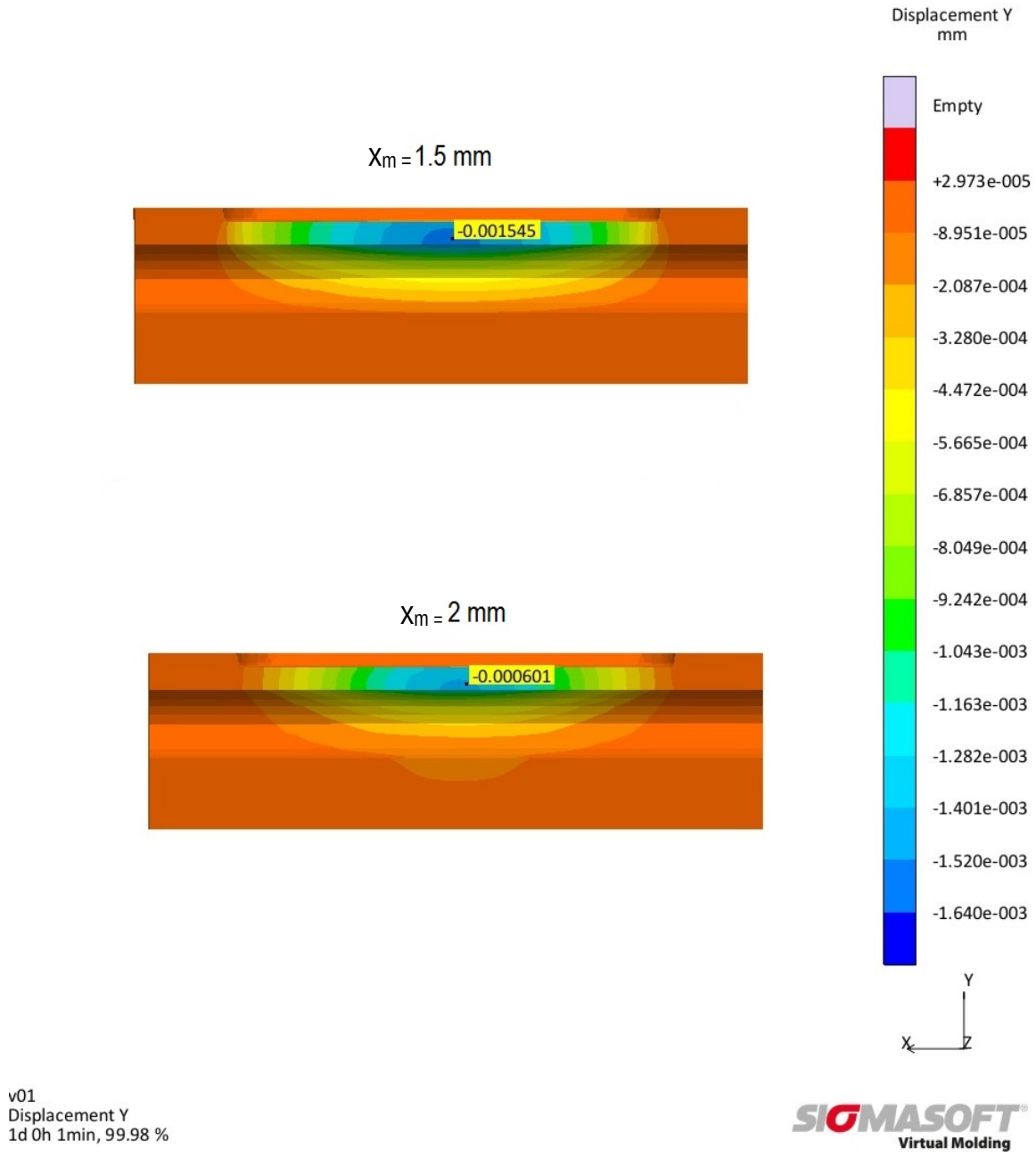


*Figure 43: SIGMASOFT® deformation prediction results for an insert having a $D_H$ of 8 mm.*

By using equation 3 as set out in section 2.6.2, it is possible to theoretically calculate the deflection of mould surface due to the injection pressure. Table 15 compares the theoretical calculated values with those achieved using SIGMASOFT® simulations.

*Table 15: Comparison between the theoretical calculated and simulated deflections*

| Channel dimensions and cooling channel distance from cavity surface | Theoretical deflection (µm) | Simulated deflection (µm) |
|---|---|---|
| | | |
| $D_H$ = 4 mm; $x_m$ = 0.8 mm | 1.450 | 1.396 |
| | | |
| $D_H$ = 4 mm; $x_m$ = 1.5 mm | 2.15 | 2.04 |
| | | |
| $D_H$ = 8 mm; $x_m$ = 1.5 mm | 15.98 | 15.45 |
| | | |
| $D_H$ = 4 mm; $x_m$ = 0.8 mm | 0.645 | 0.601 |

The calculated theoretical values are shown to be close to the simulated values, thereby indicating that SIGMASOFT® simulation software is a valuable tool to be used during the design process.

The 3D scan data for the AM inserts indicated that some deformation had occurred during the experimental trials. For the AM inserts having a $D_H$ of 4 mm and an $x_m$ of 0.8 mm, the fixed half of the IM toolset experienced an average deformation of 62.13 µm in the positive Z-direction. From the scan data for the moving half of the inserts having a $D_H$ of 4 mm and an $x_m$ of 0.8 mm, an average deformation of 19.1 µm was observed in the negative Z-direction. Figure 44 shows the scan data for inserts having a $D_H$ of 4 mm and an $x_m$ of 0.8 mm.

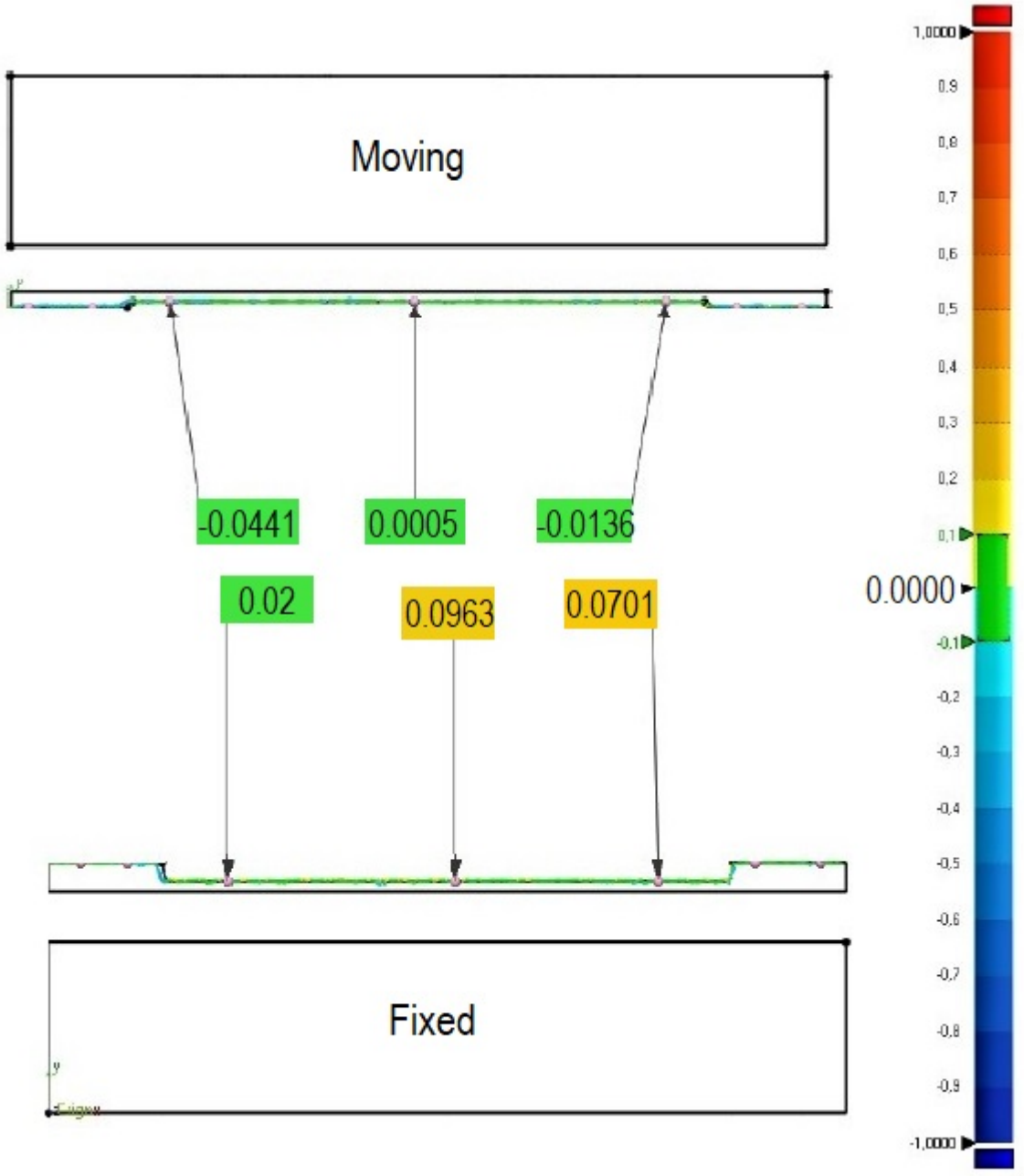


*Figure 44: Scan data of an AM insert having a channel diameter of 4 mm and $x_m$ of 0.8 mm after IM trials.*

For the AM inserts having a $D_H$ of 4 mm and an $x_m$ of 1.5 mm, the moving half of the IM toolset experienced an average deformation of 12.2 µm in the positive Z-direction. From the scan data for the fixed half of the inserts having a $D_H$ of 4 mm and an $x_m$ of 1.5 mm, a deformation of 90.2 µm was observed in the negative Z-direction. Figure 45 shows the scan data for inserts having a $D_H$ of 4 mm and an $x_m$ of 1.5 mm.

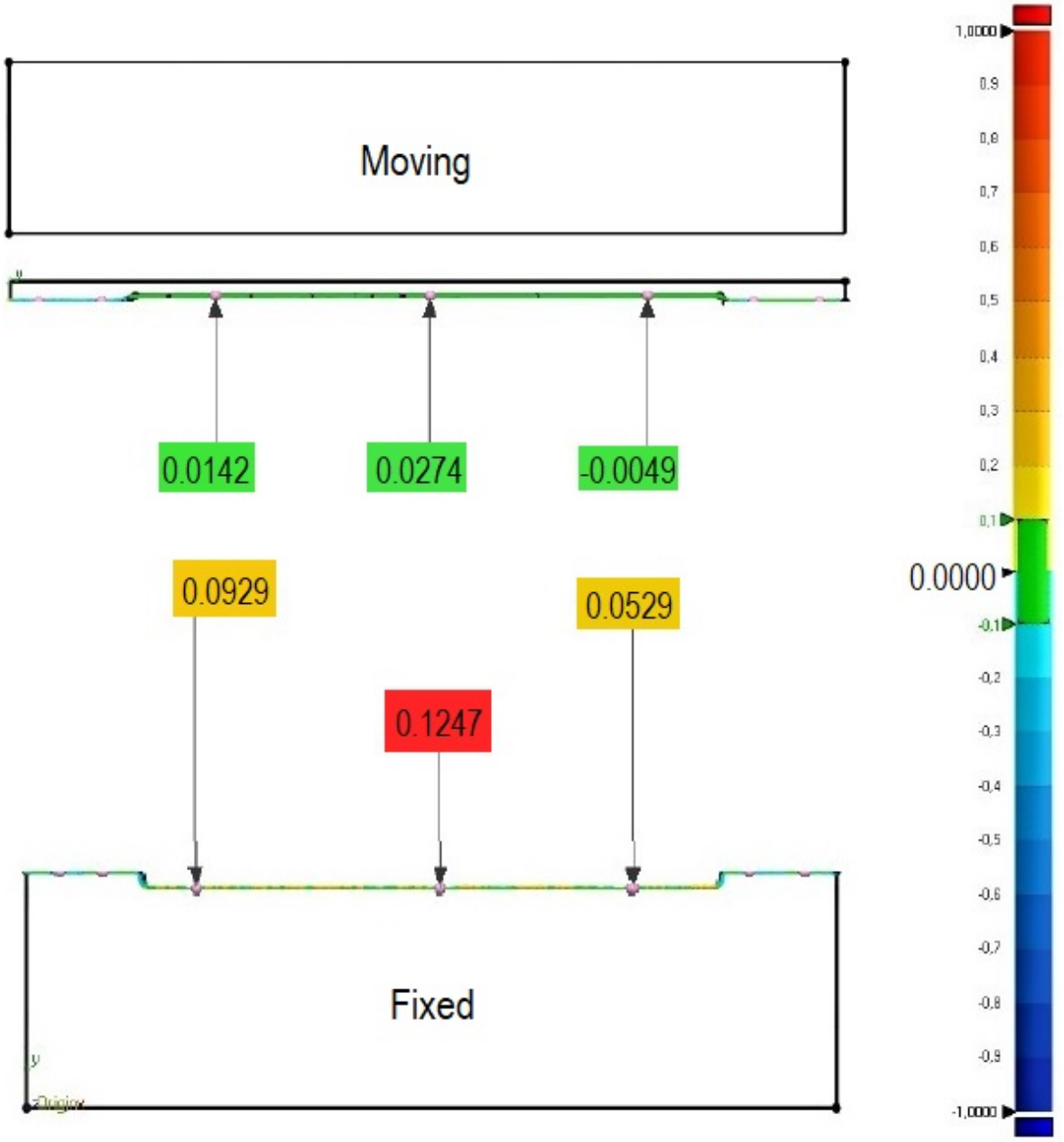


*Figure 45: Scan data of an AM insert having a channel diameter of 4 mm and $x_m$ of 1.5 mm.*

For the AM inserts having a $D_H$ of 8 mm and an $x_m$ of 1.5 mm, the moving half of the IM toolset experienced an average deformation of 16.8 µm in the negative Z-direction. From the scan data for the fixed half of the inserts having a $D_H$ of 8 mm and an $x_m$ of 1.5 mm, a deformation of 95.8 µm was observed in the positive Z-direction. Figure 46 shows the scan data for inserts having a $D_H$ of 8 mm and an $x_m$ of 1.5 mm.

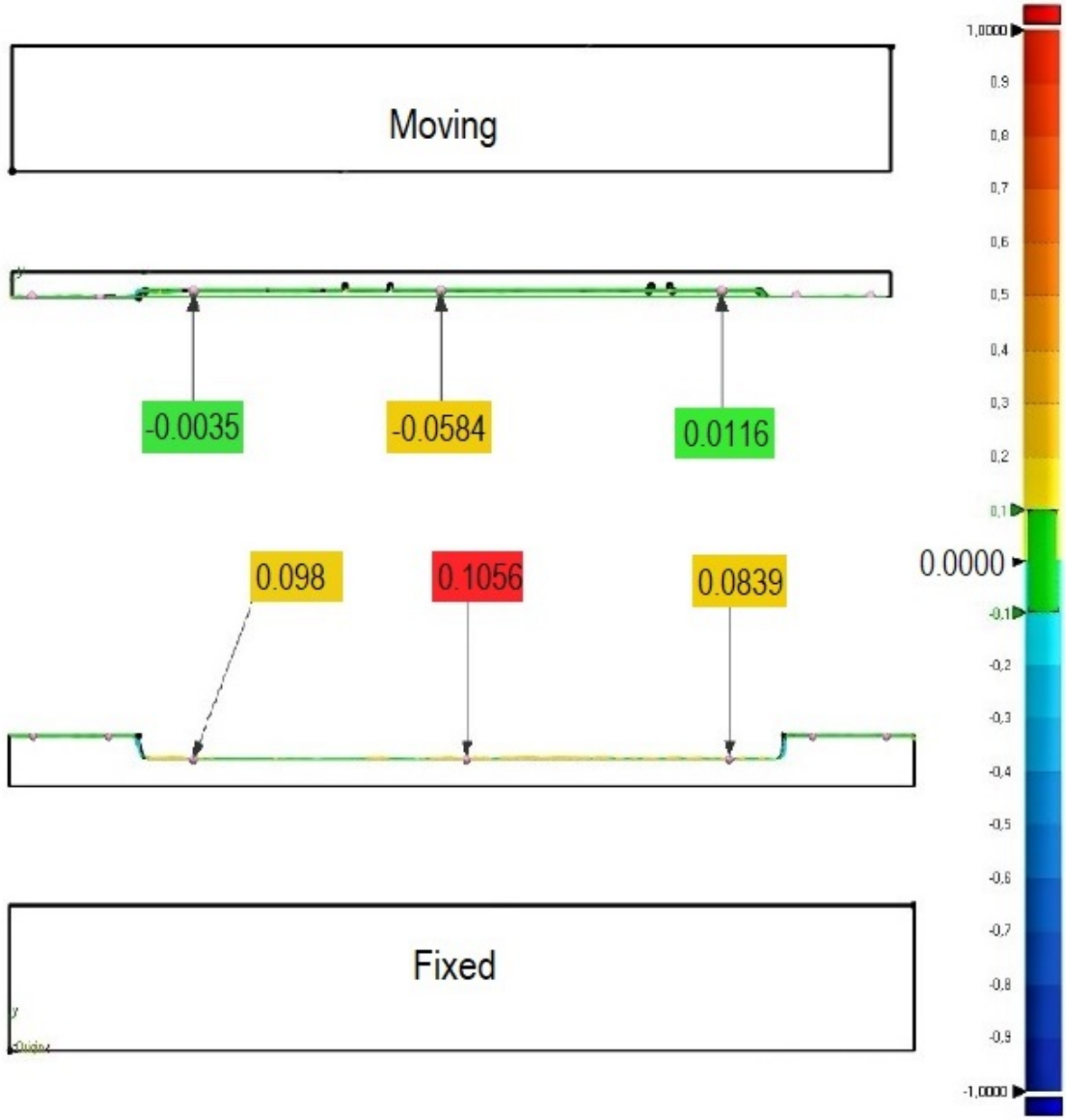


*Figure 46: Scan data of the moving half of an AM insert having a channel diameter of 8 mm and $x_m$ of 1.5 mm.*

For the AM inserts having a $D_H$ of 8 mm and an $x_m$ of 2mm, the moving half of the IM toolset experienced an average deformation of 37.2 µm in the positive Z-direction. From the scan data for the fixed half of the inserts having a $D_H$ of 8 mm and an $x_m$ of 2 mm, a deformation of 48.2 µm was observed in the positive Z-direction. Figure 47 shows the scan data for inserts having a $D_H$ of 8 mm and an $x_m$ of 2 mm.

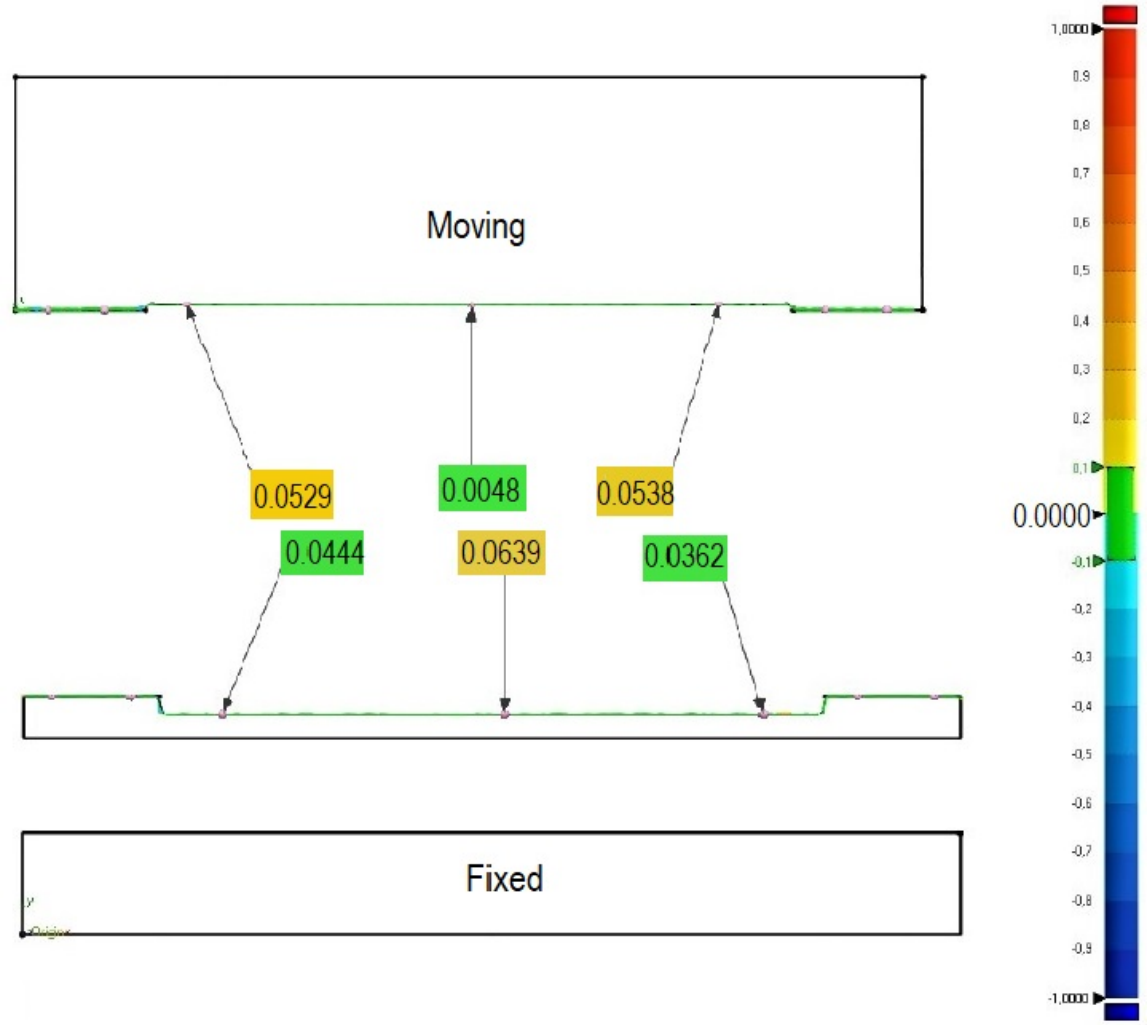


*Figure 47: Scan data of an AM insert having a channel diameter of 8 mm and $x_m$ of 2 mm.*

Table 16 shows a comparison between the experimental and simulated deflections respectively.

*Table 16: Comparison between the experimental and simulated deflections*

| Channel dimensions and cooling channel distance from cavity surface | Experimental deflection (µm) | | Simulated deflection (µm) |
|---|---|---|---|
| | Fixed | Moving | |
| $D_H$ = 4 mm; $x_m$ = 0.8 mm | 62.13 | -19.1 | 1.396 |
| | | | |
| $D_H$ = 4 mm; $x_m$ = 1.5 mm | 90.2 | 12.2 | 2.04 |
| | | | |
| $D_H$ = 8 mm; $x_m$ = 1.5 mm | 95.5 | -16.8 | 15.45 |
| | | | |
| $D_H$ = 4 mm; $x_m$ = 0.8 mm | 48.2 | 37.2 | 0.601 |

The experimental deflections showed in Table 16 appears to be quite high, however it must be noted that the theoretical and simulated results did not take into consideration the effect of the force distribution of the injected molten polymer on the fixed and moving sides of the mould, respectively. It was observed that the inserts on the fixed side of the IM machine showed a larger deformation than that of the moving side; a logical explanation for this being the difference in lateral force absorption between the moving side and the fixed side of the IM machine. The moving side, being made up of the clamping mechanism, through its design absorbs more lateral force caused by the injection pressure of the molten polymer than the fixed side, which is rigid. Furthermore, no plastic deformation occurred during the experimental tests, indicating that the selected minimum values of $x_m$ are sufficient.

In Table 17 (Hsu, 2012) provides design parameters for the general design of cooling channels for both conformal cooling channels as well as conventionally drilled cooling channels. Figure 48 gives a representation of the dimensions described in Table 16, where b represents the hydraulic diameter of the cooling channels and c denotes the distance between the cooling channel and the mould cavity. From this it is suggested that the distance between the cooling channel and the mould cavity, c, is dependent on the value of b, the hydraulic diameter of the cooling channel.

*Table 17: Cooling channel design parameters as used in the general design of cooling channels (Hsu 2012).*

| Wall thickness of product (mm) | Cooling channel diameter (mm) (b) | Distance between centre of channels and cavity (c) |
|---|---|---|
| 0–2 | 4–8 | 1.5–2 x b |
| 2–4 | 8–12 | 1.5–2 x b |
| 4–6 | 12–14 | 1.5–2 x b |

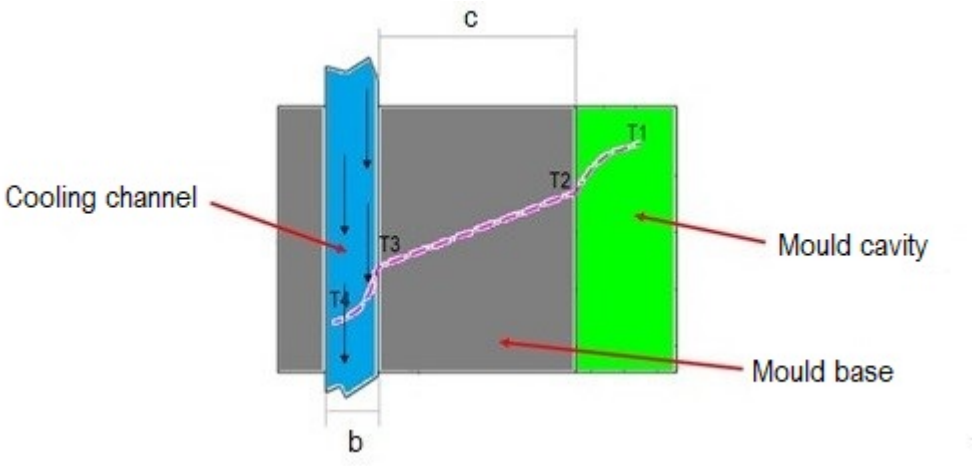


*Figure 48: Graphic representation of parameters used in the general design of cooling channels (Hsu 2012).*

It can thus be deduced that in order to increase the cooling efficiency, the distance c, should be as small as possible.

Mielonen (2016) further suggested that a minimum distance of 2.5 mm for $x_m$ was sufficient for AM conformal cooling channels which were manufactured using a laser melting process, however, no experimental data was presented. This serves to further strengthen the perception of safely guarded trade secrets as far as design rules are concerned. When compared to Mielonen's (2016) suggestion, the green edge shown in the 3D scan data, presented in Figures 44 to 47, indicates a good fit with the CAD model, thereby indicating that the deformation experienced by the AM inserts was minute and negligible.

No signs of deformation or warping were detected on the moulded part during the experimental trial, which serves to confirm that the minimum distance for $x_m$ of 0.8 mm is acceptable for an insert having a $D_H$ of 4mm, and an $x_m$ of 1.5 mm is acceptable for an insert having a $D_H$ of 8 mm.

It must, however, be noted that while the theoretical calculations indicated that the mould material would fail under the specified parameters, the experimental trials together with the 3D scanning of the inserts proved otherwise. This is due to a pressure drop across the mould assembly from the injection point to the gate of the mould cavity. Since there is no specified range for this pressure drop, it is recommended to decrease the $x_m$ value to an actual minimum through machining, until failure of the mould material during experimental trials.

### 4.2.4 Application of refined design rules

The results yielded by the virtual moulding process indicated that the use of AM conformal cooling channels showed a decrease in cycle time of three seconds compared to the conventional manufactured channels. While this might not seem significant, Figure 49 and Table 18 show that the use of conformal cooling channels leads to more efficient cooling and a lower average mould temperature. This in itself is an indication that the cooling effects of AM conformal cooling channels surpass that of conventionally manufactured cooling channels.

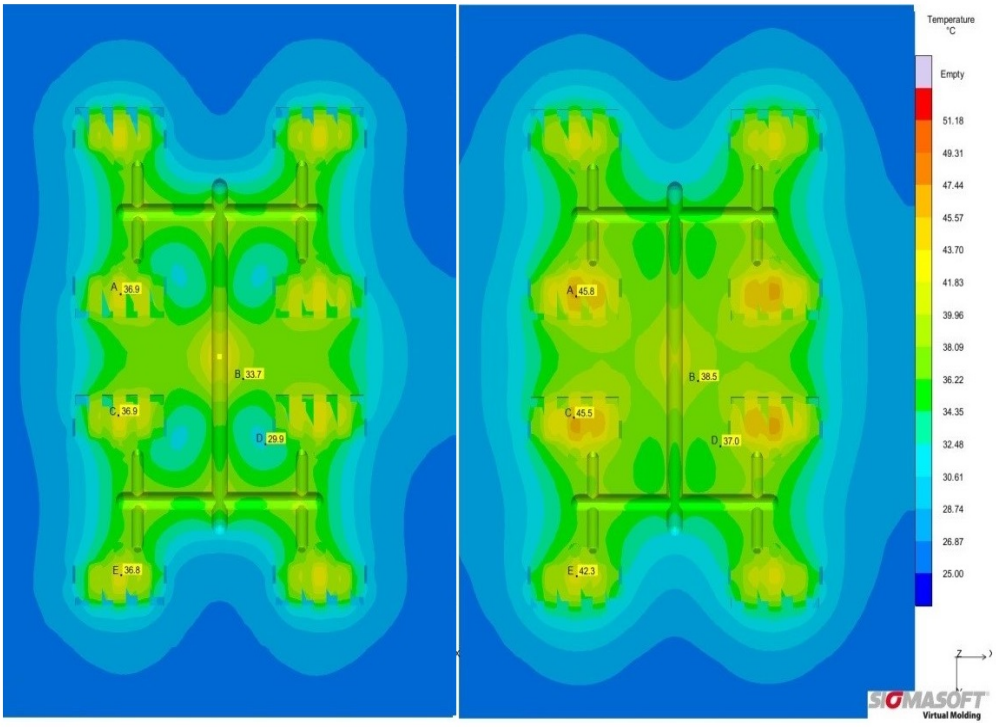


(a) (b)

*Figure 49: Temperature comparison at various mould locations for (a) conformal cooling channels and (b) conventional cooling channels.*

*Table 18: Average temperature comparison between conformal and conventional cooling channels*

| Location | Conformal (°C) | Conventional (°C) |
|---|---|---|
| A | 36.9 | 45.8 |
| B | 33.7 | 38.5 |
| C | 36.9 | 45.5 |
| D | 29.9 | 37 |
| E | 36.8 | 42.3 |
| Average temp | 34.84 | 41.82 |

In Figure 50 (a), it is evident that the AM conformal cooling channel design has led to a more efficient cooling of the mould. This is highlighted by the even temperature gradient across the mould surface.

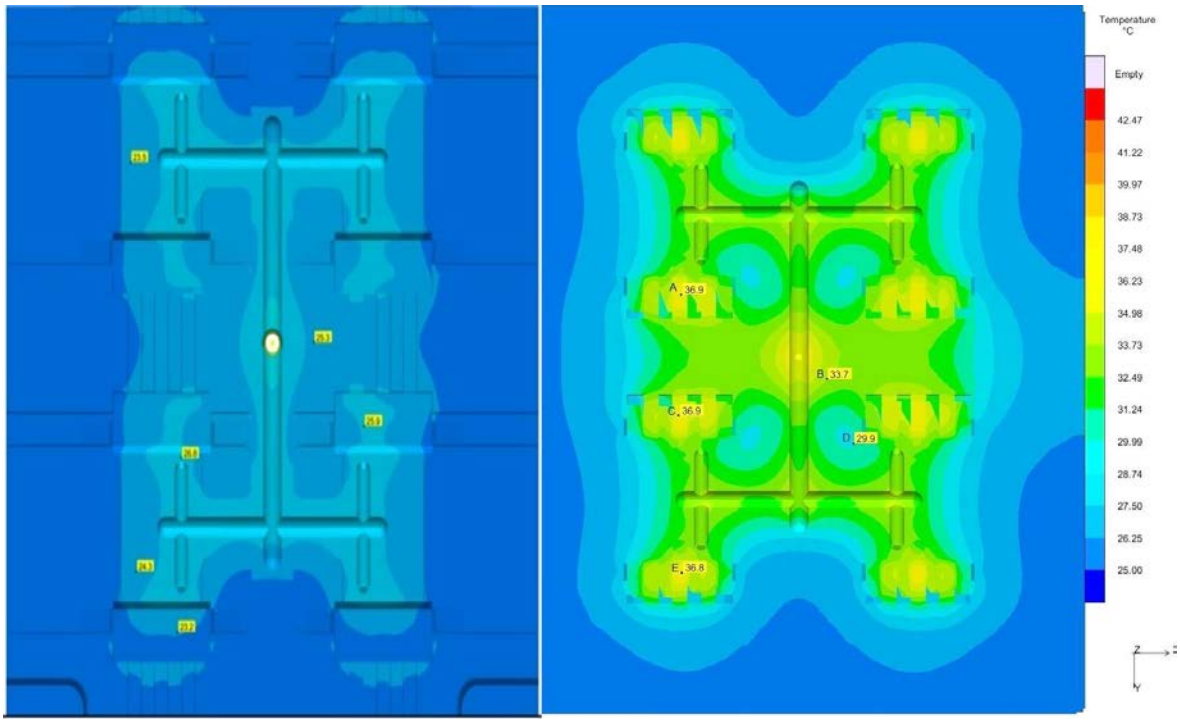


(a) (b)

*Figure 50: Temperature comparison at various mould locations for (a) updated conformal cooling channels and (b) original conformal cooling channels.*

Table 19 shows a comparison of the SIGMASOFT® simulation results between the AM-produced mould and a conventionally produced mould. While a decrease in cycle time of three seconds appears to be minimal, it results in a 12% increase in production, whereas with the conventionally machined mould, 138 parts are produced per hour; it is possible for 156 parts to be produced with the AM mould. This also results in an 11% saving in production costs per manufactured part, as calculated against the current production cost received from Altech-UEC.

*Table 19: Comparison between conformal cooling channels and conventional cooling channels.*

<table>
<tr><td></td><td>Conventionally produced mould</td><td>AM-produced mould</td></tr>
<tr><td>Cycle time (sec)</td><td>26</td><td>23</td></tr>
<tr><td colspan="2">% Time saved</td><td>12%</td></tr>
<tr><td>Production cost per part</td><td>R 0.28</td><td>R 0.25</td></tr>
<tr><td colspan="2">% Production cost saved per part</td><td>11%</td></tr>
<tr><td>Design time (CAD)</td><td colspan="2">10 hours</td></tr>
<tr><td>Manufacturing time</td><td rowspan="2">80 hours</td><td>16 hours</td></tr>
<tr><td>Finishing time</td><td>2 days</td></tr>
<tr><td>Cost to produce mould</td><td>R 136 101.91</td><td>R 60 000.00</td></tr>
</table>

Table 20 shows a comparison between the cycle times achieved during the industrial application trials with the DMLS produced mould as compared against data which was obtained from Altech-UEC. From this it is evident that a cycle time of 15 seconds was obtained using a toolset having AM conformal cooling channels. This difference in cycle time resulted in a 42% time saved which translates to a monetary saving of 12 cents. In terms of production efficiency, 138 parts produced per hour using a toolset having conventionally machined cooling channels as compared to the 240 parts being produced with a toolset having conformal cooling channels.

*Table 20: Comparison between conformal cooling channels and conventional cooling channels*

| | Conventionally produced mould | AM produced mould |
|---|---|---|
| Cycle Time (sec) | 26 | 15 |
| % Time saved | | 42% |
| Production cost per part | R 0.28 | R 0.16 |

## 4.3 Discussion of results

Due to the nature of the DMLS process, residual stresses are built up in the component during manufacture and as a result the geometric accuracy of the component is often sacrificed during removal of the components from the build platform. It was found that upon removal from the build platform, the insert showed signs of warping, which in the light of the geometric accuracy required for tooling components rendered the insert unusable. It was thus decided to apply a heat treatment while the insert was attached to the build platform. Through an iterative process of 3D scanning techniques and subsequent hardness measurements, a stress-relieving heat treatment was formulated which produced virtually stress-free IM inserts. While the stress-relieving heat treatment produced a stress-free component, there was a substantial reduction in the hardness of the components which proved to be desirable as the IM tool inserts required further machining. By applying an age-hardening heat treatment after the inserts were machined to their final dimensions, the inserts proved to be durable during the experimental trials. Through the metallographic study of the microstructure of both stress-relieved and age-hardened MS1 specimens, the microstructure of the age-hardened samples was noted as a homogenous precipitation-hardened structure, which is consistent with literature (Kempen *et al.*, 2011). The use of the developed stress-relieving heat treatment followed by age-hardening has proven to be beneficial when applied to MS1 components produced through the DMLS process.

With regard to the shape of the cooling channels used in this study, the theoretical calculations were done for a cooling channel having a rectangular cross-section since this provided a worst-case scenario for loading the cooling channels with the applied injection pressure. Since a rectangular channel would have further build limitations, a circular cross-sectional channel was used for both the SIGMASOFT® virtual mould simulations and the practical experiments. Furthermore, it should

be pointed out that since AM offers virtual freedom of design, a cooling channel having an oval cross-section might have been considered. When considering the force distribution across an oval cross-section, it would appear that an oval cross-section with the smaller radius placed perpendicular to the cavity is indeed stronger that a circular cross-section, however, when taking into consideration the aim of this study, by refining a design rule according to a circular cross-section, the minimum distance between the mould cavity surface and the cooling channel will be more than sufficient when applied to a different channel cross-section such as an oval. Channels with a hydraulic diameter $D_H$, of 4 mm and 8 mm were considered for the practical experiments, since 4 mm channels allow metal powder to be removed with ease and 8 mm channels are commonly used in the IM industry.

During the IM trials on the inserts with conformal cooling channels, no visible deformation was observed under an industry standard of a 140 MPa injection pressure. Thus it became evident that the theoretical calculations as well as experimental results verified the reliability of the SIGMASOFT® virtual mould simulation software and consequently, a minimum distance for $x_m$ could be determined. While the SIGMASOFT® virtual mould simulation software predicted the pressure exerted on the mould wall, as well as the displacement, it could not predict whether any plastic deformation would take place. Through meticulous measurement and 3D scanning techniques, no significant plastic deformation was observed during the practical trials. However, the 3D scan results indicated that deformation of a minute nature had occurred. The maximum deformation occurred at the centre of the inserts for both 4 mm and 8 mm channels. This is possibly as a result of the molten plastic being injected directly into the centre of the insert. When compared to literature, a minimum distance of $x_m$ = 2.5 mm was recommended for cooling channels of any $D_H$ which is manufactured using a laser melting process, such as DMLS (Mielonen, 2016). However, no experimental data was provided. Therefore, by determining a minimum distance for $x_m$, design boundaries for conformal cooling channels were enhanced during this study.

During the industrial application, the use of SIGMASOFT® virtual mould simulation software indicated that the use of conformal cooling channels provided a uniform temperature gradient as opposed to conventionally drilled cooling channels. From this data it was possible to predict that a saving of 12% in the cycle time was possible, which in turn would lead to an 11% increase in productivity. The practical trials with the mould toolset having conformal cooling channels achieved a cycle of 15 secs, which resulted in a 42% increase in productivity. In this specific case, further monetary savings could be achieved through the use of AM, since the estimated cost to produce the IM tool with the DMLS process was significantly less than that of conventional machining techniques.

When comparing the practical results to that achieved through SIGMASOFT® virtual mould simulation software, a difference in the cycle time of 8 seconds is observed. This can be attributed to the lower temperature of the cooling water during the practical trials. An industry expert indicated that further time savings could be achieved by tweaking the cooling water parameters.

*Summary*

*The methodology used in this study, has resulted in a series of experiments through which specific sets of data were extracted. Through this data, a set of enhanced design constraints have been achieved, which includes a stress-relieving heat treatment for DMLS-produced components, a material comparison between supplier data and experimental data, as well as a determination of a minimum distance between the mould cavity and the cooling channel. An industrial application was used as a practical comparison between an IM tool having conformal cooling channels and an IM tool having conventionally drilled channels.*

# Chapter 5

## Conclusions and Recommendations

*An evaluation of the investigations carried out provides conclusions on the aim and findings of this study. Recommendations for further studies are also highlighted in this chapter.*

---

### Conclusions

The aim of this study was to identify and refine design constraints as applied to the design of conformal cooling channels. When considering the objectives, it can be confirmed that each of the objectives has been successfully met, thereby achieving the aim of this study. Literature has shown that the use of conformal cooling channels is beneficial to the IM industry and this has been further established in this study. Through further development, the cooling potential of conformal cooling channels can be greatly enhanced. Conclusions on the attainment of the different objectives follow. Appendix 1 shows a summary of the attained objectives.

I. Research and identify existing AM design constraints as applied to IM tooling with conformal cooling channels built in maraging steel.

Literature indicated that no specific set of design guidelines existed for conformal cooling channels produced using a laser melting process, and where they do exist, any such design guidelines are considered a closely guarded “trade secret” (Mielonen, 2016). While design guidelines for conventionally drilled cooling channels have been documented (Hsu, 2012) and can be utilized in the design of conformal cooling channels, they serve no purpose in pushing the boundaries as far as design for AM tooling is concerned. With regard to the shape of the cooling channels used in this study, a channel having a circular cross-section was used for both the SIGMASOFT® virtual mould simulations as well as the practical experiments.

Research in the broader context of MS1 components produced through the DMLS process showed a lack of a documented stress-relieving heat treatment. While this is not directly applicable to the design of conformal cooling channels, it does impact the geometric constraints of IM tooling inserts. It was found that upon removal from the build platform, the insert showed signs of warping, which in the light of the geometric accuracy required for tooling components

rendered the insert unusable. While the material supplier, EOS, specified a heat treatment, this proved to be an age-hardening process which if applied to the warped insert would result in the insert being too hard to machine to final dimensions. Therefore, further work was done to develop a stress-relieving heat treatment specifically for application on maraging steel components built through the DMLS process. Through an iterative process of 3D-scanning techniques and subsequent hardness measurements, a stress-relieving heat treatment was formulated which produced virtually stress-free IM inserts. While the stress-relieving heat treatment produced a virtually stress-free component, there was a substantial reduction in the hardness of the components which proved to be desirable as the IM tool inserts required further machining. By applying an age-hardening heat treatment after the inserts were machined to their final dimensions, the inserts proved to be durable during the experimental trials. The heat-treatment processes followed are described below in Table 21.

*Table 21: Heat-treatment process followed in the post-processing of the IM inserts.*

| | |
|---|---|
| Stress-relieving heat treatment | Components to be placed in a furnace at 890 °C with a soaking time of 3 hours per 25 mm thickness and allowed to cool to room temperature.<br><br>Obtained hardness: 22 ± 0.5 HRC |
| Age-hardening heat treatment | Components to be placed in a furnace at 495 °C with a soaking time of 6 hours and allowed to cool to room temperature.<br><br>Obtained hardness: 51 ≤ 54 HRC |

II. Develop and refine specific design rules to improve the cooling efficiency of conformal cooling channels in IM tooling inserts produced in maraging steel.

From literature as well as the study done on the Altech-UEC IM tool, it became evident that the use of conformal cooling channels was beneficial to the cooling efficiency of an IM toolset. It was further proven that the use of conformal cooling channels had a significant impact on the reduction of the IM cycle time. The uncertainty regarding the minimum distance between the mould cavity surface and the cooling channel was successfully clarified. Thus, through the use

of CAD techniques, FEA-based simulation and practical experiments, the design rule for a minimum distance between the cooling channel and the mould surface was refined and documented. Table 22, describes the design rules which were formulated with consideration of the design constraints researched in this study.

*Table 22: Design rules emanating from this study*

| | |
|---|---|
| Minimum distance between the mould cavity and the cooling channel | $D_H$ = 4 mm; $x_m \geq 1$ mm<br>$D_H$ = 8 mm; $x_m \geq 1.5$ mm |

III. Demonstrate the effectiveness of the conformal cooling through application to an industry mould.

With the goal of demonstrating the effectiveness of conformal cooling channels, the CAD of an existing toolset supplied by Altech-UEC was modified using the developed design rules to have conformal cooling channels. This IM toolset was manufactured using the DMLS process using MS1 as feedstock. After heat treatment and post-processing, practical trials were conducted where the data extracted was compared to data provided by Altech-UEC, where it was seen that the cycle time for the toolset having conformal cooling channels decreased by 42%. This reduction in cycle time indicated that conformal cooling had a positive impact on increasing the efficiency of the IM process.

IV. Document a design process for conformal cooling channels in a format that would be user-friendly for practitioners in the tooling industry.

In order to augment the design process of IM tooling, the thought process behind design for IM tooling with a view to the use of AM was documented. While the steps followed in the augmented design process may not apply to any specific IM toolset, it provides a tool designer with a basic outline of necessary steps to follow when considering the use of AM in the manufacture of tooling components. Due to a lack of design rules for the distance between the mould cavity surface and the cooling channel, the design for mould strength was found to be a valuable contribution to this study.

The design approach and methodology can be documented as follows:

i. Assess the need for the use of additive manufacturing:

Implement hybrid tooling and limit the use of AM to complex geometries where possible.

ii. Design for sufficient and uniform cooling:
Plan and distribute cooling channels effectively and assess via FEA-based simulations to determine the optimal cooling strategy.

iii. Design for mould strength and deflection:
Consider mould material strength and design cooling channels to be closer to the mould cavity, thereby increasing cooling efficiency.

iv. Design for part ejection temperature:
Set the goal to reduce the cycle time and increase production.

The application of the refined design rules to a production toolset proved to be a valuable verification of the results of this study. AM was established as a valuable resource to the tool making industry. Due to the layered nature of AM, the possibilities are endless for further optimization of manufacturing processes.

In conclusion, the use of AM as applied to the IM industry in this study has provided satisfactory results and indicated that AM can be a feasible solution to future problems in the tooling industry.

## Recommendations

Recent developments in the AM sector holds promise for weight saving in the IM tooling industry. Due to the nature of the DMLS process, it is quite possible to achieve lightweight tooling by replacing bulky sections with lattice structures. The resultant requirement of less energy to move bulky tooling components further increases the efficiency of the IM process. While this has been successfully achieved, it is still a novel idea for tooling applications and provides potential for further development.

Another area of interest on IM applications is the efficiency of coolant flow through conformal cooling channels. No recent literature could be found, but there is potential for further study. By designing for balanced flow between conformal cooling channels which split, the cooling efficiency of IM tools could possibly be further enhanced, thereby leading to shorter production times and a more efficient IM process.

The nature of AM processes allows for further development of cooling strategies. Current trends in the IM industry show that two cooling strategies are favoured for conformal cooling channels, namely spiral channels and parallel channels. However, by making use of the virtual design freedom of AM, the opportunity exists for these strategies to be further enhanced. Furthermore, the placement of ribs inside cooling channels to produce turbulent flow is an area of study worth pursuing.

# References


Ahn, D., Park, S. and Kim, H. (2010) 'Manufacture of an Injection Mould with Rapid and Uniform Cooling Characteristics for the Fan Parts Using a DMT Process', *International Journal of Precision Engineering and Manufacturing*, 11(6), pp. 915–916. doi: 10.1007/s12541-010-0111-3.

van As, B., Combrinck, J., Booysen, G., de Beer, D. J., (2015) 'Direct metal laser sintering, utilising conformal cooling for high volume production tooling', *South African Journal of Industrial Engineering*, 28, pp. 170–182.

de Beer, D. J., du Preez, W. B., Greyling, H., Prinsloo, F., Sciamarillo, F., Trollip, N., Vermeulen, M., Wohlers, T., (2016) *A South African Additive Manufacturing Strategy*, pp-48.

Buijs, K. (2005) Lasercusing, Will it make removing metal by machine and casting a thing of the past?, *Stailess Steel World*, pp 31-37. http://innomet.nl/en/publications/ Accessed on 05 January 2016

Chou, K., Wang, K. (2014) 'Residual Stress in Metal Parts Produced by Powder-Bed Additive Manufacturing Processes', *Igarss 2014*, (1), pp. 1–5. doi: 10.1007/s13398-014-0173-7.2.

Clayton, J. (2014) 'Optimising metal powders for additive manufacturing', *Metal Powder Report*. Elsevier Ltd, 69(5), pp. 14–17. doi: 10.1016/S0026-0657(14)70223-1.

Combrinck, J., Booysen, G., van der Walt, J., de Beer, D. J, (2012) 'Limited run production using Alumide® tooling for the plastic injection moulding process', *South African Journal of Industrial Engineering*, 23(July 2012), pp. 131–146.

Dobransky, J., Baron, P., Simkulet, V., Kocisko, M., Ruzbarsky, J., Vojnova, E., (2015) Examination of material manufactured by direct metal laser sintering (DMLS), *METALURGIJA,* 54(3), pp. 477–480.

Elanchezhian, C., Sunder Selwyn, T. and Vijaya Ramnath, B. (2005) '*Design of Jigs-Fixtures and Press Tools,* Chennai: Eswar Press.

Elwany, B. Y. A. (2014) Making 3-D futures reality, *Industrial Engineer*, pp. 32–35.

EOS (2007) EOSINT M Technology for Direct Metal Laser-Sintering (DMLS), pp. 1–53.

EOS (2013) ‘EOS Materials Metals Brochure, pp. 9–10.

EOS (2014a) ‘Application Notes Design Rules for DMLS’, 49(0), pp. 1–14.

EOS (2014b) ‘Material Data Sheet for EOS MS1 M 270 Systems’, 49(0), pp. 1–3.

EPMA (2015) ‘Introduction to additive manufacturing technology.’, *EPMA*, pp. 1–41.

Ferreira, J. C. (2004) ‘Rapid tooling of die DMLS inserts for shoot-squeeze moulding (DISA) system’, *Journal of Materials Processing Technology*, 155–156(1–3), pp. 1111–1117. doi: 10.1016/j.jmatprotec.2004.04.404.

Feygin, M. and Sung, S. P. (1999), Laminated object manufacturing apparatus method, *Patent no. 5876550,* pp 1-52.

Gibson, I., Rosen, D. and Stucker, B. (2015) ‘“ Additive Manufacturing Technologies : 3D Printing , Rapid Prototyping , and Direct Digital Manufacturing ”, 2nd Edition’, 59(3), pp. 193–198.

Heigel, J. C., Michaleris, P. and Reutzel, E. W. (2015) ‘Thermo-mechanical model development and validation of directed energy deposition additive manufacturing of Ti–6Al–4V’, *Additive Manufacturing*. Elsevier B.V., 5, pp. 9–19. doi: 10.1016/j.addma.2014.10.003.

Hsu, A., (2012), Conformal Cooling Industrial Application and Design Optimization Technology Definition Conformal. pp 1-50

Kempen, K. *et al.* (2011) ‘Microstructure and mechanical properties of Selective Laser Melted 18ni-300 steel’, 12, pp. 255–263. doi: 10.1016/j.phpro.2011.03.033.

Knowles, C. R., Becker, T. H. and Tait, R. B. (2012) ‘The effect of heat treatment on the residual stress levels within direct metal laser sintered ti-6al-4v as measured using the hole-drilling strain gauge method’, *RAPDASA*, 23(3), pp. 119–129. 13th Annual Rapid Product Development Association of South Africa conference, 31 Oct- 2 Nov 2012, Kwa Maritane Bush Lodge, Pilanesburg, South Africa

Li, C. L. (2001) ‘A feature-based approach to injection mould cooling system design’, *Computer-Aided Design*, 33(14), pp. 1073–1090. doi: http://dx.doi.org/10.1016/S0010-4485(00)00144-5.

Matias, E. and Rao, B. (2015) ‘3D printing: On its historical evolution and the implications for business’, in *Portland International Centre on Management of Engineering and Technology*, pp. 551–558. doi: 10.1109/PICMET.2015.7273052.

Mielonen, M. (2016) Improving production efficiency of injection molding process by utilization of

laser melted tool inserts with conformal cooling, *Master's Thesis: M.Sc in Technology*, Alto University, School of Engineering, Finland

Mueller, B. and Kochan, D. (1999) 'Laminated object manufacturing for rapid tooling and patternmaking in foundry industry', *Computers in Industry*, 39(1), pp. 47–53. doi: 10.1016/S0166-3615(98)00127-4.

Rao, N. (2007) 'Manufacturing Tooling Introduction What is tool design', pp. 1–8.

Rao, N. and Schumacher, G. (2004) *Design Fomulae for Plastic Engineers*. 2nd edn. Hanser Publishers, Munich

Samperi, M. T. (2014) Development of design guidelines for metal additive manufacturing and process selection, *Master's Thesis: M.Sc in Mechanical Engineering,* Pennsylvania State University

Sandberg, M. (2007) 'Design for manufacturing using knowledge engineering', *Doctoral Thesis,* Luleâ University of Technology, Sweden.

Santos, E. C., Shiomi, M., Oskada, K., Laoui, T. (2006) 'Rapid manufacturing of metal components by laser forming', *International Journal of Machine Tools and Manufacture*, 46(12–13), pp. 1459–1468. doi: 10.1016/j.ijmachtools.2005.09.005.

Schmid, G. and Eidenschink, U. (2014) Rapid manufacturing. pp 1-7. http://docplayer.net/62670630-Rapid-manufacturing-with-fdm-in-jig-and-fixture-construction.html Accessed on 26 November 2015.

Schmolz-Bickenbach. 2015. *Materials Brochure,* viewed 25 November 2015 at https://www.dew-stahl.com/en/products/tool-steels/steels-for-plastic-moulding/

Schneider, K. and Carson, J. (2016) 'Energy-Efficient Additive Manufacturing', *NYSERDA Report*, (16), pp. 1–24.

Stratasys. (2012) A New Mindset in Product Design. pp 1-9 http://usglobalimages.stratasys.com/Main/Secure/White%20Papers/WP_FDM_NewMindset.pdf?v=635905246245235050 Accessed on 26 November 2015.

Thijs, L., van Humbeeck, J., Kempen, K., Yasa, E., Kruth, J., Romouts, M. (2011) 'Investigation on the Inclusions in Maraging Steel Produced by Selective Laser Melting'. International Conference on Advanced Research in Virtual and Rapid Prototyping (VRAP), Date: 2011/09/28 - 2011/10/01, Location: Leiria, Portugal

Whale, J. *et al.* (1995) 'A model of the injection moulding process', 37(September 1992), pp. 1–15.

*Wohlers Report 2018*, 3D Printing and Addtive Manufacturing State of the Industry Annual Worldwide Progress Report, Fort Collins, Co., Wohlers Ass, Inc.

Wong, K. V. and Hernandez, A. (2012) 'A Review of Additive Manufacturing', *ISRN Mechanical Engineering*, 2012, pp. 1–10. doi: 10.5402/2012/208760.

Wu, J. *et al.* (2016) 'Fast and stable electrical discharge machining ( EDM )', *Mechanical Systems and Signal Processing*. Elsevier, 72–73, pp. 420–431. doi: 10.1016/j.ymssp.2015.11.006.

Yadroitsev, I., Krakhmalev, P. and Yadroitsava, I. (2014) 'Hierarchical design principles of selective laser melting for high quality metallic objects', *Additive Manufacturing*, 7, pp. 45–56. doi: 10.1016/j.addma.2014.12.007

Zhang, Y. *et al.* (2014) 'Evaluating the Design for Additive Manufacturing: A Process Planning Perspective', *Procedia CIRP*. Elsevier B.V., 21, pp. 144–150. doi: 10.1016/j.procir.2014.03.179

# Appendix 1

# Design Rules for Conformal Cooling Channels in Maraging Steel Inserts

| | | |
|---|---|---|
| Recommended minimum distance between cavity and cooling channel | $D_H = 4$ mm; $x_m \geq 1$ mm<br>$D_H = 8$ mm; $x_m \geq 1.5$ mm | 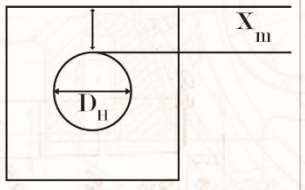 |

# Heat treatment of Maraging Steel Inserts

| | |
|---|---|
| **Stress relieving heat treatment**<br>- Reduce geometric distortion of inserts<br>- Enhance machinability | Components to be placed in a furnace at 890°C while attached to the build plate with a soaking time of 3 hours per 25mm and allowed to cool to room temperature.<br>Obtained hardness: 22 ± 0.5 HRC |
| **Age-hardening heat treatment**<br>- Enhance hardness and material strength after final machining | Components to be placed in a furnace at 495°C with a soaking time of 6 hours and allowed to cool to room temperature.<br>Obtained hardness: 51≥54 HRC |

Central University of Technology, Free State

CRPM

science & technology
Department: Science and Technology
REPUBLIC OF SOUTH AFRICA





Central University of Technology, Free State

# Appendix 2

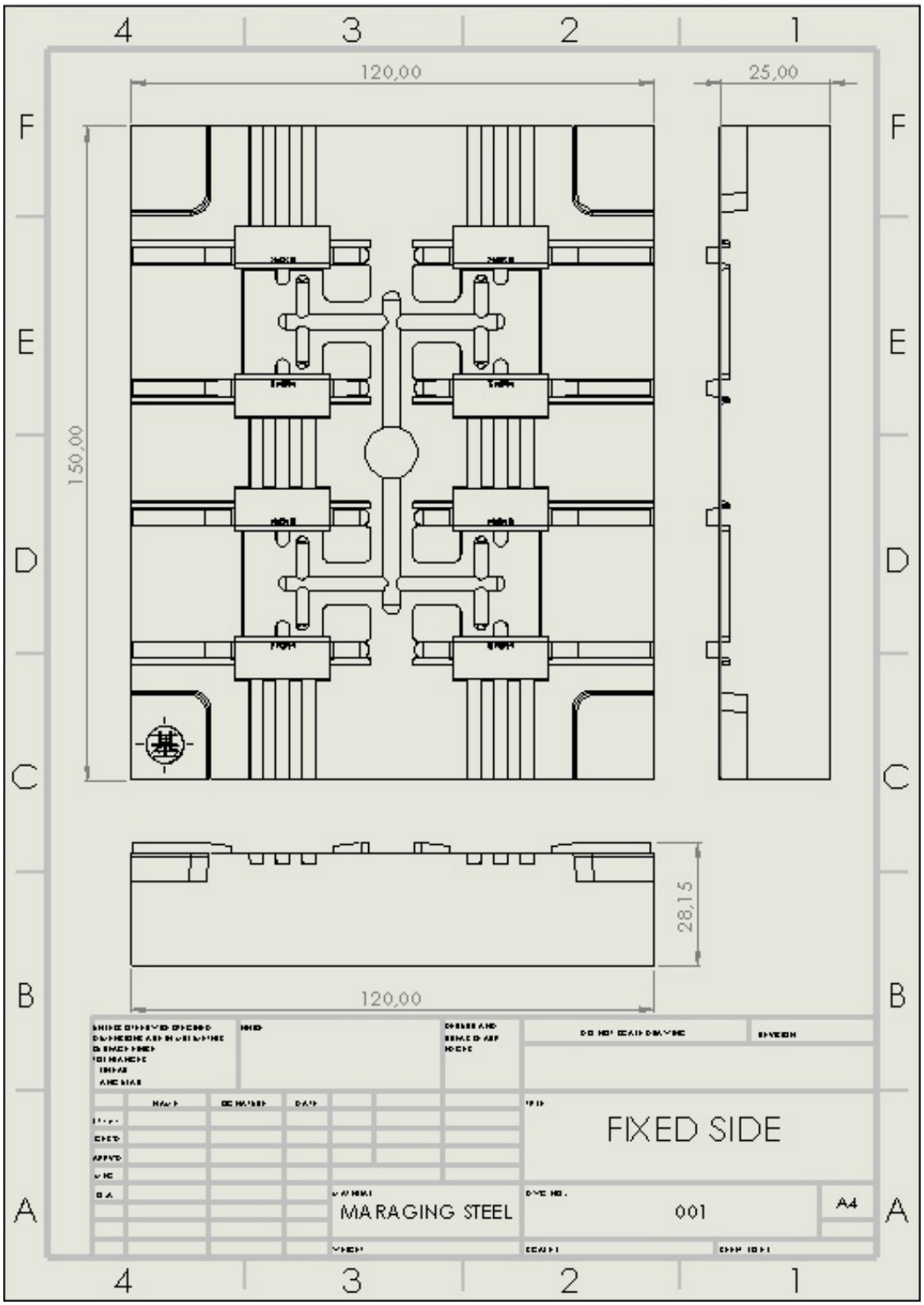


*Figure 51: CAD draft showing the fixed side of the Altech -UEC mould*

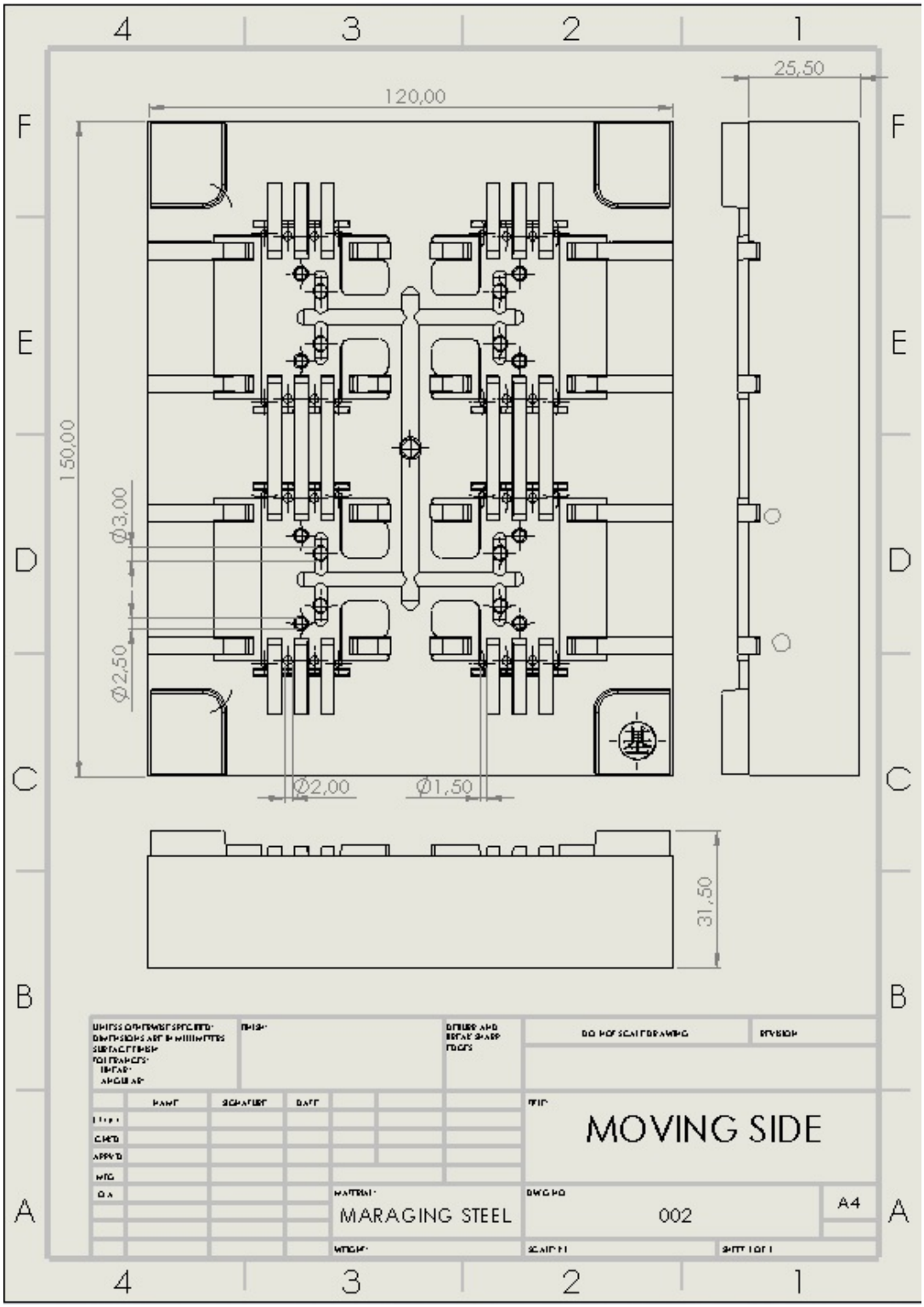


*Figure 52: CAD draft showing the moving side of the Altech -UEC mould*

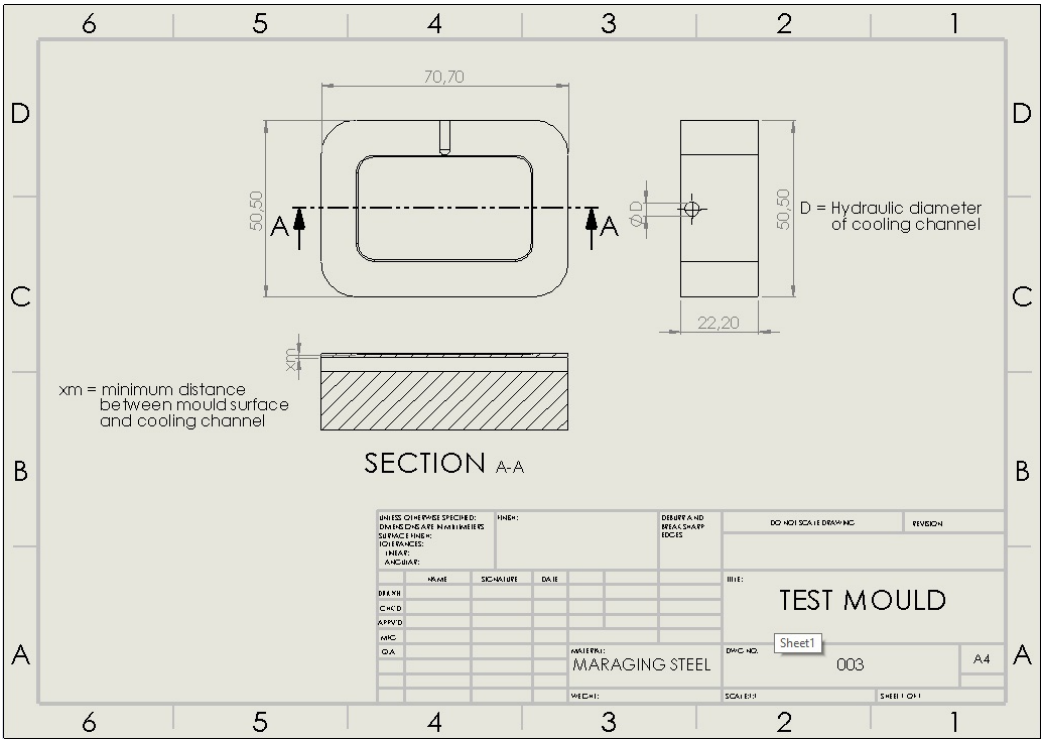


*Figure 53: CAD draft showing the dimensions of the mould strength test inserts*

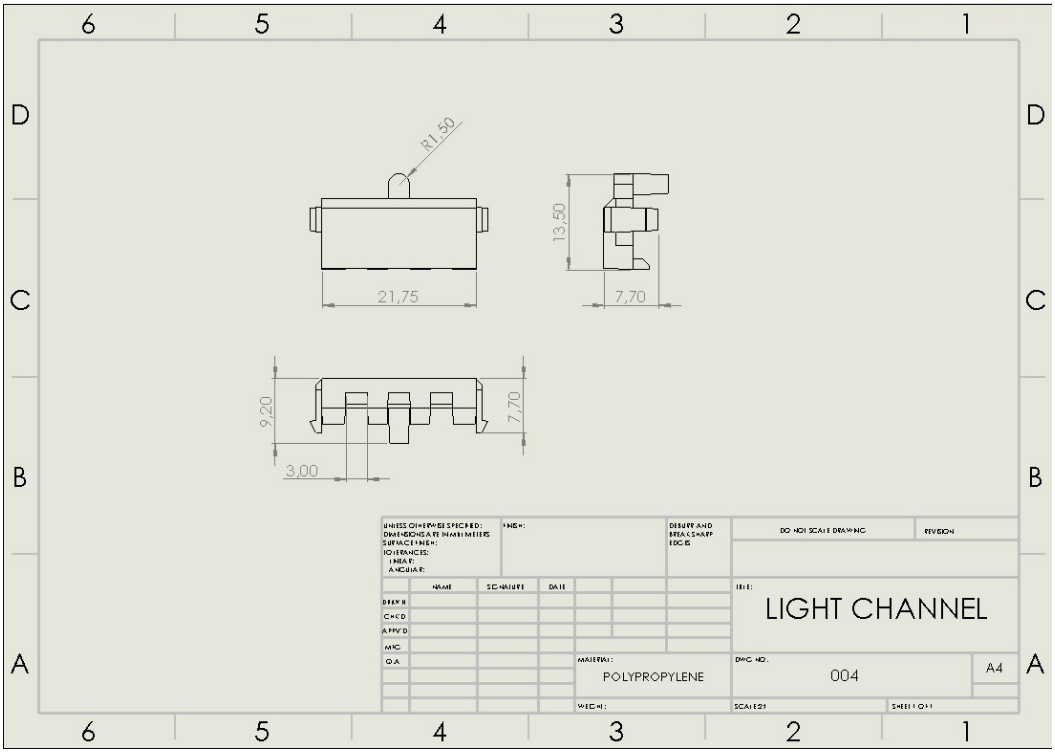


*Figure 54: CAD draft showing the dimensions of part used in the industry application of the developed design rules*

*Table 23: Heat transfer properties used in the SIGMASOFT® simulations*

| Material | Heat transfer coefficient (W/m°C) |
|---|---|
| Maraging steel | 20 |
| ABS plastic | 0.175 |
| Polypropylene plastic | 0.16 |
| Water | 0.615 |

*Table 24: Polymer material properties as used in the SIGMASOFT® simulations*

| Physical and mechanical properties | ABS | Polypropylene |
|---|---|---|
| Ultimate ensile strength (MPa) | 40.6 | 29.8 |
| Yield strength (MPa) | 44.6 | 31.6 |
| Young's modulus (GPa) | 1.98 | 1.70 |
| Density (kg/m$^3$) | 1090 | 929 |
| Melt Flow @200°C (g/10min) | 17.6 | 14.9 |